#344 OCTOBER 2018

Acoustic target classification

ICES COOPERATIVE RESEARCH REPORT

RAPPORT DES RECHERCHES COLLECTIVES

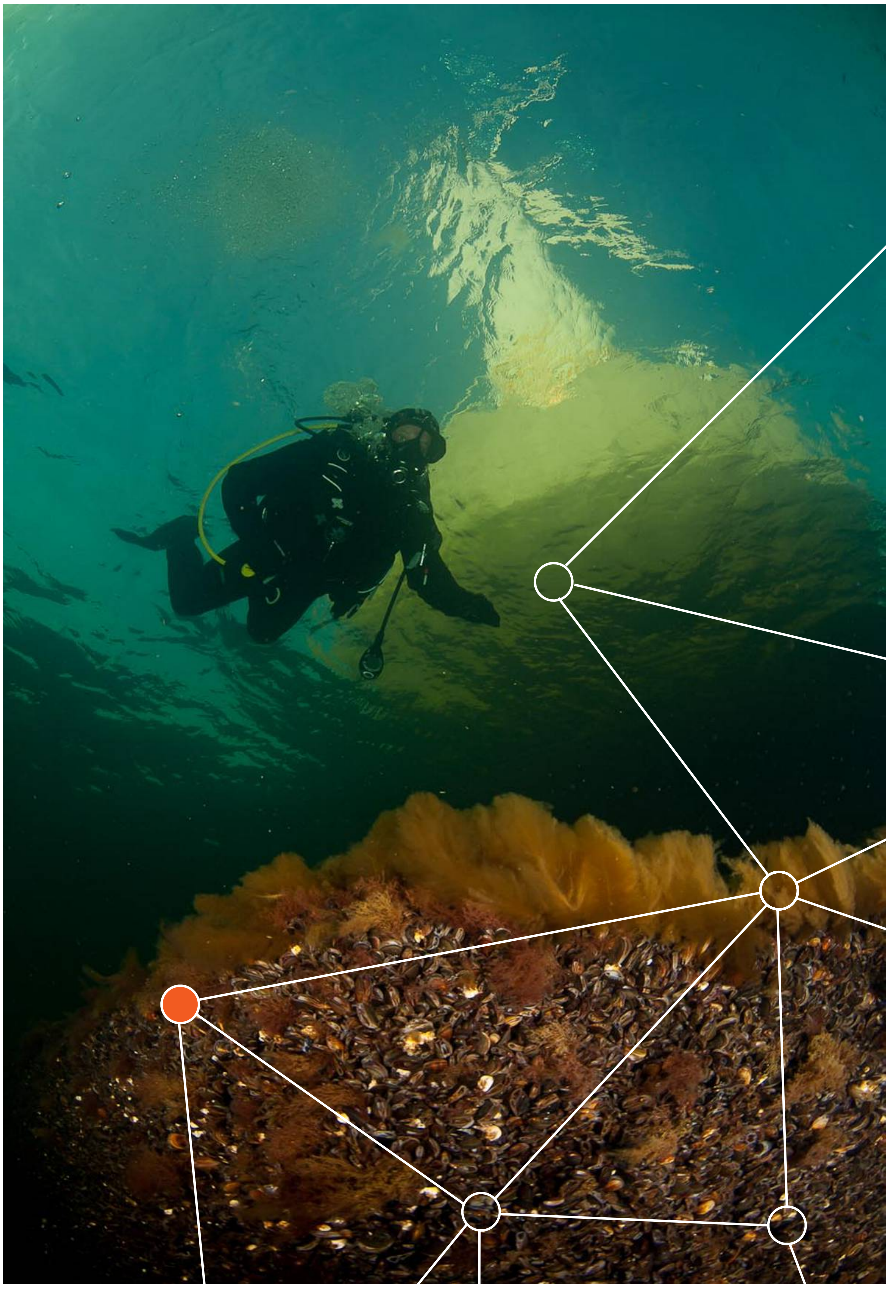

ICES INTERNATIONAL COUNCIL FOR THE EXPLORATION OF THE SEA
CIEM CONSEIL INTERNATIONAL POUR L'EXPLORATION DE LA MER

ICES COOPERATIVE RESEARCH REPORT
RAPPORT DES RECHERCHES COLLECTIVES

NO. 344

OCTOBER 2018

Acoustic target classification

Editor
Rolf J. Korneliussen

Authors
Laurent Berger ● Fabio Campanlla
Dezhang Chu● David Demer ● Alex De Robertis
Réka Domokos ● Mathieu Doray ● Sophie Fielding
Sascha M. M. Fässler ● Stéphane Gauthier ● Sven Gastauer
John Horne ● Briony Hutton ● Federico Iriarte
J. Michael Jech ● Rudy Kloser ● Gareth Lawson
Anne Lebourges-Dhaussy ● Ian McQuinn ●Marian Peña
Ben Scoulding ● Serdar Sakinan ● Matthias Schaber
J. Christopher Taylor ● Charles H. Thompson

ICES
International Council for the Exploration of the Sea
CIEM
Conseil International pour l'Exploration de la Mer

International Council for the Exploration of the Sea
Conseil International pour l'Exploration de la Mer

H. C. Andersens Boulevard 44–46
DK-1553 Copenhagen V
Denmark
Telephone (+45) 33 38 67 00
Telefax (+45) 33 93 42 15
www.ices.dk
info@ices.dk

Recommended format for purposes of citation:

Korneliussen, Rolf J. (Ed.). 2018. Acoustic target classification. ICES Cooperative Research Report No. 344. 104 pp. http://doi.org/10.17895/ices.pub.4567

Series Editor: Emory D. Anderson

DOI http://doi.org/10.17895/ices.pub.4567

ISBN 978-87-7482-218-9

ISSN 2707-7144

Contents

Foreword

Data are collected from a variety of acoustic systems in many countries to address a range of ecosystem monitoring and stock management objectives. A key step in the analysis of fisheries acoustics data is target classification, i.e. categorizing the backscatter data, ultimately by target species, so that it can be converted into estimates of abundance or biomass. The information needed to classify acoustic targets may be contained within the acoustic measurements, particularly if they are made over a range of frequencies.

The SIMFAMI project, financed by the European Union, presented some multifrequency methods for species identification (Fernandes *et al*., 2006). Readers should also note that there are two other ICES reports on related topics: CRR No. 238 Report on Echo Trace Classification (Reid, 2000) and Acoustic seabed classification of marine physical and biological landscapes (ICES, 2007). However, as these reports were written when multifrequency and wideband methods were less mature, they mostly focus on single-frequency methods.

Acoustic classification of biological targets is a fast-moving field. While most of the theoretical principles in the earlier reports are still relevant, there is a need to evaluate recent developments, expand their applications to contemporary technologies, and recommend target-classification protocols for use in fisheries research and ecosystem surveys. Several ICES Member Countries and observer countries have identified these needs and conveyed them to ICES Working Group on Fisheries Acoustics, Science, and Technology (WGFAST) and Science Committee (SCICOM). This is the first ICES CRR to detail the latest multifrequency and wideband methods for acoustic target classification.

1 Executive overview

Species identification is "the grand challenge" (MacLennan and Holliday, 1996) for acoustic methods used to estimate fish abundance (Simmonds and MacLennan, 2005). Acoustic survey methods are continuously improved to increase the accuracy of acoustic classification and thereby reduce the uncertainty of abundance estimates.

Most commonly, single-frequency acoustic data are classified using echogram features and biological samples. First, the echogram data are scrutinized (analysed, corrected, and classified) e.g. by checking for errors, removing noise, thresholding, and setting analysis depth layers. Then, target features are delineated by lines, rectangles, or polygons and ascribed to species using expert knowledge resulting from relevant biological and oceanographic samples. In most surveys, the aim is to identify echoes from one or two species, with other echoes considered less important. Acoustic target classification can be improved by using multifrequency data and exploiting its inherent information.

The target audiences for this report are:

- users who conduct surveys and derive abundance estimates;
- those who understand what can and cannot be done using existing and modified processing tools, but may not be familiar with the theory underlying acoustic target classification methods;
- developers who use and modify existing tools and develop advanced tools;
- those with advanced theoretical knowledge.

2 Terminology

The names, symbols, and units of physical quantities must be precisely defined to assure effective scientific communication. The following terminology is used consistently throughout this report and can be adopted for more general use in the field of fisheries acoustics. Terminology (Table 2.1) and symbols (Table 2.2) defined here are used consistently throughout this report, and in Demer *et al*. (2015; Calibration of acoustic instruments). Note that this terminology is used in acoustics; optics and radar may have different definitions, e.g. broadband.

Symbols uniquely represent a term. All symbols for variables are italicized. Any symbol for a variable (x) which is not logarithmically transformed is lower case. Any symbol for a variable with units of decibels, e.g. $X(\mathrm{dB}) = 10Log\left(x/x_{ref}\right)$, relative to a reference value (x_{ref}), is capitalized.

Table 2.1. Terminology used throughout this report.

Term	Description and references
Approximate model	Approximate models are modifications of exact models where boundary conditions and/or model input are simplified and/or parameter ranges and prediction ranges are restricted.
Bandwidth	The difference between half-power points in a signal, expressed in hertz, or normalized by the mid-frequency, in percent (Chatfield, 1989).
Broadband	A signal with 10% or greater bandwidth. Also known as broad bandwidth.
Classification	Apportionment of acoustic backscatter to taxon (e.g. genus, species), trophic level (e.g. secondary producer, primary consumer), or anatomical characteristics (e.g. gas-bearing, fluid-like scatterer). Synonymous with identification and categorization (Horne, 2000). See Section 3.3.
Chirp	A frequency-modulated (FM) broadband signal, e.g. frequency increasing linearly from the start to the end of the pulse.
Combined-frequency data	Data generated by combining data from two or more frequencies into a single data channel. Term used for example in Korneliussen (2000) and Korneliussen and Ona (2002, 2003).
Composite data	Data generated by combining data from two or more frequencies into a single data channel. (The term combined-frequency data was used previously, and is still used sometimes).
ΔdB	Difference (Δ) in S_v at two acoustic frequencies, f_1 and f_2, e.g. $S_v(f_1)$–$S_v(f_2)$.
Exact model	Exact models are derived from physical first principles and are accepted as theoretically correct. They are often expressed in the form of infinite series expansions valid for model–parameter ranges that ensure convergence.
Fluid	Liquids and gases that do not support shear waves.
Geometric scattering region	a/λ << 1. Sometimes called "high-frequency scattering region" although this term relates to the size of the target relative to the wavelength
Logarithmic relative frequency response	$R(f) \equiv \log_{10}\left[r(f)\right]$
Model	Mathematical expressions of acoustic backscattering cross-sectional area (Jech *et al.*, 2015).
Model input	The data used to produce a model output.
Morphology	Study of the form and structure of organisms and their features. In this document it relates to the shape, form, and structure of targets.
Morphometry	The process of measuring external shape, dimension and form.

Multifrequency	Multiple narrowband signals. In general, each narrowband signal is generated by its own individual echosounder; therefore, multifrequency data require multiple echosounders (or one echosounder with several processing units). Data from two or more frequencies. Historically, the term dual-frequency has been used for two frequencies.
Narrowband	Also known as narrow bandwidth. Narrowband is defined here as a signal with bandwidth < 10% of the centre frequency.
Noise	Unwanted component of a measurement. Ambient noise can be measured by an instrument in passive mode. Interference noise is from unsynchronized instruments.
Numerical model	Numerical models use numerical methods to solve the mathematical equations. They are approximations but can be used to predict acoustic backscatter from complex targets.
Rayleigh (Strutt, 1919) scattering region	a/λ << 1. Sometimes called "low-frequency scattering region" although this relates to the size of the target relative to the wavelength.
Relative frequency response	$r(f) \equiv \frac{s_v(f)}{s_v(f_{ref})} \equiv \frac{s_A(f)}{s_A(f_{ref})}$ Commonly, f_{ref}= 38 kHz. s_v, s_A, f in Table 1.2 (Korneliussen and Ona, 2002, 2003).
Q	The quality factor of a signal, usually related to the resonance frequency. Q is the ratio of the resonance frequency (f_r) to the bandwidth (Δf), $f_r/\Delta f$. Narrowband signals have higher Q and broadband signals have lower Q (ANSI, 1994).
Relative frequency response based on single targets	$r_T(f) \equiv \frac{\langle \sigma_{bs,T,i}(f) \rangle}{\langle \sigma_{bs,T,i}(f_{ref}) \rangle}$ Commonly, f_{ref} =38 kHz, σ_{bs} for fish *T*, ping *i*. See Pedersen and Korneliussen (2009).
Resonant scatter	Mie region. Scatter where the frequency of the ensonifying wave matches one of the targets own natural frequencies of vibration. See Urick (1983).
Scrutinization	Also called manual categorization. The process of allocating acoustic backscatter to acoustic scrutinize categories, such as "cod", "cod or haddock", "sandeel", or "possibly sandeel". Those acoustic values are validated against biological sampling and are eventually used to allocate the observed backscatter to species.
Single-frequency data	Data from one echosounder with a narrowband signal.
Target	The source of desired acoustic backscatter.
Wideband	Also known as wide bandwidth. Includes a suite of frequencies from multiple, narrowband signals, multiple broadband signals, or a combination of these.
Z-score	Method based on the normal deviate (*Z*-score) of the ΔdB for frequency pairs and classes of scatterers. Z-score is a standard statistical feature that allows comparison of two different normal distributions. See e.g. De Robertis *et al*. (2010) for use of *Z*-score in fisheries acoustics.

Table 2.2. Terms, symbols, and units

Term	Symbol	Unit	Description or defining equation
Absorption coefficient	α_a	dB m^{-1}	A metric of absorption loss. The reduction in acoustic intensity with r resulting from the conversion of p_a to heat.
Acoustic power	p_a	W	Acoustic RMS (root mean squared) energy per unit time.
Acoustic wavelength	λ	M	Distance spanned by one cycle of a periodic pressure wave.
Area backscattering coefficient	s_a	m^2 m^{-2}	The integral of s_v over a range of depths. $s_a = \int_{z_1}^{z_2} s_v dz$
Backscattering cross section	σ_{bs}	m^2	$\sigma_{bsv} = r^2 I_{bs}(r) 10^{\alpha_a r/10} / I_{inc}$ $\sigma_{bsv} = r^2 I_{bs}(r) 10^{\alpha_a r/10} / I_{inc}$
Depth	d	M	The vertical distance below the sea surface.
Frequency	f	Hz	Number of complete cycles of a periodic wave per unit time.
Nautical area scattering coefficient	s_A	Nautical mile^{-2} m^2	s_a multiplied by $4\pi 1852^2$.
Pulse duration	τ	S	The duration of a sound pulse.
Radius	a	M	Equivalent spherical radius of object.
Range	r	M	Distance between objects, e.g. the transducer and the target.
Sampled volume	V	m^3	The volume contributing to a received signal.
Signal-to-noise ratio	r_{sn}	Dimensionless	The quotient of signal to noise power.
Target strength	TS	dB re 1 m^2	$TS = 10\log_{10}(\frac{\sigma_{bs}}{A_0})$ $A_0 = 1m^2$ $TS = 10\log_{10}(\frac{\sigma}{4\pi A_0})$ $\sigma_{bs} = \sigma_{Clay\&Medwin} = \frac{\sigma}{4\pi} = \sigma_{Urick}$
Volume backscattering coefficient	s_v	m^{-1} m^2 m^{-3} dB re 1 m^2 m^{-3}	The backscattering cross section per unit of water volume. $s_v = \sum \frac{\sigma_{bs}}{V}$
Volume backscattering strength	S_v	dB re 1 m^{-1} dB re 1 m^2 m^{-3}	$S_v = 10\log_{10}(\frac{s_v}{A_0})$ $A_0 = 1m^2$

3 Introduction

3.1 Why classify acoustic data?

Classification is needed to efficiently and objectively interpret acoustic data and achieve accurate and reproducible results for stock management and ecosystem studies. Classification results can be used to guide sampling, quantify measurement and sampling uncertainty, and better assess target species and other ecosystem components. Classification results can also be used to guide sampling during a survey. Ultimately, this produces more objective data for stock management.

3.2 What this report contains

This report describes methods that can be used to classify acoustic targets in multiple narrowband frequencies data. Some of the methods may be applicable to broadband data or applied to data from narrowband frequencies that have been derived from broadband measurements. The classification methods are demonstrated through case studies.

3.3 What this report does not contain (and why)

- Seabed classification. It does not pertain to the classification of aquatic organisms, see Anderson *et al*. (2007a);
- Echotrace classification. It is based on single-frequency echogram morphology, see Reid (2000);
- Scrutinization of echograms. It focuses on the classification of single-frequency data, see ICES (2015).

3.4 Approaches to target classification

The expected relative frequency response from a few scatterer types is illustrated in Figure 3.1, with the region covered by five discrete frequencies in the range 18–200 kHz, as indicated. Under survey conditions, measurement uncertainties, available acoustic frequencies, and equipment limitations make it more appropriate, initially, to categorize echoes from scatterers with common features (e.g. fluid-like or gas filled).

Fluid-like objects have sound speed, and density properties similar to those of water, and the backscatter is characterized by fluctuations between the low-frequency (Rayleigh) and high-frequency (geometric) scattering regions (e.g. organism types 1, 2, and 3 in Figure 3.1). All gas-filled objects, such as siphonophores and fish with swimbladders, exhibit resonant scattering at a frequency that depends on depth and size of the gas inclusion (e.g. curves 5 and 7 in Figure 3.1). Backscatter from elastic-shelled zooplankton is characterized by the smooth transition between low- and high-frequency regions. There will also be differences in scattering features within each class, e.g. the rate of increase in the low-frequency region, the height and width of the resonance peak, the spacing of high-frequency oscillations, and the high-frequency backscattering strength.

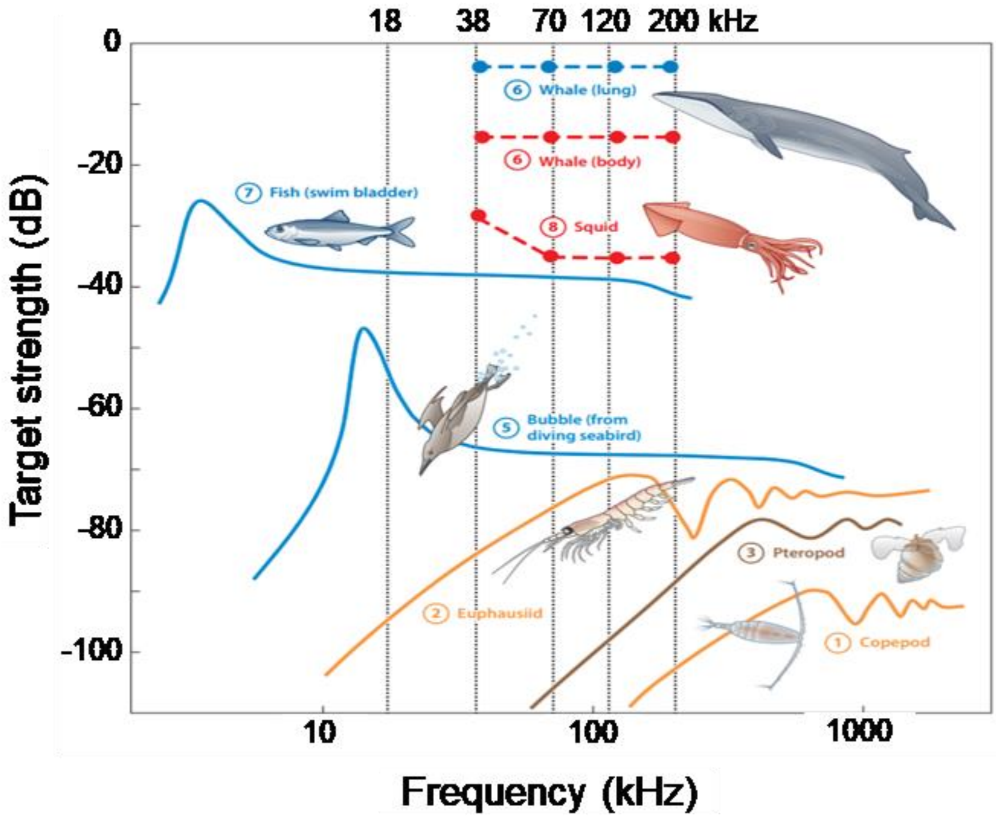

Figure 3.1. Target strength vs. frequency for different types of animals, with zooplankton in the three lower right curves. The *x*-axis location of the various curves depends on the ratio of organism size divided by acoustic wavelength. The curves are shown for typical organism sizes over the range of typical acoustic frequencies. Reproduced from Benoit-Bird and Lawson (2016).

The workflow (Figure 3.2) starts with planning (sections 5.1–5.4), followed by acquisition (Section 5.5), quality control (Section 5.6), and concludes with classification (Section 6).

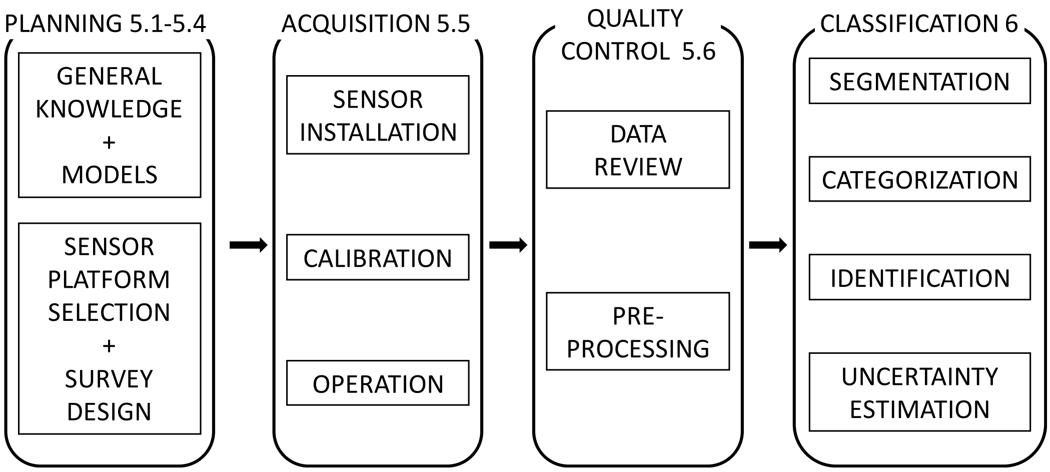

Figure 3.2. The process described in this report involves planning, data acquisition, quality control, and classification.

The aim of acoustic target classification is to categorize backscatter into groups, ultimately associated with target species, so that the data can be converted into estimates of abundance or biomass. The approach depends on a combination of perspective, available data, and the application.

Four levels of acoustic target classification include: (i) discrimination, (ii) categorization, (iii) identification, and (iv) validation. Discrimination removes unwanted data from data to be processed. For example, if the objective is to estimate the abundance of a fish species with a swimbladder, then backscatter values lower than those expected from the target species may be excluded from analysis using a threshold on the volume backscattering strength (S_V) or the difference in S_V measured with multiple frequencies (e.g. Sato *et al*., 2015). Categorization groups data that represent scatterers with common acoustic characteristics. For example, a layer of strongly scattering demersal targets can be grouped separately from discrete pelagic scatterers higher in the water column. Identification is the assignment of a taxon or species to each category. For example, the demersal-layer and pelagic-discrete scattering categories may be identified as ground and pelagic fish, respectively. With *a priori* information, bottom- and midwater-trawl data, or both, these identifications may be validated as Atlantic cod (*Gadus morhua*) and herring (*Clupea harengus)*, respectively. Thus, the results of acoustic categorization may, in many cases, be refined to species level, such as cod, capelin (*Mallotus villosus*), or herring.

4 Acoustic scattering properties of aquatic organisms

Classification of acoustic backscatter into functional groups depends on the scattering properties of the target, the instruments used, and how the instruments are operated.

When subjected to a pressure wave, aquatic organisms with an acoustic impedance different from that of the surrounding body of water scatter the wave in a characteristic way. The characteristics of acoustic scattering have only been studied for a small number of species. Factors that influence backscatter characteristics include the acoustic instrument (e.g. transmit signal), the environment (e.g. seawater density and sound speed), and the target shape and morphology (e.g. fluid-like or gas-filled). A list of parameters assumed to significantly affect the acoustic scattering properties of aquatic organisms is given in Table 4.1 (Urick, 1983; Stanton *et al*., 1996; Medwin and Clay, 1998; Lavery *et al*., 2003; Moum *et al*., 2003; Simmonds and MacLennan, 2005).

Information about the echosounder and transducer can be obtained from the manufacturer or estimated from an instrument calibration (Demer *et al*., 2015).

Table 4.1. Dominant factors affecting the acoustic scattering properties of aquatic organisms.

Instrument	Transducer	Environment (water)	Organism
Source level	Resonance frequency	Depth	Species
Frequency	Bandwidth	Temperature	Size
Bandwidth	Beam width	Salinity	Number density
Sampling frequency	Transmit sensitivity	Sound speed	Specific density
Pulse duration	Receive sensitivity	Density	Compressional wave speed
System gain	Built-in gain	Sound absorption coefficient	Shear wave speed
Electrical noise	Efficiency	Ambient noise	Sound absorption coefficient
	Electrical/mechanical noise	Dissipation rate of turbulent kinetic energy	Morphology
		Dissipation rates of temperature and salinity variances	Behaviour
		Molecular diffusivities for temperature and salt	Anatomy
		Molecular viscosity	Fecundity
			Maturity

Environmental parameters, the physical and chemical properties of water, can be measured with instruments such as conductivity temperature depth (CTD). The parameters defining the scattering properties of aquatic organisms are highly variable and mostly unknown. These parameters can be categorized into three groups:

- physical parameters such as sound speed (fluid) in the seawater, and compressional and shear wave speeds in the organisms;
- geometric parameters including those related to morphology such as shape (length, width, and height) and behaviour affecting the angle of orientation relative to the incident wave; and
- biological parameters such as anatomy and fecundity.

Although instrument and geometric parameters can generally be estimated with practical levels of uncertainty, biological factors and their influence are more variable and can rarely be described with high levels of certainty (Gross and Raymont, 1942; Lowndes, 1942; Enright, 1963; Greenlaw, 1977; Kogeler *et al*., 1987; Chu *et al*., 2000, 2003; Smith *et al*., 2010; Chu and Wiebe, 2005; Warren and Smith, 2007; Wiebe *et al*., 2010; Becker and Warren, 2014). There is interspecies variability (different species have different parameters), instability (properties change significantly with environmental conditions, life-history traits, behavioural characteristics, etc.), and intraspecies differences (e.g. ontogenetic stage). The paucity of information on biological parameters limits the characterization of acoustic scattering from marine organisms that is needed for species identification and target classification.

4.1 Variability of scattering characteristics of aquatic organisms

Variation in the scattering characteristics of aquatic organisms relates to environmental, biological, and behavioural parameters (Table 4.1). The dominant behavioural factor is generally the orientation angle relative to the incident wave (i.e. tilt angle), e.g. resulting from swimming behaviours such as vertical migration or prey–predator interaction (Torgersen and Kaartvedt, 2001). Backscatter also varies due to changes in swimbladder morphology vs. life stage (Chu *et al*., 2003) and depth (pressure; see Figure 8 in Horne *et al*., 2009). Scattering properties also vary geographically. The temporal and spatial variability of acoustic scattering must be considered when applying classification algorithms because it increases classification uncertainty.

4.2 Stochastic acoustic scattering properties

Stochastic variables, notably target strength (TS), are imprecisely known or incompletely characterized. While the underlying physical theory is determinate, the echo measurements are stochastic due to unobserved changes in the environment (e.g. temperature fluctuations) or target properties such as acoustic-wave incidence angles or school structure. Observed temporal variation in TS may be described by a probability-density function (PDF), in which case the mean over many measurements can be estimated precisely. The stochastic characteristics of echoes have been modelled theoretically (Rice, 1954; Ehrenberg, 1972; Baraket, 1974; Jao and Elbaum, 1978; Stanton, 1985; Stanton *et al*., 1993, Chu and Stanton, 2010).

4.3 Mixed species assemblages

Total acoustic backscatter may be the sum of echoes from different species comprising the aggregation. If the backscatter from one species is dominant, classification is relatively simple (Stanton *et al*., 1998a, 1998b; Traykovski *et al*., 1998; Hammond and Swartzman, 2001; Korneliussen *et al*., 2009; Korneliussen, 2010; Pedersen and Korneliussen, 2009; De Robertis *et al*., 2010). However, if backscatter from multiple species is not resolvable and is similar in strength, then classification, if possible, is difficult (Campanella and Taylor, 2016; Korneliussen *et al*., 2016; Gastauer *et al*., 2017a, 2017b). For mixed-species aggregations, classification to species requires ancillary information such as from trawl catches or camera images (see e.g. Simmonds and McLennan, 2005, p. 340).

5 Steps prior to target classification

5.1 Considerations related to instrumentation and installation

The first step in data collection is planning (Figure 3.2) and the first part of the planning process is to understand the scattering properties of targets and select appropriate instrumentation. Acoustic data collected at multiple frequencies should be comparable both physically and spatially. Requirements for the collection of comparable multifrequency data (Korneliussen *et al.*, 2008) include:

Physically comparable data

- Echosounder systems are expected to operate such that the linear wave equation applies;
- All systems of echosounders and transducers must be calibrated;
- Noise must be insignificant;
- Insignificant interference between acoustic systems.

Spatially comparable data (at high spatial resolution)

- Identical pulse lengths and pulse shapes at all frequencies;
- Individual pings should always be identifiable in the data files;
- Similar acoustic sampling volume at all frequencies for comparable ranges to the scatterers;
- Simultaneous transmission of pulses at all acoustic frequencies.

5.2 Requirements for physically comparable data

5.2.1 Echosounder systems are expected to operate such that the linear wave equation applies

Explanation: The equations used to estimate fish stock abundance are far-field approximations of the linear wave equation. The sound speed in water is pressure dependent, so propagation of a pressure wave (sound) inherently propagates non-linearly. Therefore, some energy leaks from the original acoustic frequency to other frequencies, e.g. to the double and triple of the original frequency (i.e. harmonic frequencies). The linear wave equation is a low-power approximation of wave propagation, while one of the more general and far more complicated non-linear wave equations is required to better approximate high-power sound. See e.g. Korneliussen (2002), Tichy *et al*. (2003), Simmons and MacLennan (2005, p. 37) or (in particular) Pedersen (2006) for description of non-linear sound propagation in fisheries acoustics. Non-linear generation of sound depends on several parameters, of which sound pressure level and frequency are two. Standard target calibration compensates for most of the non-linear loss until the depth of the calibration sphere, e.g. at 20 m below the hull, but the non-linear loss continues beyond that depth.

Suggested solution: A solution is to use power low enough that the linear wave equation applies or, more correctly, power low enough that – combined with calibration – the non-linear loss can be ignored. Transducers generating 7° beams have a smaller area at increasing frequencies. At the danger of oversimplifying, a simple rule of thumb is to use < 25 kW m^{-2} active area transducer ceramics for transducers of 60% efficiency (20 kW m^{-2} power input on transducers of 75% efficiency, which is typical for Simrad composite transducers). A more exact approach is to estimate non-linear loss from the equations given in Pedersen (2006). If data have already been collected with too high a power, a method to estimate the losses due to non-linear effects is given by Pedersen (2006, p. 170).

5.2.2 All systems of echosounders and transducers must be calibrated

Explanation: Use sonars that can be calibrated (see Demer *et al*., 2015). The term "sonar" includes vertically oriented sonars also known as echosounders. Note that the calibration methods inherently require sound propagation to follow the linear wave equation.

Suggested solution: Follow the guidelines in Demer *et al*. (2015) to calibrate.

5.2.3 Noise must be insignificant

Measurements should not be biased by noise and noise should not reduce the sampling volume (see point 5.3.2 below; Ona, 1987; Foote, 1991)

Explanation: Ambient noise will inherently limit the sampling volume, i.e. the usable range (at a given maximum off-axis angle). Absorption and ambient noise are frequency-dependent, which gives a frequency-dependent usable range. The maximum usable range also depends on the scattering properties of the targets (i.e. on the target strength) as well as the acoustic frequency. Signal-to-noise ratios (r_{sn}) should be high as ratios like the relative frequency responses, $r(f)$, used for categorization, are sensitive to both the numerator and the denominators.

Suggested solution: Passive data should be collected regularly so that ambient noise can be estimated and later removed from the data. Noise measurements should be recorded at different water depths, vessel speeds, engine revolutions, and propeller tilts. In bad weather, if possible, change vessel bearing and speed (and put out the protruding keel if you have one). Note that signals received some time after the detection of the first bottom echo can be considered passive (depending on range, ping rate, bottom type, etc; Korneliussen, 2000). In other words, this means that noise can be estimated continuously while actively pinging, provided the recording is sufficiently long (i.e. the receiver is listening for long enough after transmission) after the first bottom echo is received (e.g. see Korneliussen, 2000). The ambient noise can be used to estimate the maximum usable range, which depends on the scattering properties of the targets (i.e. on the target strength; Foote, 1991).

5.2.4 Insignificant interference between acoustic systems

Explanation: Acoustic instruments should not influence each other appreciably. The worst-case situation is two unsynchronized systems transmitting in the same frequency band. Similarly, internal echosounder electronics used at one frequency should not influence another, and the sound transmitted at one frequency should not influence another frequency. This requires synchronization, i.e. simultaneous transmission of sound at all frequencies, or alternating pings from systems that would otherwise interfere with each other. Acoustic energy leakage cannot occur from one frequency to another, which, in practice, means no non-linear effects. This in turn requires that the transmission power should be kept low. It also requires that there is no transfer of electric energy (i.e. crosstalk), e.g. between the electronics or between the cables carrying the energy to the transducers that convert the electrical energy to sound.

Suggested solution: This is an issue that manufacturers need to solve but customers may put effort into ensuring that manufacturers do so. Good electrical earth connections for all the instrumentation are essential to avoid interference that may be picked up by electrical signal cables. The transducer cables should be as short as possible to reduce electrical interference from outside sources. If AC power supply is noisy, it may be replaced by a linear DC power supply if possible. Furthermore, limit any unnecessary ship-based noise.

5.3 Spatially comparable data

5.3.1 Identical pulse lengths and pulse shapes at all frequencies

Explanation: The requirement for identical pulse lengths and pulse shapes at all frequencies is necessary to ensure that samples are directly comparable at the highest spatial resolution. See Figure 5.1a.

Suggested solution: The use of identical pulse lengths and pulse shapes at all frequencies should be made possible by the manufacturer. There may be different solutions to this, e.g. reduction of vertical resolution in the data which naturally reduces the achievable spatial resolution.

5.3.2 Individual pings should always be identifiable in the data files

Explanation: More than having the measurements comparable physically and spatially, the coherent pings at different frequencies must be identified in the data files. One should know which pings to compare between frequencies – it is not very useful to compare current ping at one frequency with a ping from 2 min earlier at another frequency.

Suggested solution: Individual pings always identifiable in the data files require high enough time-resolution in the data.

5.3.3 Similar acoustic sampling volume at all frequencies for comparable ranges to the scatterers

Targets of interest should be acoustically visible in all parts of the sampled volumes for the ranges used. Provided that signal-to-noise is high, this implies (i) same half-power beam widths at all frequencies, (ii) same acoustic centre of all transducers (includes same transducer depth), and (iii) same orientation for the acoustic axis for all transducers.

Explanation: It is currently unrealistic to cover a wide acoustic bandwidth with a single transducer that has the same opening angle at all frequencies, so any solution would be a compromise. See Figure 5.1 b for illustration of point (i). Higher s_v measured in wider beams may indicate that scatterers are avoiding the sampling platform, and lower s_v measured in wider beams may indicate that scatterers are attracted to the sampling platform. Since direction to the target is not available (in s_v-data!), comparing data from a wide 18-kHz beam and a narrow 38-kHz beam may indicate either a target resonant at 18 kHz or a target on the outer edge of the narrow 38 kHz beam. The use of multiple transducers inherently means that points (ii) and (iii) cannot be fulfilled.

Suggested solution: Similar acoustic sampling volume at all frequencies for comparable ranges to the scatterers. Having the same half-power beam width (determined where the acoustic power is half of the value in the centre of the beam) for a transducer at its resonance frequency is achievable, and manufacturers have been encouraged to produce transducers with 7° beam width at its resonance frequency. Achieving the same half-power beam width for a single transducer over a wide bandwidth is challenging, especially when high efficiency is required, but it is possible (Sæther, 2009). Such a transducer inherently also has the same acoustic centre and acoustic axis over the frequency range. A more realistic solution is to cluster multiple transducers together and thus optimize beam overlap by minimizing distances between the transducers.

5.3.4 Simultaneous transmission of pulses at all acoustic frequencies

Explanation: There will be a lot of spike (i.e. impulse) noise if the pulse transmission of multiple acoustic sources is unsynchronized. For sequential pinging, spike noise may be avoided, but the pings then ensonify different volumes (and thereby different targets) at different frequencies. Furthermore, for sequential pinging one frequency at a time, the specimens could have moved and changed orientation from one ping/frequency to the next. A non-moving target measured from a moving platform will appear as a moving target. Since measurements can be averaged across pings, this is a smaller problem if there are many targets in the sampling volume since. Finally, different bandwidths of echosounder subsystems at different frequencies may result in frequency-dependent pulse delays (as shown in Figure 5.1 c).

Suggested solution: Synchronization should include other ship-based acoustic devices (e.g. sonars and non-scientific echosounders). Any acoustic devices which cannot be synchronized should be switched off. Frequency-dependent pulse delays can easily be compensated for by applying frequency-dependent vertical shift, so that samples at the same depth are compared.

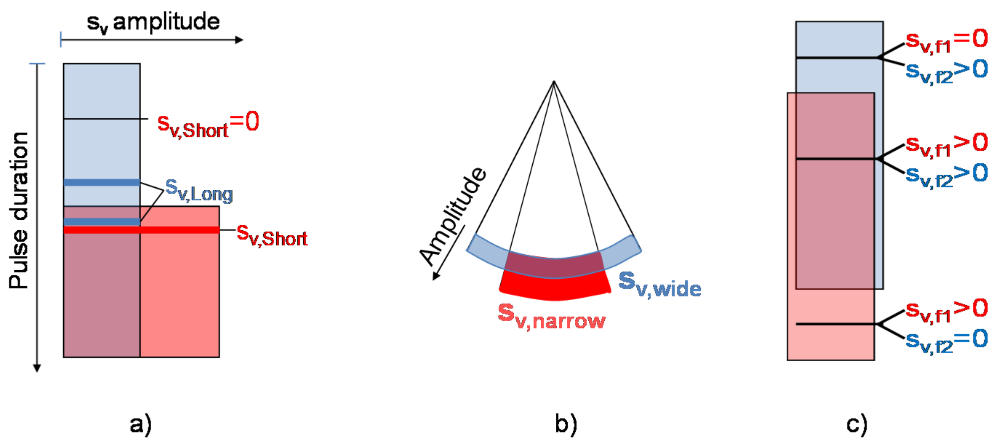

Figure 5.1. Illustration of some requirements to make s_v or s_A samples physically comparable. (a) Integrated backscatter is independent of pulse durations due to calibration, but the individual samples will differ for different pulse duration (Section 5.3.1). (b) Backscatter of homogeneous layers are independent of beam width due to calibration, therefore evenly distributed targets in a layer will give same value. The integral will differ if the targets are not homogeneously distributed, e.g. most targets at the edges due to avoidance [Section 5.3.3]. (c) If pulses at different frequencies are not simultaneous, sample by sample comparison will be incorrect (Section 5.3.4).

The use of a high ping rate makes it easier to improve data after collection, e.g. estimating and removing noise, smoothing data, or using different ping numbers to compensate for a long-ship distance between transducers. A further reason is to achieve high spatial resolution in the ship cruise direction. It is, therefore, advisable to use as high a ping-rate as practically possible.

For a flat bottom and fixed ping rate, false seabed detections appear at a predictable depth in the echogram. Therefore, it is possible to optimize ping rate to avoid false seabed detections at the same time as maintaining a high ping rate (Renfree and Demer, 2016).

To reduce bias induced by sampling different volumes with different transducers, Berger *et al.* (2009) developed a method for filtering fish school frequency response observed by several beams coming from different transducers and with different beam widths. The filtering method makes use of the true school position provided by the roll and pitch stabilized Simrad ME70 multibeam echosounder (Trenkel *et al.*, 2008), the positions and orientations of the transducers, and the dynamic position of the vessel. Echoes from the single-beam echosounders that were not simultaneously observed by all frequencies are removed, hence allowing for the study of *in situ* frequency response from fish schools with increased accuracy. The method is available in the MOVIES 3D software (Trenkel *et al.*, 2009).

5.4 Survey planning

5.4.1 Goals and logistics

The first and most important consideration is the question being asked or the goal of the project or survey, as all decisions are dependent on this. Will the data be for management purposes, such as stock assessments? If so, what is required from the assessment (species identification, target size, etc.)? The following are points that need to be considered:

- biology (e.g. spawning)
- behaviour (e.g. migration)
- historical information (e.g. past surveys or fisheries-dependent data can help inform survey design)
- temporal distribution (e.g. seasonal changes or day/night effects which will affect acoustic detectability and survey efficiency)
- spatial distribution (e.g. do the species inhabit deep or shallow water?)
- conditions at time of data collection
- utilize existing knowledge to inform survey decisions (e.g. literature, local knowledge from fishers, etc.)
- permit requirements
- ethical approval
- funding
- expertise and availability of personal

5.4.2 Sampling for species verification and validation

Robust classifications based on acoustic methods ideally rely on accurate knowledge of the organisms responsible for the backscattering responses. This is usually obtained from dedicated and concurrent sampling using capture devices such as nets, optical methods, or other forms of physical sampling (e.g. Fernandes *et al.*, 2016). In practice, acoustic target identification will only be as good as the validation tools used. This requirement poses a challenge, as validation of acoustic targets is subject to many uncertainties. In the context of fisheries acoustics, where the primary goal is generally classification of acoustic backscatter as species and size classes, this often means comparison of acoustic classifications with the results of sampling with nets and/or optical instruments (Ona, 2003; Doray *et al.*, 2007, 2016; Ryan *et al.*, 2009; Sawada *et al.*, 2009; Kubilius and Ona, 2012; O'Driscoll *et al.*, 2013; Fernandes *et al.*, 2016). These samples are size- and species-selective (Wileman *et al.*, 1996), and the animals captured or imaged are unlikely to accurately represent the species and size composition of acoustic scatters. In addition, organisms have complex behaviours and may react to sampling platforms such as vessels (De Robertis and Handegard, 2013) and underwater vehicles (Koslow *et al.*, 1995; Stoner *et al.*, 1998).

The details of biases introduced by factors such as reactions to sampling platforms, nets, and cameras are outside the scope of this report. However, the basic methods of conducting validation sampling for comparison to acoustic classification are discussed in Section 6. It should be emphasized that while validation is critical to the success of an acoustic classification method, it is complicated by uncertainties in the methods used.

Extrapolation error is also a possibility. The efficacy of an acoustic classification method is often situation-dependent (e.g. which species are present, the behaviour of these species, etc.), and acoustic target identification is unlikely to be generally applicable. Where possible, potential biases in both the target classification and the validation methods with their associated uncertainties should be considered explicitly under realistic local conditions (even if they are poorly understood). Given the large potential biases in these measures, multiple lines of validation may prove effective in addressing issues of species- and size-specific catchability and availability to sampling tools. In addition, comparison with prior knowledge, laboratory measurements, and model predictions may help build confidence in classification results. Model predictions are also subject to potentially large and poorly understood biases.

The species and size classes estimated from sampling may correspond to those dominating the environment, but they may not necessarily dominate the acoustic scattering due to large differences in acoustic scattering properties of various organisms (e.g. Stanton *et al*., 1993, 1994a, 1994b; Gauthier and Horne, 2004). For example, in mixed assemblages, a small proportion of swimbladder-bearing fish can dominate the backscatter at low frequency (38 kHz) even if they do not dominate the biomass or numerical densities (McClatchie and Coombs, 2005). Therefore, the abundance of organisms and their scattering properties must both be considered. Computing expected backscatter based on animal abundance and their scattering properties is referred to as the forward problem (Lavery *et al*., 2007). This approach can also be used to assess if the biological sampling is representative of the organisms acoustically sampled (Mair *et al*., 2005; Peña *et al*., 2015).

The level of identification depends on the species present, the availability of validation data, and the need to identify species. Validation data typically include coincident samples obtained during the acoustic survey. Direct sampling uses nets or other technologies to obtain representative samples from observed patterns on echograms of individual or aggregated targets. Qualitative or quantitative use of these supplementary samples depends on the "representativeness" of the validation data, such as catch or photos. Criteria for representativeness include how well the samples reflect the size and species composition of the acoustically detected organisms and the spatial resolution of acoustic samples.

It is important to remember that all sampling technologies, direct or remote sensing, have constraints, resulting in biased samples. The most appropriate sampling technology will maximize the probability of obtaining representative samples and minimize bias in catches (i.e. the selectivity of the gear), however the definition of "appropriate" is not simple. Choosing which sampling gear to use will be dictated by the location being sampled, organism behaviour relative to the sampling gear, the platform used to conduct the sampling, the construction of the sampling gear, how the gear is deployed, knowledge of the selectivity of the sampler, and the competency of the operator. Ideally, the selectivity of a sampler will be quantified (e.g. Nakashima, 1990; Williams *et al*., 2011; De Robertis *et al*., 2017). In cases where validation samples contribute to time-series for abundance or biomass estimates of commercially important species, effects of changing the sampling gear and/or the sampling method should be quantified, as a conversion factor is needed to scale data from samples obtained using the modified gear to samples collected from the existing dataseries.

5.4.3 Modelling the scattering properties

Models of the scattering properties of aquatic organisms can assist in understanding the effects described in Table 5.1. Scattering models can be used to guide or inform classification. Mathematical models are important in understanding what affects the scattering properties at a given frequency. The anatomy of the species, e.g. possession or lack of a swimbladder, affects the scattering strength, as does orientation behaviour, but not to the same degree at all frequencies. Ona (1990) describes several physiological factors that cause natural variations in acoustic TS of fish. Several scattering models of zooplankton and fish (e.g. Stanton, 1988, 1989; Clay, 1992; Stanton *et al.*, 1993, 1994a, 1994b, 1996, 1998a, 1998b; Stanton and Chu, 2004; Clay and Horne, 1994; Demer and Conti, 2003) show that orientation, morphology, and physical properties (e.g. density and sound speed contrasts (g and h) affect scattering properties. An effective scattering model needs to be complex enough to describe the real scattering properties and simple enough for practical use.

5.4.3.1 Types of models

Acoustic scattering models can be categorized into two types: (i) analytical and (ii) numerical. A detailed summary of these models can be found in Jech *et al*. (2015) and are listed in Table 5.1.

Analytical expressions of scattering models can be further divided into two forms: exact and approximate. Exact solutions are limited to a few targets with regular geometric shapes expressed as modal series solutions. They are applicable for targets with a low ka value, where k is the acoustic wave number and a is the characteristic dimension of the target, e.g. the radius of a sphere. When the ka is very large, the exact modal series solutions may suffer from convergence problems, especially for prolate spheroids. Approximate models normally have either closed-form solutions or forms that can be computed easily and can describe targets with more complicated geometry and material properties. These models can describe most of the practical scattering by aquatic organisms in the field of fisheries and zooplankton acoustics (Jech *et al*., 2016; Table 5.1).

Numerical models are normally discrete forms of the exact integral solutions and can describe the scattering by targets with complex geometry and material properties (boundary conditions). There are two major methods: (i) boundary element and (ii) finite element. Although these methods are exact and more flexible in dealing with complicated shapes and material properties, they are computationally expensive, requiring computers with large memory and fast computation speed (Jech *et al*., 2015; Table 5.1).

Table 5.1. Types of acoustic scattering models

Model/approximation solution	Shape	Use	Limitations	Advantages	Reference
ANALYTICAL MODELS					
Exact model					
Spheres	Simple geometric shape	Siphonopores	Limited to spheres	Simple to use	Anderson (1950); Faran (1951)
Infinitely long cylinder	Simple geometric shape	Fish body and krill/shrimp	Not morphologically realistic	Simple to use	Faran (1951); Stanton (1988)
Prolate spheroid	Simple geometric shape	Copepods, swimbladder, and fish body	Numerically difficult for *k*a<<1	Simple to use	Flammer (1957); Yeh (1967); Furusawa (1988); Reeder and Stanton (2004)
Approximate model					
Fourier Matching Method (FMM)	Axisymmetric simple geometric shape	Swimbladder and fish body	Axisymmetric representation	Valid over wide range of frequencies, body shapes, tilt angles, and material properties	Reeder and Stanton (2004)
Deform and Finite cylinder (DFC)					Stanton (1989); Ye *et al*. (1997)
Modal Series Based Deformed Cylinder Model (MSB-DCM)	Axisymmetric simple geometric shape	Swimbladder and fish body	Axisymmetric representation	Low computational requirements	Stanton (1989)
Resonance scattering	Simple geometric shape	Swimbladder	Not accurate for high frequencies, where *k*a>>1	Low computational requirements	Weston (1967); Love (1978); Ye (1997a, b); Scoulding *et al*. (2015)

Ray-based approximation					Clay (1992); Stanton *et al*. (1993)
Kirchhoff approximation (KA)	True shape	Swimbladder and fish body	Computationally intensive, not accurate for long thin objects	Valid over wide range of frequencies, body shapes, tilt angles, and material properties	Foote (1985); Clay and Horne (1994)
Distorted Wave Born Approximation	Simple geometric shape	Fish body	Applicable only for weak scatterers	Low computational requirements	Chu *et al*. (1993); Stanton *et al*. (1994a, 1994b); Demer and Conti (2003); Jones *et al*. (2009)
Hybrid model					
Kirchhoff Ray Mode Approximation (KRM)	Simplified shape	Swimbladder and fish body	Not valid at high tilt angles and low frequencies, where ka<=1	Low computational requirements	Clay and Horne (1994)
DWBA and DFC	Axisymmetric (bent) shape	Swimbladder and fish body	Axisymmetric: with equals height	May represent relatively complex shapes	Gorska *et al*. (2005)
NUMERICAL MODELS					
Boundary Element Model (BEM)	Complex shape	Swimbladder and fish body		Not as computationally intensive as FEM	Chen and Scheikert (1963); Chertock (1964); Copley (1967); Okumura *et al*. (2003)
Finite Element Model (FEM)	Complex shape	Swimbladder and fish body	Computationally intensive. Requires a lot of computer memory at high frequencies.	Valid over wide range of frequencies, body shapes, tilt angles, and material properties	Berenger (1996); Ihlenburg (1998); Lilja *et al*. (2004); Zampolli *et al*. (2009)

5.4.3.2 Model input parameters

There are several parameters that are crucial to model-based classification, therefore the list below is not exhaustive. Some parameters (e.g. absorption) are frequency-specific. As the absorption coefficient strongly depends on acoustic frequency, any classification schemes based on the spectral characteristics of the organisms could be affected if the water absorption coefficients are incorrect. According to Doonan *et al*. (2003), commonly used estimates of acoustic absorptions in seawater (Francois and Garrison, 1982) are inaccurate above 200 kHz. Thus, variables based on frequency ratios, such as the relative frequency responses, *r(f)*, will vary with depth, and if those variables are used in target classification, the results may be incorrect. Models require input parameters based on what they are modelling. Different input parameters will affect different models in different ways.

- material properties: e.g. density, sound speed, viscosity, specific heat ratio, surface tension, conductivity
- biological/anatomical: e.g. bone, flesh, gas bearing vs. non-gas bearing, age, sex, maturity, life history
- morphology: e.g. geometric shape, i.e. length, height, and width (typically mean and standard deviation)
- physiology: e.g. fat content, ontogeny, stomach fullness
- behaviour: e.g. angle of orientation relative to the receiver (typically mean and standard deviation) often associated with diel vertical migration
- environmental: e.g. sound speed, density, salinity, temperature, depth, pH, absorption coefficient
- instrumental: e.g. transmit power, frequency, pulse duration, bandwidth

Material properties inside aquatic organisms will be inhomogeneous. Numerical models, such as finite element models, can handle such inhomogeneous material properties, but cannot realistically be used for classification due to computational demands. In such a scenario, a three-dimensional DWBA model can be used for weakly scattering objects (Jones *et al*., 2009).

5.4.4 Platform selection

Platform selection for echosounders should be based on: (i) cost, (ii) required temporal and/or spatial and/or vertical coverage, (iii) whether results need to be quantitative or qualitative, and (iv) additional ancillary data required for quality and validation (e.g. net samples, CTD data). Platform choice should minimize noise and interference and maximize coverage.

Echosounders were originally ship-borne, mounted on the hull, drop keel, or a pole (Sund, 1935; Simmonds and MacLennan, 2005), and were used to provide large spatial-scale surveys of fish and plankton distribution, within relatively synoptic time-scales (e.g. Hewitt *et al*., 2004). However, given the large temporal and geographic scales involved and the cost of research vessels, alternative means are being explored to collect data where possible (Greene *et al*., 2014). These include using echosounders on fishing vessels (Watkins and Brierley, 2016), autonomous underwater gliders (Guihen *et al*., 2014), and autonomous surface vehicles (Ghania *et al*., 2014; Greene *et al*., 2014).

Alternatively, when research questions require acoustic observations over long periods, moored instruments are now commonly used (Brierley *et al*., 2006; Urmy and Horne, 2016). The sample rate from moorings is typically constrained by the size of mooring and battery capacity, except where cabled observatories permit permanent operation (e.g. LoVe observatory, Godø *et al*., 2014; Venus observatory, Lemon *et al*., 2012).

Finally, platforms such as towed and lowered systems, remotely operated vehicles (ROVs), and autonomous underwater vehicles (AUVs) have been used to provide novel insights into target identification at depth (Kloser *et al*., 2002), vessel avoidance (Fernandes *et al*., 2000, 2003), and hard-to-reach locations such as undersea ice (Brierley *et al*., 2002). The resulting platform should minimize noise and interference and maximize the spatial and temporal coverage. Simmonds and MacLennan (2005) is a useful reference for using acoustics in fisheries science.

5.4.5 Survey design

Simmonds *et al*. (1992) deals with survey design. Simmonds and MacLennan (2005), Shotton and Bazigos (1984), and Jolly and Hampton (1990) are also useful documents for survey design.

The following topics should be considered when designing a survey:

- The key objectives of the survey (e.g. assessment of spawning-stock biomass would require a different survey design than determining *in situ* target strength).
- If the focus of the survey is acquisition of multifrequency data, ensure that the data are physically and spatially comparable (see Section 5.1).
- Consider a contingency plan in case of unforeseen circumstances (e.g. equipment malfunctions or bad weather).
- Consider an adaptive survey design which permits a degree of flexibility to reflect survey conditions (e.g. too much or too little time to complete survey objectives).
- Expertise and availability of personnel.
- Allocation of time to carry out pilot studies and equipment tests.
- Allowing enough time for calibration.
- Allowing enough time to collect validation data (e.g. biological samples using trawls).
- Time is usually the limiting factor.A vessel intercalibration can be performed when multiple vessels are used (see Simmonds and MacLennan, 2005, p. 326).

5.4.5.1 Survey design principle

Survey design is platform- and instrument-specific. It also depends on the survey objectives. One can, for example, classify echotraces to assess the marine organism biomass in a given area, study their spatial distribution, or analyse their temporal dynamics. Achieving each of these objectives will likely require different survey designs. Designing a survey consists of defining a sound cruise track and an efficient sampling strategy in order to make the best use of the time and resources available. Good references on survey design for acoustic biomass assessment include Simmonds *et al*. (1992) and Simmonds and MacLennan (2005). Although these provide guidance on how to design a single-frequency survey for fish biomass assessment, they are generally valid in the multifrequency context of this report. The following section builds on these references to provide a general overview of survey design best practice in the specific context of multifrequency target classification.

5.4.5.2 Procedure

Simmonds and MacLennan (2005) provide a general procedure to be worked through when designing a survey:

1. Defining the geographical area to be covered and the sampling strategy

   There are two main sampling strategies in the design of an acoustic survey: pre-planned or adaptive sampling. Pre-planned sampling involves predefining a fixed cruise track in the case of a mobile platform, or a predetermined sampling timetable in the case of a fixed observatory. Adaptive sampling allows the cruise track or the sampling rate to change according to observations made during a predefined outline survey. Results of acoustic target classification themselves can also be used to guide sampling during survey (see e.g. Case study 1 in Annex 1). When designing a survey, the first step is to decide whether to conduct pre-planned or adaptive sampling and, in the case of an adaptive strategy, to decide on the principles to be applied in adjusting the sampling coverage or rate and the data analysis methods.

   Survey limits can be predefined based on natural boundaries, knowledge of organisms' distribution, or a controlling variable (e.g. water depth or other habitat characteristics, Zwolinski *et al*., 2011). If the boundaries of the organism of interest distribution are unknown, using an adaptive strategy could be taken.

2. Estimating the resources

   With a moving platform, the density of sampling should be adjusted to optimize the limited sampling resources, i.e. principally platform time, but also the availability of trained crew or scientists to perform specific tasks. In the case of a platform such as a mooring or autonomous vehicle, limited energy supply and/or storage space may require adapting the sampling rate in order to capture the biological patterns of interest.

   If the final objective is to derive biomass estimates, the precision required can also define the density of sampling in space and time. . In the case of a moving platform, the spatial error made when using a specific survey track to assess the abundance of organisms can be estimated beforehand using geostatistics if quantitative information on the organisms' spatial distribution are available (Petitgas, 2001; Doray et al., 2008).

3. Calculating the time available for the survey

   Practitioners should calculate the amount of resources available for the actual survey, making due allowance for other activities such as fishing (Simmonds and MacLennan, 2005). All activities require time allocation, which must be carefully estimated beforehand: logistics, transit, calibration, trawl or camera sampling, hydrographic stations, and track running time. A schedule must be in place before the survey takes place.

   When planning to acquire multifrequency data for classification purposes, a specific consideration is adjusting the ping rate and/or vessel speed in order to optimize the sampling resolution in the along-ship direction and to plan eventual specific deployments (e.g. switching from hull-mounted to lowered or ROV-based echosounders). Dedicated time should be allocated for addressing classification specifically. Trawl and optical measurements should be performed as close as possible in space and time to the acoustic data collection. It is advisable to allocate survey time for conducting pilot studies and equipment tests.

4. Deciding on sampling strategy and cruise track

   In the case of a systematic survey conducted on a moving platform, practitioners choose between random or systematic survey tracks and then define the shape of the survey grid (triangular, rectangular, etc.). If estimating biomass is not a survey goal, running a random survey track is inadvisable, as it would increase transit time. If a map of the organisms' distribution is required, a random survey track would also generally provide suboptimal spatial coverage, compared to a systematic survey track designed to sample the area homogeneously.

   Common survey shapes include parallel (see e.g. case studies 2 and 5 in Annex 1), triangular (Simmonds *et al*., 1992) or star designs (Doray *et al*., 2008). Small-scale (~ 5 km) square tracks can also be surveyed repetitively to characterize diel dynamics and submesoscale behaviour of marine organisms using multifrequency acoustic data (e.g. Bertrand et al., 2008). Simmonds *et al*. (1992), Simmonds and Fryer (1996), and Simmonds and MacLennan (2005) extensively discuss the pros and cons of survey-track options and shapes for fish biomass assessment surveys.

   Adaptive surveys on a moving platform generally follow a predefined survey track whose shape can be adapted to concentrate efforts in areas with higher abundance or by reducing/removing effort in areas of low abundance (Simmonds and MacLennan, 2005). One can, for example, choose to (i) increase sampling intensity in high-density areas when they are encountered or after a preliminary scouting survey, or (ii) adjust the transect length to map the organism's distribution (Simmonds et al., 1992).

   In the case of a fixed platform, acoustic samples can be collected at regular (Kaartvedt *et al*., 2009; Urmy *et al*., 2012) and irregular (Doksæter *et al*., 2009) intervals or in an adaptive manner, depending on survey objectives, power supply, and data-storage limitations.

5. Adapting the sampling strategy to the survey area/time frame

   This step consists of drawing the calculated length of the cruise track on a map to ensure good spatial coverage when surveying on a mobile platform (Simmonds and MacLennan, 2005). If stratified sampling is required, the sampling intensities applied to the different regions of the map must be calculated to check that the survey track complies with the sampling strategy.

   In the case of a fixed platform, the acoustic sampling timetable must be fit into the deployment/survey time frame. The practitioner should also check that the sampling timetable is adequate to capture (or avoid) specific ecological processes known to occur at given times or frequency (i.e. diel vertical migration).

Annex 1 contains case studies (A1.1, A1.2, A1.3, A1.4 and A1.5) that contain a need for survey design.

5.5 Data acquisition

The physical and spatial characteristics, as discussed in Section 5.1, should be as similar as possible for detailed analysis of the acoustic data. While absolute comparability is impossible in all situations, we propose that ''ideal data'' are considered as a reference point with the purpose of co-analysis of data at multiple frequencies (Korneliussen *et al*., 2008). Acoustic data are defined as ''ideal'' in this context if data from several frequencies can be used to generate combined-frequency data at the same resolution as the original data. This requires measurements that are physically comparable (and of the same quality at all frequencies), that recordings are made simultaneously from identical volumes, and are limited only by the effective range of the higher frequencies. Therefore, it is proposed that the requirements outlined in Section 5.1 should be followed if ideal multifrequency or broadband acoustic data are to be obtained.

Different platforms may be used: ships (hull or drop keel mounted echosounders), moorings, towed bodies, gliders, or autonomous underwater vehicles. On vessels, transducers are typically mounted close together on the hull (mounted directly or on a blister) or drop keel (which can protrude more than 3 m below the hull). Transducers should be mounted as deep as possible to reduce the negative influence of unwanted surface signals caused by bad weather (i.e. wind- and wave-generated bubbles), but also shallow enough to include enough near-surface fish registrations. Transducers mounted on a 2.5 m retractable drop keel at the bottom of a 5 m deep ship hull may be only 0.5 m below the hull in good weather and 2.5 m in bad weather, i.e. 5.5 or 7.5 m below the sea surface, respectively.

5.6 Preprocessing

Good data analysis starts with good quality data (Figure 3.2). Although this is important with any data analysis, high quality data are essential with multifrequency classification (MFC) as algorithms could be applied indiscriminately on all biological targets rather than on a narrow subset of specific, preselected echoes. Standards of best practice for data acquisition should be followed (see Sections 5.4 and 5.5) to ensure optimal data quality and coherency among frequencies. However, if for whatever reason they are not or that uncontrollable factors compromise data quality, recorded artefacts or noise must be excluded from further analyses. To do so, the raw data are preprocessed through a quality-control filtering process, whereby unwanted data (mostly signals from non-biological scatterers or external sources such as nearby ships) are identified through manual scrutiny and/or by automated algorithms.

5.6.1 Unwanted data – noise

"Wanted" signals/data include all backscatter from intended or desired biological targets. Therefore, "unwanted" or bad data occurs when noise, unwanted signals, or other inadequacies are recorded in the data acquisition process (see Section 5.5) having both physical and biological origins (Table 5.2). Often bad data are associated with noise. Noise can be defined as uncorrelated interference or unwanted sound, i.e. a signal processed by the receiver that is independent of the generated ping. This can include internal noise, platform-related noise (e.g. machinery), or asynchronous electronic or acoustic interference (e.g. other echosounders). However, uncorrelated interference can also include signals with biological origins, such as whale clicks and fish vocalizations. Korneliussen (2000) defined noise as the opposite of wanted signal: "if the intended signal is defined as all transmitted sound backscattered onto the transducer surface, then noise is everything else". In the present context, unwanted signal is separate from noise. Unwanted signal is backscatter received by the transducer that is correlated with the transmit pulse, but originates from non-targeted objects. This is predominantly from physical entities (air bubbles, the seabed, sampling equipment such as CTDs, vertical nets, etc.) or from physical, data-logging artefacts (second echo from seabed, ringing, etc.) but may include non-targeted biological organisms such as marine mammals or certain zooplankton assemblages, for example. Determining what is noise and what is unwanted or non-targeted signals is important when deciding how to preprocess the data (e.g. zooplankton are unwanted signal in the context of analysing swimbladder-bearing fish).

Table 5.2. Classification of bad data.

Noise – uncorrelated interference		Unwanted signal* – correlated backscatter	
Physical	**Biological**	**Physical**	**Biological**
Asynchronous electronic and acoustic pulsed interference (other echosounders, pingers, ADCP, 60-Hz equipment crosstalk, etc.)	Biologically produced sounds (clicks, vocalizations, etc.)	Sampling equipment (profilers, vertical nets, etc.)	Non-targeted organisms (marine mammals, some zooplankton assemblages
Internal "self-noise"		Seabed and double seabed, side lobes	
Platform-related noise		Surface reverberation, ringing	
		Air bubbles (wind- or vessel-generated), gas plumes (seeps)	

* The definition of unwanted signal is subjective and dependent on the project objectives, although in most cases, signal from a physical source (other than the transducer used to both transmit and measure) will be unwanted.

5.6.2 Ambient noise and uncorrelated interference

5.6.2.1 Physical

Internal noise independent of the transmit pulse can be caused by the electronic circuitry of the sounder or the noise from other electronics that are not electrically isolated from the sounder. This is often referred to as ambient noise as it is amplified by the sounders time-varied gain (TVG) to produce coloured bands with depth range on the echogram.

Platform-related noise can also be called TVG noise because it also passes through the time-varied gain. However, this noise often varies over time or even from ping to ping. It includes broadband vessel- or platform-generated noise, e.g. flow noise, engine noise, generators, vibrations, etc., but also has an environmental component as it increases with wind and sea state.

Asynchronous electronic and acoustic pulsed interference is caused by uncorrelated signal produced by independent transmitting equipment such as other echosounders, pingers, ADCPs, AC equipment crosstalk, etc. that have not been synchronized to the master sounder and, therefore, produce incoherent pulsed signals that are processed by the receiver. These received signals are not necessarily from the main pulse of the offending instrument, but can originate in one of the generated harmonics.

5.6.2.2 Biological

Although considerably less common than the other types of uncorrelated interference, biologically produced sounds such as clicks, e.g. sperm whales and shrimp, and vocalizations, e.g. fish and seals, can produce interference on echograms, depending on the context.

5.6.3 Unwanted signal or backscatter correlated with transmit pulse

5.6.3.1 Physical

Not all unwanted signals are strictly speaking noise, as they may be backscatter from unwanted targets such as bubbles and are therefore correlated with the transmit pulse. Ringing, caused by the transceiver picking up the transmit pulse directly or after it has bounced around the installation casing, limits what can be detected within a couple of metres of the transducer. This reverberation usually dissipates within a fixed range from the transducer and is transducer-dependent (pulse duration, power setting, etc.). Ringing can usually be mitigated by applying absorbing material behind the transducer. For horizontally oriented transducers in sonars, backscatter from surface is also undesired

Another common source of surface-related, unwanted signal is wind-generated air bubbles. As wind and sea state increase, air bubbles are generated at the air–sea interface and are exacerbated by the pitching of the vessel. As these bubbles are entrained below the vessel over the transducer faces (bubble sweep-down), large echo returns are produced. Furthermore, as the bubble layer increases with windspeed and sea state, significant signal attenuation can affect the acoustic return (Novarini and Bruno, 1982) which, in the extreme, can block out the transmitted signal completely.

During surveys, non-biological backscatter can be recorded from sampling equipment suspended below the vessel, e.g. profilers, vertical nets, etc. In addition, rising gas plumes (seeps) can be quite common when surveying methane-laden seabeds, and at times difficult to distinguish from schools of swimbladdered fish.

Of course, the dominant backscatter of physical origin in acoustic data comes from the seabed. Although automatic seabed-detection algorithms are quite effective for removing the seabed echo from further analyses, the occasional unwanted seabed detection can occur. However, missed seabed detections will result in large anomalies in the cumulative echo integration of the water column and can therefore be easily identified and corrected.

Other seabed related issues include alias seabed echoes, which can occur above the true seabed and, therefore, be misidentified as biological in nature. A false seabed can occur when the ping rate is too fast, resulting in the residual echo from the previous ping being recorded during the subsequent ping-recording interval (Tomczak *et al.*, 2002). These conditions are exacerbated with seabed depth and hardness. The alias seabed appears as a scattering layer in midwater, however it can easily be identified as it mimics the form of the true seabed.

A false seabed can also occur when an echo is produced from a side lobe along a cliff face or regions of highly fluctuating seabed depths. Given that the side lobe echo arrives from a shorter range than the true seabed beneath the vessel, the false seabed will appear as a biological scattering layer, although this time close to the true seabed.

5.6.3.2 Biological

Unwanted signal can also include non-targeted biological backscatter. These unwanted signals can be caused by large unknown objects, which produce significant backscatter anomalies but are not from a physical or inanimate source. The most common large unknown objects are marine mammals, e.g. whales and seals, although turtles and large fish such as tuna will produce similar anomalies. These objects can often be detected by isolating them using a low-pass threshold or data spike check.

Non-targeted biological backscatter can also mean weaker echoes such as plankton scattering layers when one is interested in fish echoes, which are most commonly removed with a high-pass threshold.

5.6.4 Data processing prior to classification

Data editing the removal of unwanted signals, either via manual or algorithm-based methods. Once the echoes from noise and unwanted signals have been identified, they must then be excluded from further processing through data editing. The preferred method to eliminate unwanted signal is to classify it as "bad" or "missing" data. It is important to emphasize that these data should be treated as missing, i.e. that these data should not (i) be interpolated or averaged between adjacent data cells or (ii) be replaced by zeros.

There are cleaning and filtering algorithms that can be applied automatically, such as for internal "self-noise" removal. The simplest method for filtering TVG noise is with a time-varied threshold (TVT). This will eliminate all noise below the TVG-amplified threshold which can be estimated by recording in passive mode (receiving, but not transmitting) and fitting a regression to the noise curve. However, a TVT is difficult to implement if that threshold is changing over time (e.g. due to changes in ship speed or bottom depth). In addition, since noise and signal are additive, self-noise should be subtracted from the signal, not thresholded, especially in a situation of low signal-to-noise ratio (r_{sn}). Therefore, several methods of estimating and subtracting self-noise have been developed (see Watkins and Brierley, 1996; Korneliussen, 2000; De Robertis and Higginbottom, 2007; McQuinn *et al*., 2013).

The r_{sn} needs to be sufficiently high for the relative frequency response $r(f)$ to be reliable. Generally, noise is stochastic with a non-symmetric probability density function (pdf). Resampling to a lower resolution will reduce stochastic noise, but will also reduce the spatial resolution; thus, if data are going to be smoothed, that should be done prior to noise removal. In practice, an r_{sn} in the range of 6–10 should be sufficient for measurements of volume scattering, depending on the degree of averaging used (less for heavy smoothing).

Most methods that quantify noise rely on empirically estimating the self-noise profile,using the background or minimum noise level once the TVG function has been removed, and applying a buffer to the fitted relationship associated with either the r_{sn} (e.g Korneliussen, 2000; De Robertis and Higginbottom, 2007) or the error distribution of the noise values around the mean response (e.g. McQuinn *et al*., 2013). An alternate method, which is not widely implemented in instruments used in fisheries acoustics, would be to switch between active and passive modes, i.e. pause transmitting and estimate passive noise via passive listening after a given number of transmissions.

Surface reverberation, ringing, and the bubble layer can easily be removed by automatically blanking a fixed range from the transducer face. This blanking range will vary as reverberation and ringing are transducer-dependent, i.e. depending on installation and transmit configuration. However, special attention is required when removing the bubble layer as it increases with sea state, and bubbles can produce very strong echoes and attenuation of the acoustic signal. Bubble layers can be detected either through visual scrutinization or with a low-pass threshold detector. When editing data collected in rough weather, significantly attenuated pings should be classified as bad data.

Seabed detection and removal should be carried out with automatic algorithms, followed by manual verification and correction if needed. In most situations, automatic seabed detection algorithms are efficient. However, quickly shifting seabed depths from irregular seabeds and fish aggregations close to or on the seabed may introduce errors that need to be edited manually. As a first filter, applying a small backstep of 0.5–1.0 m above the detected seabed is usually sufficient to remove most seabed signals left in the integrated water column. However, in situations with fast-rising slopes or where the seabed has been missed completely, a check for data spikes will most often identify any seabed echoes that are still above the detected seabed, which can then be corrected manually. Specifically, for MFC, using the average of bottom channels may be helpful. Thus, all detected seabed depths should be synchronized among channels to avoid unequal bin sizes between channels close to the seabed. Unequal bin sizes will result in comparing unequal sample volumes, giving erroneous frequency responses.

Side-lobe echoes can be mistaken for biological layers near the seabed and are difficult to detect automatically. When surveying in areas with fast-rising slopes or when running transect lines parallel with cliff faces, echograms should be scrutinized for so-called false seabeds or "second bottom echoes" (i.e. a multipath seabed signal from the previous ping appearing in the water column) which should then be classified as unwanted data.

5.6.5 Data averaging

Small-scale acoustic data are inherently highly variable. Attempts to classify data at the resolution of the echosounder's sampling resolution are unlikely to be effective as variability of classifiers from different scatters are likely to overlap. The data should be vertically and temporally averaged or smoothed to reduce variability prior to classification, although as little as possible to keep high spatial resolution. Averaging samples reduces random variability of measurements of relative frequency response and minimizes biases introduced by differences in the volume sampled at the different frequencies (Korneliussen and Ona, 2002). If transducers are not colocated, a first-order correction can be made prior to averaging by shifting the data in time to correspond as closely as possible to the spatial location sampled by the other frequencies (Demer *et al.*, 1999; Conti *et al.*, 2005; Korneliussen *et al.*, 2008). Thus, selection of an appropriate scale of spatial averaging (i.e. smoothing) is a central consideration in many methods of backscatter classification. Note that data samples below a specified threshold should not be set to zero prior to averaging (Korneliussen, 2000; Fernandes *et al.*, 2006).

The choice of analysis cell size represents a trade-off between decreasing variability of the observed relative frequency response and minimizing violations of the assumption that backscatter is dominated by a single organism. At the same time, relatively fine-scale averaging is desirable to minimize the extent to which backscatter from multiple taxa will be observed in a single analysis cell (Demer *et al.*, 2009). Either very low or very high levels of averaging are likely to yield poor results. The affect of averaging on variance can be evaluated via a sensitivity analysis (e.g. Gorska *et al.*, 2005, 2007; De Robertis *et al.*, 2010), but understanding the degree to which different types of scatterers will overlap in analysis cells of a given size remains a challenge as this will change over space and time. Conducting analyses of the sensitivity of classification results to data averaging is recommended.

Classifications can be improved in cases where organisms form well-defined mono-specific aggregations by preclassifying fish aggregations and combining all samples in an aggregation prior to multifrequency analysis to maximize the degree of averaging (Fernandes, 2009; Korneliussen *et al.*, 2009, 2016). In addition, combining preclassification at a fine spatial resolution to remove samples that are inconsistent with the taxon of interest, followed by classification based on the relative frequency response in spatially averaged analysis cells (Demer *et al*., 2009), or classifying pixels based on the classification results of their neighbours (De Robertis *et al*., 2010; Korneliussen *et al*., 2016) are promising approaches as they may allow for averaging of many samples, while minimizing the degree to which backscatter from different types of scatterers will be averaged together.

6 Approaches to multifrequency target classification

Models and measurements are dependent on each other. Scattering models must be verified by measurements, and measurements not described by current scattering models require new or improved models to be developed. A model should be complex enough to approximate the real world, but simple enough to apply. In general, models need to be supported through measurements to have confidence that they are consistent with our understanding of the physical world. In fisheries acoustics, scattering models are needed to understand empirical backscatter and translate observed patterns into viable biological densities.

Both modelling and empirical techniques are used to classify acoustic targets. Theoretical and numerical scattering models are used to understand how sound interacts with biology to reflect energy and to aid in the classification of aquatic organisms. Representation of aquatic organisms in scattering models began with geometric shapes, e.g. bubbles (Anderson, 1950) and evolved to direct representations of bodies and scattering inclusions, e.g. swimbladders in fish (Clay and Horne, 1994) and invertebrates, e.g. zooplankton (Chu *et al*., 1993) and cephalopods (Lee *et al*., 2012). For target classification, model predictions may be extracted from a particular scattering region, e.g. resonance or from amplitude differences among multiple frequencies (see Section 4).

The advantages of using a model-based approach instead of an empirical approach to classify backscatter include: (a) permitting the validation and theoretical interpretation of the empirical approach; (b) allowing the performance of emulations and simulations with controlled input parameters and variables to assess the efficiency, effectiveness, robustness, and uniqueness of the classification; and (c) extending the classification (frequency) ranges to those beyond measurements that are achievable with current technologies.

Although an empirically approach to classification is based on some *á priori* knowledge of scattering properties, it primarily relies on comparison of observed patterns of relative frequency response to some known monospecific scatterers at a set of given biological and physical conditions measured with a defined set of instrument settings. It may be possible to classify scatterers where the scattering properties are not fully understood, but where the species and their behaviour (e.g. spawning migration, feeding migration, wintering, etc.) are known. A major challenge to the empirical description of scattering properties is access to measurements of monospecific registrations with similar behaviour as the one being investigated. Although monospecific aggregations are used to extract scattering properties such as the relative frequency responses, the latter may not be sufficiently unique to acoustically differentiate species (e.g. echoes from herring vs. sardine).

Thus, a combined use of scattering models and measured backscatter with verified origin is the ideal scenario and an important step towards a reduction in the overall uncertainty of the final density estimates.

There are a range of classification methods that can be used either alone or in combination with multifrequency methods. Statistical descriptions of ensemble echo envelopes and image-analysis techniques have been used to characterize and classify acoustic targets. If aggregations of a species have unique shapes or sizes, then constituent species may be identified based on metrics derived from time-dependent amplitudes (i.e. echo envelopes) that describe the aggregations (e.g. Rose and Leggett, 1988). This approach has been applied to pixels in echograms (e.g. Nero and Magnuson, 1989; Scalabrin *et al*.,

1994) and extended to characterize pelagic fish aggregations (e.g. Barange, 1994; Coetzee, 2000).

Individual echo and aggregation descriptors have been used, often in conjunction with physical variables, as input to multivariate statistic techniques to classify targets. Discriminant function analysis (e.g. Rose and Leggett, 1988), cluster analysis (Weill *et al.*, 1993; Campanella and Taylor, 2016; Gastauer *et al.*, 2017a), and ordination techniques such as principle components analysis (e.g. Scalabrin *et al.*, 1994) are the most common tools used to classify fish species. An extension of the use of statistical descriptors is to use them as input to artificial neural networks, which have been used to classify anchovy (*Engraulis encrasicolus*), sardine (*Sardina pilchardus*), and horse mackerel (*Trachurus trachurus*) aggregations (e.g. Haralabous and Georgakarakos, 1996).

The availability of machine-learning techniques has led to additional acoustic target classification approaches, which can include probability-based classification of targets. Supervised classification uses validation samples to predict known species classes (e.g. Fernandes, 2009; Korneliussen *et al.*, 2009; De Robertis *et al.*, 2010). Unsupervised classification does not use validation samples, and the number of classes is not specified (e.g. Anderson *et al.*, 2007a, 2007b; Campanella and Taylor, 2016; Gastauer *et al.*, 2017a). A hybrid approach (semi-supervised learning) allows large datasets to be classified if validation samples from known classes are contained in the data (e.g. Woillez *et al.*, 2012).

6.1 Target classification based on scattering models

6.1.1 Theoretical basis for classification

In contrast to the empirical approach to target classification (Section 6.2), which can be very effective under certain circumstances, the model-based approach requires knowledge of both the data and the physical mechanisms from which the data are produced. Here, the word model represents the acoustic scattering by targets. Target backscattering is mostly monostatic (i.e. same source and receiver) but can be bistatic (different source and receiver).

Holliday (1972) combined model predictions with empirical measurements and samples to demonstrate that resonant peaks corresponded to distinct organism sizes. This logic was extended to the identification of fish species using maximum target strengths. Over the next decade, classification of fish targets to species was aligned with maximum observed target strengths. Unfortunately, two implicit assumptions were not appropriate to this extension:

1. that a maximum peak would also occur at the frequencies commonly used in fisheries acoustics (i.e. geometric scattering frequencies where ka or $L/\lambda > 1$), and,
2. that intraspecies maximum target strengths variability was low relative to species variability.

Non-unique and highly variable echo amplitudes of acoustic targets within the geometric scattering region negate the use of maximum target strength as a target classifier. While maximum backscatter amplitudes may separate acoustically large targets from smaller targets (e.g. predators and prey), stochastic variability of backscatter amplitudes (from individual organisms due to orientation or among morphologically similar species due to differences in material properties) reduces the utility of this approach.

6.1.2 Inversion – using scattering models in classification

Inversion is similar to the approach described by Fernandes *et al*. (Chapter 6 in Fernandes *et al*., 2006). The purpose of an inversion algorithm is to fit the gathered volume backscatter coefficients for multiple frequencies to analytical plankton backscatter models. The data are fit to each scattering model by the non-negative least-squares algorithm (Lawson and Hanson, 1974). The model with the smallest residual is selected as the best-fit model if the residual is smaller than a configurable maximal residual. A cost function corresponding to the k[th] model (organism) can be formulated as (Tarantola, 2005; Menke, 2012):

$$Q_k = \sum_{i=1}^{N} \left[d_i - f_i^{(k)}(\mathbf{m}_k) \right]^2 \qquad k = 1,2,\dots,K \tag{1}$$

where K is the number of models under consideration, N is the number of discrete data such as the number of frequencies, d_i is the i[th] datum, $f_i^{(k)}(\mathbf{m}_k)$ is the theoretical model (linear or non-linear) for the k[th] organism with a feature or parameter vector, $\mathbf{m}_k$, corresponding to the i[th] datum. In our applications, d_i is the measured acoustic quantity ($S_v, TS, s_v, \sigma_{bs}$, etc.) at the i[th] frequency. Our task is to find the model that minimizes the cost function Q_k:

$$\min_k (Q_k) \Rightarrow f^{(k)}(\mathbf{m}_k) \tag{2}$$

In the implementation originally described by Holliday (1977) and Holliday *et al*. (1989), the inversion is performed with a given size vector chosen by the user. The size vector contains assumed sizes for the zooplankton specimens. Often there is a desire to estimate more sizes than the available number of acoustic frequencies, i.e. the problem is underdetermination (i.e. the ratio "number of unknowns"/"number of measurements"). In Fernandes *et al*. (2006), an iterative optimization of the size vector was proposed; after a first estimate of the size distribution of the scatterers, the size vector is redistributed. The purpose of the optimization is to redistribute the size vector around the sizes where non-null abundance has been found. The number of sizes in the size vector is kept constant. If the number of sizes is not a multiple of non-null elements, the elements with the smallest size are divided first. This method helped Mair *et al*. (2005) in the interpretation of particularly strong acoustic scattering layers at 38 kHz in the northern North Sea in summer; it suggested the contribution of gas-filled gas-including organisms, which were not sampled by nets. It has also been successfully applied by Korneliussen *et al.* (2009) on pure krill concentrations, resulting in an estimate close to the mean length of organisms. In this case, the species and the appropriate model to use were both known, therefore only the sizes were anticipated. Cox *et al*. (2013) applied this to a more complex situation where the type of organisms, the sizes, and the abundance were unknown. In this case, the inversion supports the existence of an expected north–south change in the population, but does not reach a satisfactory classification of organisms. At this scale, dealing with the volumes of mixed populations sampled, classification is challenging, as is biological ground-truthing because dominant organisms in a net are rarely the dominant acoustic scatterers. Pearlside (*Maurolicus muelleri*) is an example of this: it dominates the acoustic backscatter as it feeds on the krill that dominates the biomass.

Simple inversions that have been previously performed in more focused situations are more likely to succeed (Trevorrow *et al*., 2005; Lavery *et al*., 2007), but require prior conditions for the processed data, e.g. to work on a sample where a known scatterer dominates the scattering for all the frequencies considered in the inversion.

Case study 2 in Annex 1 applies a related method to determine organism size for krill.

6.2 Empirical approach to classification

6.2.1 Frequency-dependent scattering – relative frequency response

The frequency dependence of acoustic targets (Section 3.4) is a key characteristic used in categorization. There is often clear frequency-dependent scattering in backscatter data (e.g. Figure 6.1), and this can be used as the basis for classification.

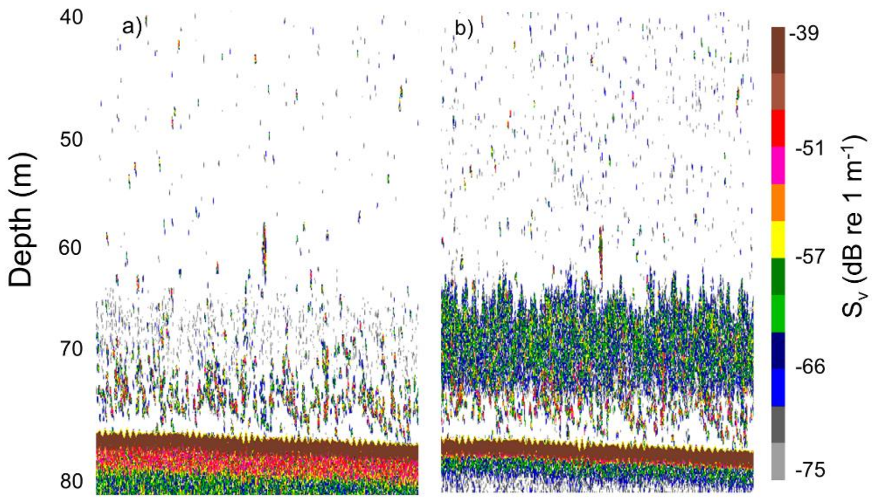

Figure 6.1. Example of frequency-dependent backscatter from fish and zooplankton. a) 38-kHz echogram showing backscatter from fish. b) 120-kHz echogram showing backscatter from fish as well as a band of zooplankton backscatter between 65 and 75 m which is not evident at 38 kHz.

This frequency dependence is typically characterized by normalizing the observed backscatter to a reference frequency (by convention often 38 kHz, Korneliussen and Ona, 2002; Korneliussen *et al*., 2016). In linear terms, the relative frequency response *r(f)* of volume backscattering coefficients measured at two frequencies (f_1, f_2) is defined in Table 2.1 for both volume scatterers and single targets. The key advantage of using a ratio for classification over other metrics, based on absolute volume backscatter, is that the frequency ratio depends only on the frequency-dependent properties of the targets rather than their absolute abundance.

A variety of equivalent terms has been used to describe the relative frequency response in the literature (Korneliussen and Ona, 2002; Pedersen and Korneliussen, 2009; McQuinn *et a*l., 2013). For example, $R(f) = \log_{10}[r(f)]$ is sometimes referred to as a "dB-difference" and can be expressed as follows for volume scattering:

$$R(f) = \log_{10}[r(f)] = S_v(f_1) - S_v(f_2) = \Delta MVBS_{f_1-f_2} = \langle TS(f_1)\rangle - \langle TS(f_2)\rangle \tag{3}$$

In practice, the measurement of *r(f)* can be limited by noise, as the targets must be observed at all frequencies in overlapping beams and with a significantly high r_{sn} to allow *r(f)*. At low r_{sn} (i.e. long ranges, weak scatterers, frequencies with low *r(f)*), the effects of noise will bias the estimates of *r(f)*.

Methods for acoustic target classification based on *r(f)* are described in increasing complexity in the following sections.

6.2.1.1 Manual categorization

Manual data scrutiny typically starts with excluding unwanted areas (e.g. transit between transects, trawl, and CTD stations) followed by the removal of unwanted backscatter (e.g. bottom echoes and noise spikes). Operators then identify and select regions with similar acoustic properties. The subjective analyst scrutiny may be supported by objective information e.g. relative frequency response, *r(f)*, including resonance peaks. Furthermore, some fish species typically appear as single individuals, while other species are usually seen in schools, layers, or loose aggregations at certain times and locations. Geographical location, distance to sea surface, and distance to seabed are also used to support the species identification process. The mean *r(f)* and the scattering coefficient (s_A) of an encircled region (e.g. a fish aggregation) are often efficient at differentiating between species, especially when those species form single-species aggregations. Sometimes *r(f)* and (s_A) are efficient at partitioning the total s_A of that region between different species. The scrutiny of acoustic backscatter is supported by results of directed biological samples when available (see Section 5.4.2 for description of sampling methods). During manual categorization, the measured *r(f)* in each volume may be compared to a reference of *r(f)* of known scatterers, thereby making the categorization process more objective and aiding the interpretation of the echogram.

If several species are present in the same volume, the resulting *r(f)* will be the sum of the individual species *r(f)*. The composite total *r(f)* may, in this case, be less useful for characterizing weak scattering species as the *r(f)* of weaker scatterers may be masked by stronger ones or the global *r(f)* will not resemble any single-species *r(f)*. Increasing the resolution of echosounders, reducing the degree of averaging used (Section 5.6.5), or decreasing the observation distances can help to reduce sampling volume and improve target classification.

Case studies 3 and 4 compare manual categorization to categorization based on an acoustic feature library. (See Annex 1).

6.2.1.2 Automatic use of frequency-dependent backscatter

The volume backscatter relative frequency response has successfully been applied to assign species of zooplankton and fish where the species being studied are in homogeneous aggregations of a relatively uniform size class. Examples of this are krill in the Antarctic (Brierley *et al*., 1998) and eastern Canada (McQuinn *et al*., 2013), the deep-water orange roughy (*Hoplostethus atlanticus*; Kloser *et al*., 2002), and herring (*Clupea harengus*), mackerel (*Scomber scombrus*), and capelin (*Mallotus villosus*) in the North Sea and the Barents Sea (Korneliussen and Ona, 2002, 2003; Fernandes *et al*., 2006; Korneliussen *et al*., 2009). The assignment of species is often supported with empirical data based on multiple lines of evidence including trawl catch, behaviour, optical verification, and target strength (e.g. Fernandes *et al*., 2006, 2016; McQuinn *et al*., 2013; Ryan and Kloser, 2016) or knowledge of the model scattering characteristics of the species (Fernandes *et al*., 2006; Kloser *et al*., 2002). The relative frequency response method works best when there are large differences (e.g. > ca. 3 dB) in the species groups being discriminated either due to size (Raleigh, resonance and geometric scattering regions – Figure 3.1) or different composition (e.g. fluid-filled and gas-bladder organisms). Resonance scattering is often used to distinguish species or size classes of species that possess gas bladders at various depths (e.g. Kloser *et al*., 2002).

There has been a long history of using resonance scattering volume reverberation methods to estimate the average size of the species gas-bladder by comparing the frequency response, using broadband with low- and high- frequency ranges as well as using several discrete frequencies, to a scattering model (Andreeva, 1964; Holliday, 1972; Kalish *et al*., 1986; Stanton *et al*., 2010). These volume reverberation methods are range limited due to sound absorption at higher frequencies (Francois and Garrison, 1982) and due to spherical spreading increasing the ensonified volume. A large ensonified volume creates classification uncertainty by increases the number of potential scatterers of different species and sizes. These range dependent effects can be minimized using deeply towing systems (Kloser *et al*., 2002). To avoid multi-scatterer volume reverberation classification errors single target frequency response methods can be used (Demer *et al*., 1999; Conti *et al*., 2005). These methods generally require a profiling probe to ensure one target is detected within the ensonified beam. Using lowered probes it is possible to obtain an individual frequency response for an organisms with optical verification (e.g. Kloser *et al*., 2016).

6.2.1.3 Objective categorization using reference libraries

An acoustic reference library is one that contains measured scattering properties originating in known species. It could be a set of measured relative frequency responses used for reference during manual scrutiny or it could be a digital reference of acoustic data that is automatically or semi-automatically compared with the digital acoustic data being scrutinized.

The Bergen echo integrator (BEI; Foote *et al*., 1991; Korneliussen, 2010) began by allowing observations to be compared with a library of relative frequency responses of known scatterers during manual scrutiny and then evolved such that those results of automatic categorization (species identification) were available during scrutiny (Korneliussen and Ona, 2002, 2003). Data from multifrequency echosounders working simultaneously with nearly identical and overlapping acoustic beams are processed stepwise in a modular sequence. This is to remove noise and bad data and to average data. Similarly, data from wideband echosounders could be converted to multifrequency data and processed in the same way as multifrequency data. In later systems, data were processed in a similar manner, e.g. by Korneliussen *et al*. (2009) and using Z-score in De Robertis *et al*. (2010).

Case study 3 in Annex 1 details a relatively simple application of this approach where species classification during acoustic surveys in Alaska were based on the mean and standard deviation of trawl ground-truthed frequency response.

6.2.1.4 Library of statistical features of acoustic variables from known species

The overall approach of this method is to extract statistical descriptors of acoustic variables from a known target and store them in a library. The descriptors are used to classify new targets based on their similarity to taxa in the library. Prior to extracting features into a library, data should be processed as described above (Section 6.2.1.3) to remove noise and bad data and to average data. This should be done in a standardized mannerto ensure data in a library containingstatistical properties of acoustical variables are as comparable as possible. Statistical properties of acoustical variables based on measured backscatter from known species, such as relative frequency responses and s_v, can then be extracted from these high-quality data and stored in a reference library.

Other variables such as geographical position, temperature, and depth can also be contained in a library. More sophisticated implementations of an acoustic library have the potential to work well in more challenging situations.

One procedure of extracting such statistical properties is described in Figure 4 in Korneliussen *et al*. (2016). The driving idea, to be able to extract features that are later used to distinguish species in unknown data, is quite general, however, and is not connected to any software.

Case study 4 in Annex 1 uses a library containing statistical properties of acoustical variables.

6.3 Machine learning methods

Machine learning techniques can be classified in supervised and unsupervised algorithms. Supervised algorithms include a known response variable that acts as "teacher" for the algorithm. The most commonly used techniques are described in the subsections below. Principal component analysis, clustering (e.g. K-means), neural networks (e.g. self-organizing maps; Kohonen, 1982; Peña *et al*., 2008), and other topology-preserving mappings (Peña, 2007) are the most used unsupervised techniques.

If ground-truth data are reliable, then supervised classification methods are the preferred approach. However, target classification can be problematic in areas with many species and where the collection of ground-truth data is limited or unreliable: unsupervised classification techniques can be helpful in this case. With unsupervised learning, the data do not have class attributes *a priori* and the classification is based on the intrinsic characteristics of the data. The assumption behind this approach is that the groups of aggregations/schools identified by the classification correspond to biologically meaningful structures that can be related, for example, to morphological and/or behavioural similarity between species. Unless the species investigated have very different patterns, it is unlikely that this method could identify groups at a high taxonomic level, but it can provide useful information on a broader scale (e.g. family, functional groups, guilds).

Machine learning techniques can be applied at the school level, and a large list of features describing the characteristics of the aggregations can be used in the classification process. Metrics describing the energetic and geometric properties and multifrequency response of schools are the most common categories of variables used for this purpose, and thorough description of these can be found in the literature (Nero and Magnuson, 1989; Scalabrin and Massè, 1993; Haralabous and Georgarakos, 1996; Reid, 2000; Korneliussen *et al*., 2009).

6.3.1 Supervised

6.3.1.1 Feed forward neural networks

Artificial neural networks (ANN) are a family of statistical models that mimic the design of biological neural networks, such as the human brain. ANNs can recognize patterns and learn from their interactions with the environment. Every connection between the nodes (or neurons) is referred to as "weight", with all connections being iterative: "feed forward" means that information is transferred from the previous to the next layer. Different forms of ANNs exist, but the most commonly used ones are multilayer feed-forward networks (Rumelhart *et al*., 1986), which are supervised methods. "Learning"' or "training" is achieved through an iterative process where a fraction of the validation information is used for training and the remaining fraction is used for testing. A cross-validation process is often used to maintain equal representation of the labelled information for both training and validation. During the iteration, the detected error is propagated backwards through the network to adjust weights to decrease the error. Once the training is achieved, the feed-forward structure is used for the classification of the entire dataset.

One of the main advantages of ANNs is their capacity to account for non-linear relationships between input and outputs, which make it an effective classification method. ANNs are effective when dealing with extreme values, as their affect is minimized (Lek *et al*., 1996). On the other hand, ANNs have been recognized as a "black box'', due to a lack of information regarding the relative influence of the metrics used as input for the classification (Olden and Jackson, 2002).

ANNs are mainly applied to categorized acoustic data based on echotrace characteristics (Ramani and Patrick, 1992; Haralabous and Georgakarakos, 1996; Cabreira *et al*., 2009), but also based on multifrequency data (Simmonds *et al*., 1996).

6.3.1.2 Random forests

Random forests are a machine-learning method for data classification or regression analysis (Breiman, 2001). Random-forest classification (or "walks") grow a multitude of classification decision trees during the training process, outputting the mode of the classes (classification, discrete values) or the mean prediction (regression, continuous values). The main strengths of random forests include their ability to run efficiently over large datasets. This allows for large numbers (e.g. thousands) of input variables without variable deletion, and the results provide an overview of the importance or influence of the different variables to the final classification (Breiman, 2001). It provides an in-built quality check as an alternative to cross-validation checks. The error (uncertainty) is computed as each tree is constructed using a different bootstrap sample from the original data.

With a few exceptions, random forests have seldom been used in classification of multifrequency fisheries acoustics data. Fallon *et al*. (2016) used random forests to classify krill (Euphausia superba), icefish (Champsocephalus gunnari), and mixed aggregations of weakly scattering fish with 95% accuracy. Antona (2016) used Breiman's random forests to classify herring, sprat (*Sprattus sprattus*), and Norway pout (*Trisopterus esmarkii*) based on broadband acoustic data collected with Simrad EK80 echosounders operating at six frequencies (18, 38, 70, 120, 200, and 333 kHz). In their study, the accuracy of the random forests improved with the inclusion of auxiliary data (e.g. latitude, longitude, and depth). Lefort *et al*. (2012) used random forests as a classification tool for characterizing pelagic fish schools from data collected with single-beam (two-dimensional) and multibeam (three-dimensional) sonar images.

Single classification or regression trees (a variant of decision trees; Breiman *et al*., 1984) are suitable for analyses of ecological data (De'ath and Fabricius, 2000) and have been used as such (De'ath, 2007). However, despite their suitability for use with active-acoustic data, few studies have applied these methods. Fernandes (2009) identified species based on multifrequency acoustic data using classification trees; however, the presented methods are more prone to overfitting and hence have comparatively poor predictive performance. At the same time, they have the advantage of being intuitive (Fernandes, 2009).

6.3.2 Unsupervised

6.3.2.1 Multivariate ordination in reduced space

Multivariate ordination methods are commonly used in numerical ecology and can reveal the major variance trends contained in multifrequency data. Ordination methods project the scatter of objects (e.g. acoustic elementary sampling volumes) in a multidimensional (e.g. multifrequency) diagram onto two-dimensional bivariate graphs (biplots). The axes (or components) of these graphs are chosen to represent a large fraction of the variability of the multidimensional data matrix in a space with reduced (i.e. lower) dimensionality relative to the original dataset. Methods for ordination in reduced space also allow one to derive quantitative information on the quality of the projections and study the relationships among descriptors as well as among objects (Legendre and Legendre, 2012).

Principal component analysis (PCA) is the most commonly used ordination technique in reduced space; however, it is limited to quantitative descriptors.

Doray *et al*. (2009) applied PCA on s_A profiles at 38 and 120 kHz to identify the principal components of micronektonic sound-scattering layers observed at moored fishing aggregation devices at a vertical resolution of 10 m depth. Other commonly used multivariate ordination methods include (i) correspondence analysis (CA) to analyse presence/absence or zero-inflated data and (ii) principal coordinate analysis (metric scaling, PCoA) or nonmetric multidimensional scaling (nMDS) to handle quantitative, semiquantitative, qualitative, or mixed descriptors (Legendre and Legendre, 2012). Borcard *et al.* (2011) show how to carry out calculations for the methods described in Legendre and Legendre (2012) using the programming language of R (R Core Team, 2016). Campanella and Taylor (2016) and Gastauer *et al*. (2017a) classified acoustically detected schools by applying a clustering algorithm on multifrequency descriptors of the fish schools and plotted the clustering results on a PCA biplot derived from the same dataset.

6.3.2.2 Clustering

Clustering is an unsupervised multivariate approach that partitions the data into a set of clusters based on a collection of objects or descriptors (Legendre and Legendre, 2012). Clustering is classically performed on association matrices, which describe the similarity or dissimilarity between the different objects. Legendre and Legendre (2012) provide an extensive description of the clustering methods principles and algorithms that are used in numerical ecology.

The most commonly used clustering methods are k-means (MacQueen, 1967), methods, and derivatives thereof (Kondo *et al*., 2012). K-means partitions the data into a predetermined number of clusters. The goal of this method is to minimize the total intracluster variance (the squared error function) or to reduce dissimilarity within groups typically assessed through Euclidean distance measures. K-means is a relatively efficient method but has several drawbacks that need considering. First, choosing the number of clusters must be done *a priori*, which can be problematic especially if little is known about the expected number of clusters. The most objective way to determine the ideal number of clusters is through an iterative approach. The most common approaches used are based on the evaluation of the "quality" of the clustering using different types or a combination of internal indices (sum of squared error, silhouette, gap statistics) and external indices (e.g. Rand index, entropy; Rand, 1971; Rouesseeuw, 1987; Jain and Dubes, 1988; Tibshirani *et al*., 2001; Handl *et al*., 2005; Theodoridis and Koutroubas, 2008). Another approach is the "Clest" algorithm which is a prediction-based resampling method (Dudoit and Fridlyand, 2002; Kondo *et al*., 2012; Campanella and Taylor, 2016; Gastauer *et al*., 2017a). The algorithm selects the optimal number of clusters based on the evaluation of the predictive power of the classification using a set of validation datasets iteratively selected randomly from the original dataset, similar to bootstrapping methods. To address uncertainty in the number of clusters, expectation maximization (EM) for finite mixture models (Dempster *et al*., 1977) can identify the probability of a given data point belonging to a given group (e.g. Anderson *et al*., 2007b). Cluster metrics (e.g. Bayesian information criterion, Schwarz, 1978) can assess the fit of clusters to data (Fraley and Raftery, 1998) and to iteratively determine the optimum number of clusters. A further weakness of the traditional k-means method is its limited ability to deal with outliers or noise data: it uses the squared Euclidean distance to determine the dissimilarity matrix, giving more weight to outliers. The characteristics of each cluster can provide insights into biologically or ecologically relevant features. Moreover, any other form of biological validation can contribute to the speculation of what could be described by the clusters or indicator species and can be attributed to the different clusters (Gastauer *et al*., 2017a).

K-means classification has been applied to broadband acoustic data in Ross *et al*. (2013) and combined multifrequency split-beam and multibeam data in Buelens *et al*. (2009). A review of clustering applied to multifrequency data in Peña (2018) highlights the importance of considering variance and cluster geometry. It also includes a new technique to initialize clustering that helps the algorithm find less abundant groups.

Case study 5 in Annex 1 illustrates the use of clustering.

6.3.2.3 Self-organizing maps

The self-organizing map (SOM; Kohonen, 1982) searches for hidden structure in unlabelled data, producing a low-dimensional, discretized representation of the input space. It computes a set of reference vectors (prototypes or neurons) representing local means of the data. In this way, redundancy in the variables is reduced, projecting the data into a two-dimensional space (similar to principal components analysis), while redundancy in the samples is reduced creating these prototypes (like in k-means).

The algorithm organizes the positions of the neurons in an unsupervised competitive learning mechanism. The SOM can be considered a non-linear extension of the scatterplot technique often used in acoustics, but the SOM is able to employ all available mean volume backscattering strengths (ΔMVBS) simultaneously (Peña and Calise, 2016). The SOM can also search for linear and non-linear correlations between variables (Peña *et al*., 2015). Different relationships may arise in this way for intercorrelated variables, allowing a more in-depth analysis of the data. The SOM is also robust to errors/outliers that are usually embedded in the acoustic data. The maximum number of variables used in supervised techniques depend on the number of observations (fivefold less as a rule of thumb), while the SOM is often used for feature selection, even with more variables than samples. These advantages improve the ability of researchers to identify potential effects not considered *a priori* and help them to establish new hypotheses about causal relations.

6.4 Other classification methods

There are several classification methods that are not yet common but that may be used either alone or in combination with other multifrequency or broadband analysis methods.

6.4.1 Phase coherence

A low standard deviation of the phase samples within an echo is a metric typically used to identify echoes from acoustically resolvable individual scatterers (Soule *et al.*, 1995). However, if multiple targets are spaced with radial ranges differing by an integer multiple of a half-wavelength, their combined echoes interfere constructively and have a coherent phase (Demer *et al.*, 1999). Consequently, measurements with interferometric systems (e.g. split-beam echosounders) may be inaccurate in cases of echoes coincidentally arriving from multiple sources (Soule *et al.*, 1995; Foote, 1996; Yang and Taxt, 1997) or directions (e.g. multipath reverberation; Kraeutner and Bird, 1999). However, coincident echoes can be better rejected, thus significantly improving measurement accuracy, by using co-located, multifrequency, split-aperture transducers and interferometric processing (Demer *et al.*, 1999; Conti *et al.*, 2005). This is because it is unlikely for echoes from multiple targets to constructively interfere at multiple frequencies. Therefore, high coherence in the target phase and estimated three-dimensional location (Demer *et al.*, 1999) are good indicators of a resolvable single target. The frequency responses of accurate TS measurements at multiple frequencies can then be used for acoustic target classifications (Figure 6.2; Demer *et al.*, 1999).

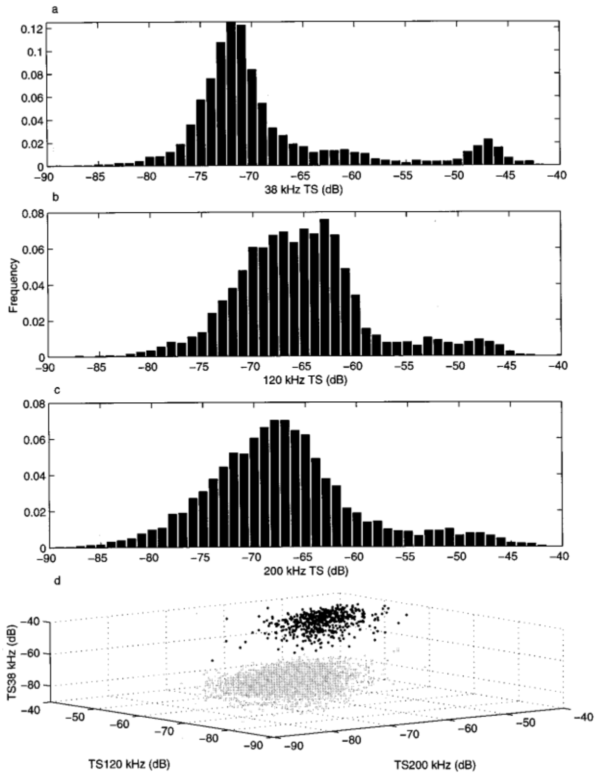

Figure 6.2. Target strength of Southern Ocean scatterers at 38, 120, and 200 kHz. Spatial matches of single-target detections at all three frequencies totaled 5690. The 38 kHz histogram (a) contains three modes: mode 1, −85 to −65 dB; mode 2, −65 to −55 dB; and mode 3, −55 to 40 dB. In (d), mode 1 (black dots) and mode 3 (grey dots) are clearly separable by the three-frequency target strength classification. (Reproduced from Figure 14 in Demer *et al.*, 1999).

Even for resolvable single targets, however, some degree of incoherence results from the target size, shape, and behaviour (Stanton and Clay, 1986) and the signal-to-noise ratio (r_{sn}; Ehrenberg and Torkelson, 1996). For resolvable single targets that are small compared to the acoustic wavelength, the echoes are weak and coherent (Stanton and Clay, 1986). For larger scatterers, interference caused by echoes from distributed anatomical features will cause phase fluctuations (e.g. Demer and Conti, 2003), introducing some incoherence in the larger returns. For multiple unresolved scatterers, the incoherence increases further, more so for swarming vs. schooling organisms. Thus, varying degrees of incoherence occur when echoes originate in a stationary or moving single target, multiple features of a single organism, swarming or schooling multiple organisms, or single or multiple facets of the seabed. In other words, there is a spectrum of echo coherence.

6.4.2 Statistical-spectral identification

Target identification may be improved by exploiting information contained in both the statistics and the spectra of the backscatter amplitude (Demer *et al.*, 2009). Backscatter intensity, proportional to the square of echo amplitude, is usually measured as TS (dB re 1 m^2) for resolvable individual targets, or volume backscattering strength (S_v; dB re 1 m^{-1}) for backscatter from multiple non-resolvable targets in a volume. In some cases, the multifrequency backscatter-intensity information is sufficient to remotely identify target sizes, morphologies, taxa, or perhaps species (Demer *et al.*, 1999). In other cases, echo statistics may provide additional useful information to characterize single targets and aggregations.

Backscatter amplitude, $e = 10^{S_v/20}$, deconvolved from the transducer beam-directivity pattern (Clay, 1983), can be modelled as the sum of coherent (e_c) and incoherent (e_d) components (Clay and Heist, 1984; Stanton and Clay, 1986):

$$e = ec + ed \tag{4}$$

The probability density function (PDF) of e is described by the single-parameter ($\gamma = e_c^2/e_d^2$) Rician distribution. When the echo amplitude is mostly coherent (the target is stable or small relative to a wavelength), γ is large and the Rician PDF approaches a Gaussian PDF. Conversely, when the echo amplitude is mostly incoherent (the target is active or large relative to a wavelength), γ is small, approaching zero, and the Rician PDF conforms to the Rayleigh PDF. In this case, the mean echo amplitude decreases, and the variance increases (Figure 6.3; Demer *et al.*, 2009).

The ratio of the variance and the mean of echo amplitude (VMR; dB) can be used to estimate the magnitude of γ; if calculated from measurements of e at multiple frequencies, it can be used for pixel-wise classification of S_v data (Demer *et al.*, 2009). In addition to describing echo-phase stability, the VMR also includes information about the mean echo amplitude. Consequently, high values of VMR indicate high phase coherence and thus highly resolved or schooling targets; low VMR indicates low phase coherence resulting from large or active single targets or both, or unresolved targets, perhaps swarming. For example, the authors demonstrated that the VMR of echo amplitudes measured at three or more frequencies can be used to classify backscatter from zooplankton (low VMR), fish schools (intermediate VMR), and resolvable single targets and initial seabed reflections (high VMR).

For studies of targets located near a boundary (e.g. demersal fish), the statistical-spectral method for identification (SSID) also provides estimates of the height of the region near the boundary in which targets cannot be resolved (Demer *et al.*, 2009), the so-called acoustic dead zone (ADZ; Ona and Mitson, 1996).

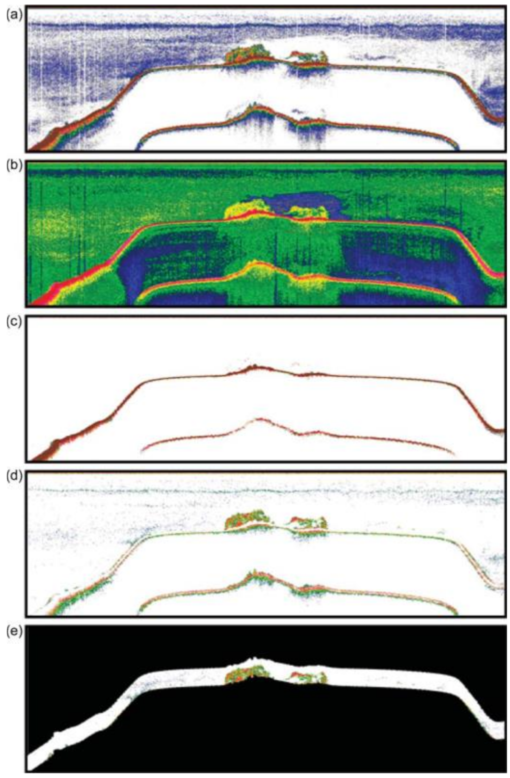

Figure 6.3. (a) A 38 kHz echogram illustrating aggregations over a high-relief rocky seabed; (b) A VMR echogram providing high temporal-spatial resolution of the incoherent scatter from the aggregations of rockfish, the coherent initial reflection from the seabed, and the subsequent incoherent reflection, primarily from the rough seabed; (c) the coherent (reflected) echo from the seabed at 38 kHz; (d) the incoherent echoes from the aggregations of rockfish (*Sebastes* spp.) and the rough seabed; and (e) echoes at 38 kHz from the putative aggregations of rockfish. (Reproduced from Figure 2 in Demer *et al.*, 2009).

6.4.3 Scattering spectra and directivity

Target strength, TS, and hence S_v, is a function of the target size, shape, and morphology, as well as acoustic frequency (f; Hz) and incidence angle (θ; °). In the Rayleigh scattering region, where λ is large compared to the target size, acoustic scatter is omnidirectional, independent of θ, and TS and S_v increase vs. f and target length (L; m). In the geometric scattering region, where the acoustic wavelength (λ; m) is small compared to the target size, echoes from the facets comprising a target will interfere constructively and destructively causing peaks and nulls in the scattering spectra. In the geometric region, TS and S_v are dependent on θ, and this backscattering directivity increases with f and L. Consequently, when θ varies around normal incidence, S_v increases with increasing f or L when λ is large compared to the target size (Rayleigh region), and decreases with increasing f or L when λ is small compared to the target size (geometric region). The effects of scattering directivity can be exploited for acoustic target classification.

6.4.4 Multifrequency biplanar split-aperture processing

With a focus on high-resolution seabed imaging and classification, Cutter and Demer (2010) showed that each coherent sample from the measurement frequencies could be positioned in geographic coordinates. Their multifrequency biplanar interferometric (MBI) imaging technique provides data for estimating within-beam seabed range, slope, hardness, and roughness (Demer *et al.*, 2009; Cutter and Demer, 2010). Demer *et al.*

(2009) showed that the MBI technique could also be applied to data from a multifrequency multibeam echosounder to image and identify targets both in the water column and on the seabed. With measurements made over a range of incidence angles, the angular dependence of backscattering from the targets, the target directivity, may also be exploited to further enhance the accuracy of target identification and size estimation.

Using the multifrequency biplanar interferometric technique (MBI; Cutter and Demer, 2010), the three-dimensional positions of resolved targets can be compensated for transducer location, transducer motion, transducer directivity, and propagation losses. The geographic coordinates can also be located. Coherent, resolved targets may be biotic or abiotic, entire individuals or aggregations of animals, facets of animals or the seabed. Thus, MBI can estimate fish aggregation shape, density, abundance, and behaviour as well as detect and classify echoes from animals and the seabed using the same dataset. MBI allows greatly improved estimations of seabed depth; sub-beam slope, hardness, and roughness; and the height of the unresolved region near the seabed, the ADZ (Demer *et al*., 2009; Cutter and Demer, 2010, 2014).

7 Future objectives, recommendations, and conclusions

National and international directives for marine governance, typical in broad ecosystem monitoring for state-of-the-environment reporting (ecosystem health) and fisheries maangement through stock assessments, will drive the future objectives of target classification. Ecosystem monitoring will require better knowledge of species/group allocations with metrics on lower trophic levels, changes in community composition, and size changes. Likewise, effective fisheries management has an ongoing need for more precise stock assessments with a trend to have real-time management for some species. The advent of real-time management will require better real-time species identification with ascribed uncertainty.

To address the objectives of target classification, advances in technology and methodology are expected. Of recent interest are acoustic systems with wider frequency ranges; however, the same principles and challenges described in this document for narrowband multifrequency classification still apply, along with new challenges including data volume (and hence processing efficiency) and frequency variability due to stochasticity.

Other advances are likely to include systems with broader coverage used on new platforms taking advantage of lower power requirements. Lower power requirements will also make it possible to perform on-board processing for real-time target classification and reporting, creating a need for more automatic classification for efficient data processing. Advanced platforms are expected to have more integrated sensors of physical, chemical, and biological parameters. The newest sensors and platforms in use include low-frequency broadband on a towed body (Stanton *et al*., 2012) and array systems with reduced noise pollution (Diachok, 2016). Both of which provide insight into fish size classes. Combined acoustic and optical probes that can be deployed to deep layers reduce the sampling volume, thus providing better species/group resolution (Kloser *et al*., 2016), such as differentiating between phytoplankton and zooplankton (Benoit-Bird *et al*., 2010).

These advances require ongoing development of data preparation, calibration, feature extraction, grouping, and validation of acoustic data.

8 Acknowledgements

The authors wish to thank the hosts of ICES Working Group on Target Classification (WGTC) meetings 2014, NOAA, New Bedford, USA; 2015, Ifremer, Nantes, France; 2016, IEO, Vigo, Spain). Thank you also to the journals that reprint the figures and to the institutions financing travel to the WGTC meetings. Finally, we are grateful to the reviewers of this CRR.

9 References

Anderson, V. C. 1950. Sound scattering from a fluid sphere. The Journal of the Acoustical Society of America, 22: 426–431. https://doi.org/10.1121/1.1906621

Anderson, J. T., Holliday, D. V., Kloser, R., Reid, D., Simard, Y., Brown, C. J., Chapman, R., *et al*. 2007a. Acoustic seabed classification of marine physical and biological landscapes. ICES Cooperative Research Report No. 286. 183 pp.

Anderson, C. I. H., J. K. Horne, and J. Boyle. 2007b. Classifying multifrequency fisheries acoustic data using a robust probabilistic classification technique. The Journal of the Acoustical Society of America, 121: 230–237. https://doi.org/10.1121/1.2731016

Andreeva, I. B. 1964. Scattering of sound by air bladders of fish in deep sound-scattering ocean layers. Soviet physics. Acoustics, 10: 17–20.

ANSI. 1994. American National Standard: Acoustical Terminology. ANSI S1.1-1994. Acoustical Society of America, New York. 58 pp.

Antona, A. 2016. Remote fish species and size identification using broadband echosounders. Institute for Marine Resources and Ecosystem Studies (IMARES), Wageningen University. http://edepot.wur.nl/378294

Barakat, R. 1974. First-order statistics of combined random sinusoidal waves with applications to laser speckle patterns. Optica Acta, 21: 903–921. https://doi.org/10.1080/713818862

Barange, M. 1994. Acoustic identification, classification and structure of biological patchiness on the edge of the Agulhas Bank and its relation to frontal features. South African Journal of Marine Science, 14: 333–347. https://doi.org/10.2989/025776194784286969

Becker, K. N., and Warren, J. D. 2014. Material properties of Northeast Pacific zooplankton. ICES Journal of Marine Science, 71: 2550–2563. https://doi.org/10.1093/icesjms/fsu109

Benoit-Bird, K. J., and Lawson, G. L. 2016. Ecological insights from pelagic habitats acquired using active acoustic techniques. Annual Review of Marine Science, 8: 463–490. https://doi.org/10.1146/annurev-marine-122414-034001

Benoit-Bird, K. J., Moline, M. A., Waluk, C. M., and Robbins, I. C. 2010. Integrated measurements of acoustical and optical thin layers I: Vertical scales of association. Continental Shelf Research, 30: 17–28. https://doi.org/10.1016/j.csr.2009.08.001

Berenger, J. P. 1996. Three-dimensional perfectly matched layer for the absorption of electromagnetic waves. Journal of Computational Physics, 127: 363–379. https://doi.org/10.1006/jcph.1996.0181

Berger, L., Poncelet, C., and Trenkel, V. M. 2009. A method for reducing uncertainty in estimates of fish-school frequency response using data from multifrequency and multibeam echosounders. ICES Journal of Marine Science, 66: 1155–1161. https://doi.org/10.1093/icesjms/fsp113

Bertrand, A., Gerlotto, F., Bertrand, S., Gutiérrez, M., Alza, L., Chipollini, A., Díaz, E., *et al*. 2008. Schooling behaviour and environmental forcing in relation to anchoveta distribution: An analysis across multiple spatial scales. Progress in Oceanography, 79: 264–277. https://doi.org/10.1016/j.pocean.2008.10.018

Borcard, D., Gillet, F., and Legendre, P. 2011. Numerical Ecology with R. Springer, New York. 306 pp. https://doi.org/10.1007/978-1-4419-7976-6

Breiman, L. 2001. Random forests. Machine Learning, 45: 5–32. https://doi.org/10.1023/A:1010933404324

Breiman, L., Friedman, J. H., Olshen, R. A., and Stone, C. J. 1984. Classification and Regression Trees. Chapman and Hall, Boca Raton, FL. 368 pp.

Brierley, A. S., Fernandes, P. G., Brandon, M. A., Armstrong, F., Millard, N. W., McPhail, A. D., Stevenson, P., *et al*. 2002. Antarctic krill under sea ice: elevated abundance in a narrow band just south of the ice edge. Science, 295: 1890–1892. https://doi.org/10.1126/science.1068574

Brierley, A. S., Goss, C., Watkins, J. L., and Woodroffe, P. 1998. Variations in echosounder calibration with temperature, and some possible implications for acoustic surveys of krill biomass. CCAMLR Science, 5: 273–281.

Brierley, A. S., Saunders, R. A., Bone, D. G., Murphy, E. J., Enderlein, P., Conti, S. G., and Demer, D. A. 2006. Use of moored acoustic instruments to measure short-term variability in abundance of Antarctic krill. Limnology and Oceanography: Methods 4, 18–29. https://doi.org/10.4319/lom.2006.4.18

Buelens, B., Pauly, T., Williams, R., and Sale, A. 2009. Kernel methods for the detection and classification of fish schools in single-beam and multibeam acoustic data. ICES Journal of Marine Science, 66: 1130–1135. https://doi.org/10.1093/icesjms/fsp004

Cabreira, A. G., Tripode, M., and Madirolas, A. 2009. Artificial neural networks for fish-species identification. ICES Journal of Marine Science, 66: 1119–1129. https://doi.org/10.1093/icesjms/fsp009

Campanella, F., and Taylor, J. C. 2016. Investigating acoustic diversity of fish aggregations in coral reef ecosystems from multifrequency fishery sonar surveys. Fisheries Research, 181: 63–76. https://doi.org/10.1016/j.fishres.2016.03.027

Chatfield, C. 1989. The Analysis of Time Series: An Introduction, Fourth edition. Chapman & Hall, London, UK. 241 pp.

Chen, L. H., and Scheikert, D. G. 1963. Sound radiation from an arbitrary body. The Journal of the Acoustical Society of America, 35: 1626–1632. https://doi.org/10.1121/1.1918770

Chertock, G. 1964. Sound radiation from vibrating surfaces. The Journal of the Acoustical Society of America, 36: 1305–1313. https://doi.org/10.1121/1.1919203

Chu, D., Foote, K. G., and Stanton, T. K. 1993. Further analysis of target strength measurements of Antarctic krill at 38 kHz and 120 kHz: Comparison with deformed cylinder model and inference of orientation distribution. The Journal of the Acoustical Society of America, 93: 2985–2988. https://doi.org/10.1121/1.405818

Chu, D., and Stanton, T. K. 2010. Statistics of echoes from a directional sonar beam insonifying finite numbers of single scatterers and patches of scatterers. IEEE Journal of Oceanic Engineering, 35: 267–277. https://doi.org/10.1109/JOE.2009.2037988

Chu, D., and Wiebe, P. 2005. Measurements of acoustic material properties of zooplankton in Antarctic waters. ICES Journal of Marine Science, 62: 818–831. https://doi.org/10.1016/j.icesjms.2004.12.020

Chu, D., Wiebe, P., and Copley, N. 2000. Inference of material properties of zooplankton from acoustic and resistivity measurements. ICES Journal of Marine Science, 57: 1128–1142. https://doi.org/10.1006/jmsc.2000.0800

Chu, D., Wiebe, P. H., Copley, N. J., Lawson, G. L., and Puvanendran, V. 2003. Material properties of North Atlantic cod eggs and early-stage larvae and their influence on acoustic scattering. ICES Journal of Marine Science, 60: 508–515. https://doi.org/10.1016/S1054-3139(03)00047-X

Clay, C. S. 1983. Deconvolution of the fish scattering PDF from the echo PDF for a single transducer sonar. The Journal of the Acoustical Society of America, 73: 1989–1994. https://doi.org/10.1121/1.389564

Clay, C. S. 1992. Composite ray-mode approximations for backscattered sound from gas-filled cylinders and swimbladders. The Journal of the Acoustical Society of America, 92: 2173–2180. https://doi.org/10.1121/1.405211

Clay, C. S, and Heist, B. G. 1984. Acoustic scattering by fish–Acoustic models and a two-parameter fit. The Journal of the Acoustical Society of America, 75: 1077–1083. https://doi.org/10.1121/1.390781

Clay, C. S., and Horne, J. K. 1994. Acoustic models of fish: The Atlantic cod (*Gadus morhua*). The Journal of the Acoustical Society of America, 96: 1661–1668. https://doi.org/10.1121/1.410245

Coetzee, J. 2000. Use of a shoal analysis and patch estimation system (SHAPES) to characterise sardine schools. Aquatic Living Resources, 13: 1–10. https://doi.org/10.1016/S0990-7440(00)00139-X

Conti, S. G., Demer, D. A., Soule, M. A., and Conti, J. H. E. 2005. An improved multiple-frequency method for measuring *in-situ* target strengths. ICES Journal of Marine Science, 62: 1636–1646. https://doi.org/10.1016/j.icesjms.2005.06.008

Copley, L. G. 1967. Integral equation method for radiation from vibrating bodies. Journal of the Acoustical Society of America, 41: 807–816. https://doi.org/10.1121/1.1910410

Cox, M. J., Letessier, T. B., and Brierley, A. S. 2013. Zooplankton and micronekton biovolume at the Mid-Atlantic Ridge and Charlie–Gibbs Fracture Zone estimated by multi-frequency acoustic survey. Deep-Sea Research Part II: Topical Studies in Oceanography, 98: 269–278. https://doi.org/10.1016/j.dsr2.2013.07.020

Cutter, G. R. Jr, and Demer, D. A. 2010. Multifrequency biplanar interferometric imaging. IEEE Geoscience and Remote Sensing Letters, 7: 171–175. https://doi.org/10.1109/LGRS.2009.2029533

Cutter, G. R. Jr, and Demer, D. A. 2014. Seabed classification using surface backscattering strength versus acoustic frequency and incidence angle measured with vertical, split-beam echosounders. ICES Journal of Marine Science, 71: 882–894.

De'ath, G. 2007. Boosted trees for ecological modeling and prediction. Ecology, 88: 243–251. https://doi.org/10.1890/0012-9658(2007)88[243:BTFEMA]2.0.CO;2

De'ath, G., and Fabricius, K. E. 2000. Classification and regression trees: a powerful yet simple technique for ecological data analysis. Ecology, 81: 3178–3192. https://doi.org/10.1890/0012-9658(2000)081[3178:CARTAP]2.0.CO;2

Demer, D. A., Berger, L., Bernasconi, M., Bethke, E., Boswell, K., Chu, D., Domokos, R., *et al*. 2015. Calibration of acoustic instruments. ICES Cooperative Research Report No. 326. 136 pp.

Demer, D. A., and Conti, S. G. 2003. Reconciling theoretical versus empirical target strengths of krill: effects of phase variability on the distorted-wave Born approximation. ICES Journal of Marine Science, 60: 429–434. Erratum, 2004. 61: 157–158. https://doi.org/10.1016/j.icesjms.2003.12.003

Demer, D. A., Cutter, G. R., Renfree, J. S., and Butler, J. L. 2009. A statistical-spectral method for echo classification. ICES Journal of Marine Science, 66: 1081–1090. https://doi.org/10.1093/icesjms/fsp054

Demer, D. A., Soule M. A., and Hewitt, R. P. 1999. A multifrequency method for improved accuracy and precision of *in-situ* target strength measurements. The Journal of the Acoustical Society of America, 105(4): 2359–2376. https://doi.org/10.1121/1.426841

Dempster, A. P., Laird, N. M., and Rubin, D. B. 1977. Maximum likelihood from incomplete data via EM algorithm. Journal of the Royal Statistical Society, Series B (Methodological) 39: 1–38.

De Robertis, A., and Handegard, N. O. 2013. Fish avoidance of research vessels and the efficacy of noise-reduced vessels: a review. ICES Journal of Marine Science, 70: 34–45. https://doi.org/10.1093/icesjms/fss155

De Robertis, A., and Higginbottom, I. 2007. A post-processing technique to estimate the signal-to-noise ratio and remove echosounder background noise. ICES Journal of Marine Science, 64: 1282–1291. https://doi.org/10.1093/icesjms/fsm112

De Robertis, A., McKelvey, R., and Ressler, P. H. 2010. Development and application of an empirical multifrequency method for backscatter classification. Canadian Journal of Fisheries and Aquatic Sciences, 67: 1459–1474. https://doi.org/10.1139/F10-075

De Robertis, A., Taylor, K., Williams, K., and Wilson, C. D. 2017. Species and size selectivity of two midwater trawls used in an acoustic survey of the Alaska Arctic. Deep-Sea Research II, 135: 40–50. https://doi.org/10.1016/j.dsr2.2015.11.014

Diachok, O. 2016. Bioacoustic absorption spectroscopy: An acoustical oceanography method for the study of marine ecosystems. The Journal of the Acoustical Society of America, 139: 2174, https://doi.org/10.1121/1.4950455

Doksæter, L., Godø, O. R., Olsen, E., Nøttestad, L., and Patel, R. 2009. Ecological studies of marine mammals using a seabed-mounted echosounder. ICES Journal of Marine Science, 66: 1029–1036. https://doi.org/10.1093/icesjms/fsp130

Doonan, I. J., Coombs, R. F., and McClatchie, S. 2003. The absorption of sound in seawater in relation to the estimation of deep-water fish biomass. ICES Journal of Marine Science, 60: 1047–1055. https://doi.org/10.1016/S1054-3139(03)00120-6

Doray, M., Berger, L., Le Bouffant, N., Coail, J. Y., Vacherot, J. P., de La Bernardie, X., Morinière, P., *et al*. 2016. A method for controlled target strength measurements of pelagic fish, with application to European anchovy (*Engraulis encrasicolus*). ICES Journal of Marine Science, 73: 1987–1997. https://doi.org/10.1093/icesjms/fsw084

Doray, M., Josse, E., Gervain, P., Reynal, L., and Chantrel, J. 2007. Joint use of echosounding, fishing and video techniques to assess the structure of fish aggregations around moored fish aggregating devices in Martinique (Lesser Antilles). Aquatic Living Resources, 20: 357–366. https://doi.org/10.1051/alr:2008004

Doray, M., Petitgas, P., and Josse, E. 2008. A geostatistical method for assessing biomass of tuna aggregations around moored fish aggregating devices with star acoustic surveys. Canadian Journal of Fisheries and Aquatic Sciences, 65: 1193–1205. https://doi.org/10.1139/F08-050

Doray, M., Petitgas, P., Nelson, L., Mahévas, S., Josse, E., and Reynal, L. 2009. Influence of environment on the variability of monthly tuna biomass around a moored, fish aggregating device. ICES Journal of Marine Science, 66: 1410–1416. https://doi.org/10.1093/icesjms/fsp039

Dudoit, S., and Fridlyand, J. 2002. A prediction-based resampling method for estimating the number of clusters in a dataset. Genome Biology, 3: research0036. https://doi.org/10.1186/gb-2002-3-7-research0036

Ehrenberg, J. E. 1972. A method for extracting the fish target strength distribution from acoustic echoes. Proceedings of the 1972 IEEE Conference on Engineering in the Ocean Environment, Newport, RI, pp. 61–64. https://doi.org/10.1109/OCEANS.1972.1161176

Ehrenberg, J. E., and Torkelson, T. C. 1996. Application of dual-beam and split-beam target tracking in fisheries acoustics. ICES Journal of Marine Science, 53: 329–334.

Enright, J. T. 1963. Estimates of the compressibility of some marine crustaceans. Limnology and Oceanography, 8: 382–387. https://doi.org/10.4319/lo.1963.8.4.0382

Fallon, N. G., Fielding, S., and Fernandes, P. G. 2016. Classification of Southern Ocean krill and icefish echoes using random forests. ICES Journal of Marine Science, 73: 1998–2008. https://doi.org/10.1093/icesjms/fsw057

Faran, J. J. Jr. 1951. Sound scattering by solid cylinders and spheres. The Journal of the Acoustical Society of America, 23: 405–418. https://doi.org/10.1121/1.1906780

Fernandes, P. G. 2009. Classification trees for species identification of fish-school echotraces. ICES Journal of Marine Science, 66: 1073–1080. https://doi.org/10.1093/icesjms/fsp060

Fernandes, P. G, Brierley, A. S., Simmonds, E. J., Millard, N. W., McPhail, S. D., Armstrong, F., Stevenson, P., *et al*. 2000. Fish do not avoid survey vessels. Nature, 404: 35–36. https://doi.org/10.1038/35003648

Fernandes, P. G., Copland, P., Garcia, R., Nicosevici, T., and Scoulding, B. 2016. Additional evidence for fisheries acoustics: small cameras and angling gear provide tilt angle distributions and other relevant data for mackerel surveys. ICES Journal of Marine Science, 73: 2009–2019. https://doi.org/10.1093/icesjms/fsw091

Fernandes, P. G., Korneliussen, R. J., Lebourges-Dhaussy, A., Masse, J., Iglesias, M., Diner, N., Ona, E., *et al*. 2006. The SIMFAMI project: Species Identification Methods From Acoustic Multifrequency Information. Final Report to the EC Number Q5RS-2001-02054 (Report accessible from any of the authors).

Fernandes, P. G., Stevenson, P., Brierley, A. S., Armstrong, F., and Simmonds, E. J. 2003. Autonomous underwater vehicles: future platforms for fisheries acoustics. ICES Journal of Marine Science, 60: 684–691. https://doi.org/10.1016/S1054-3139(03)00038-9

Flammer, C. 1957. Spheroidal Wave Functions. Stanford University Press, Stanford, CA. 220 pp.

Foote, K. G. 1985. Rather-high-frequency sound scattering of swimbladdered fish. The Journal of the Acoustical Society of America, 78: 688–700, https://doi.org/10.1121/1.392438

Foote, K. G. 1991. Acoustic-sampling volume. The Journal of the Acoustical Society of America, 90: 959–964. https://doi.org/10.1121/1.401963

Foote, K. G. 1996. Coincidence echo statistics. The Journal of the Acoustical Society of America, 99: 266–271. https://doi.org/10.1121/1.414537

Foote, K. G., Knudsen, H. P., Korneliussen, R. J., Nordbø, P. E., and Røang, K. 1991. Postprocessing system for echo sounder data. The Journal of the Acoustical Society of America, 90: 37–47. https://doi.org/10.1121/1.401261

Fraley, C., and Raftery, A. E. 1998. How many clusters? Which clustering method? Answers via model-based cluster analysis. The Computer Journal, 41: 578–588. https://doi.org/10.1093/comjnl/41.8.578

Francois, R. E., and Garrison, G. R. 1982. Sound absorption based on ocean measurements. Part I: Pure water and magnesium sulphate contributions. The Journal of the Acoustical Society of America, 72: 896–907. https://doi.org/10.1121/1.388170

Furusawa, M. 1988. Prolate spheroidal models for predicting general trends of fish target strength. Journal of the Acoustical Society of Japan (E), 9: 13–24. https://doi.org/10.1250/ast.9.13

Gastauer, S., Scoulding, B., and Parsons, M. 2017a. An unsupervised acoustic description of fish schools and the seabed in three fishing regions within the Northern Demersal Scalefish Fishery (NDSF, Western Australia). Acoustics Australia, 45: 363–380. https://doi.org/10.1007/s40857-017-0100-0

Gastauer, S., Scoulding, B., and Parsons, M. 2017b. Towards acoustic monitoring of a mixed demersal fishery based on commercial data: The case of the Northern Demersal Scalefish Fishery (Western Australia). Fisheries Research, 195: 91–104. https://doi.org/10.1016/j.fishres.2017.07.008

Gauthier, S., and Horne, J. K. 2004. Potential acoustic discrimination within boreal fish assemblages. ICES Journal of Marine Science, 61: 836–845. https://doi.org/10.1016/j.icesjms.2004.03.033

Ghania, M. H., Hole, L. R., Fer, I., Kourafalou, V. H., Wienders, N., Kang, H., Drushka, K., *et al*. 2014. The SailBuoy remotely-controlled unmanned vessel: Measurements of near surface temperature, salinity and oxygen concentration in the Northern Gulf of Mexico. Methods in Oceanography, 10: 104–121. https://doi.org/10.1016/j.mio.2014.08.001

Godø, O. R., Johnsen, S., and Torkelsen, T. 2014 The LoVe Ocean Observatory is in Operation. Marine Technology Society Journal, 48(2): 24–30. https://doi.org/10.4031/MTSJ.48.2.2

Gorska, N., Korneliussen, R. J., and Ona, E. 2007. Acoustic backscatter by schools of adult Atlantic mackerel. ICES Journal of Marine Science, 64: 1145–1151. https://doi.org/10.1093/icesjms/fsm094

Gorska, N., Ona, E., and Korneliussen, R. 2005. Acoustic backscattering by Atlantic mackerel as being representative of fish that lack a swimbladder. Backscattering by individual fish. ICES Journal of Marine Science, 62: 984–995. https://doi.org/10.1016/j.icesjms.2005.03.010

Greene, C. H., Meyer-Gutbrod, E. L., McGarry, L. P., Hufnagle, L. C. Jr., Chu, D., McClatchie, S., Packer, A., *et al*. 2014. A wave glider approach to fisheries acoustics: Transforming how we monitor the nation's commercial fisheries in the 21st century. Oceanography, 27(4): 168–174, https://doi.org/10.5670/oceanog.2014.82

Greenlaw, C. F. 1977. Backscattering spectra of preserved zooplankton. The Journal of the Acoustical Society of America, 62: 44–52. https://doi.org/10.1121/1.381503

Gross, F., and Raymont, J. E. G. 1942. The Specific Gravity of *Calanus finmarchicus*. Proceedings of the Royal Society of Edinburgh, B., 61: 288–296. Proceedings of the Royal Society of Edinburgh, B., 61: 288–296.

Guihen, D., Fielding, S., Murphy, E. J., Heywood, K. J., and Griffiths, G. 2014 An assessment of the use of ocean gliders to undertake acoustic measurements of zooplankton: the distribution and density of Antarctic krill (*Euphausia superba*) in the Weddell Sea. Limnology and Oceanography: Methods, 12: 373–389. https://doi.org/10.4319/lom.2014.12.373

Handl, J., Knowles, J., and Kell. D. B. 2005. Computational cluster validation in post-genomic data analysis. Bioinformatics, 21(15): 3201–3212. https://doi.org/10.1093/bioinformatics/bti517

Haralabous, J., and Georgakarakos, S. 1996. Artificial neural networks as a tool for species identification of fish schools. ICES Journal of Marine Science, 53: 173–180. https://doi.org/10.1006/jmsc.1996.0019

Hammond, T. R., and Swartzman, G. L. 2001. A general procedure for estimating the composition of fish school clusters using standard acoustic survey data. ICES Journal of Marine Science, 58: 1115–1132. https://doi.org/10.1006/jmsc.2001.1102

Hewitt, R. P., Watkins, J., Naganobu, M., Sushin, V., Brierley, A. S., Demer, D., Kasatkina, S., *et al*. 2004. Biomass of Antarctic krill in the Scotia Sea in January/February 2000 and its use in revising an estimate of precautionary yield. Deep-Sea Research Part II: Topical Studies in Oceanography, 51: 1215–1236. https://doi.org/10.1016/j.dsr2.2004.06.011

Holliday, D. V. 1972. Resonance Structure in Echoes from Schooled Pelagic Fish. The Journal of the Acoustical Society of America, 51: 1322–1332. https://doi.org/10.1121/1.1912978

Holliday, D. V. 1977. Extracting bio-physical information from the acoustic signature of marine organisms. *In* Oceanic Sound Scattering Prediction, pp. 619–624. Ed. by N. R. Andersen, and B. J. Zahuranec. Plenum Press, New York. 859 pp.

Holliday, D. V., Pieper, R. E., and Kleppel, G. S. 1989. Determination of zooplankton size and distribution with multifrequency acoustic technology. Journal du Conseil International pour l'Exploration de la Mer, 46: 52–61. https://doi.org/10.1093/icesjms/46.1.52

Horne, J. K. 2000. Acoustic approaches to remote species identification: a review. Fisheries Oceanography, 9(4): 356–371. https://doi.org/10.1046/j.1365-2419.2000.00143.x

Horne, J. K., Sawada, K., Abe, K., Kreisberg, R. B., Barbee, D. H., and Sadayasu, K. 2009. Swimbladders under pressure: anatomical and acoustic responses by walleye pollock. ICES Journal of Marine Science, 66: 1162–1168. https://doi.org/10.1093/icesjms/fsp101

ICES. 2015. Report of the Workshop on scrutinisation procedures for pelagic ecosystem surveys (WKSCRUT), 7–11 September 2015, Hamburg, Germany. ICES Document CM 2015/SSGIEOM: 18. 103 pp.

Ihlenburg, F. 1998. Finite Element Analysis of Acoustic Scattering. Applied Mathematical Sciences, Volume 132. Springer-Verlag, New York. 226 pp. https://doi.org/10.1007/b98828

Jain, A. K., and Dubes, R. C. 1988. Algorithms for Clustering Data. Prentice-Hall, Englewood Cliffs, New Jersey. 320 pp.

Jao, J. K., and Elbaum, M. 1978. First-order statistics of a non-Rayleigh fading signal and its detection. Proceedings of the IEEE, 66: 781–789. https://doi.org/10.1109/PROC.1978.11015

Jech, J. M. Horne, J. K., Chu, D., Demer, D. A., Francis, D. T. I., Gorska, N., Jones, B. *et al*. 2015. Comparisons among ten models of acoustic backscattering used in aquatic ecosystem research. The Journal of the Acoustical Society of America, 138: 3742–3764. https://doi.org/10.1121/1.4937607

Jolly, G. M., and Hampton, I. 1990. A Stratified Random Transect Design for Acoustic Surveys of Fish Stocks. Canadian Journal of Fisheries and Aquatic Sciences, 47: 1282–1291. https://doi.org/10.1139/f90-147

Jones, B. A., Lavery, A. C., and Stanton, T. K. 2009. Use of the distorted wave Born approximation to predict scattering by inhomogeneous objects: Application to squid. The Journal of the Acoustical Society of America, 125: 73–88. https://doi.org/10.1121/1.3021298

Kaartvedt, S., Røstad, A., Klevjer, T. A., and Staby, A. 2009. Use of bottom-mounted echo sounders in exploring behavior of mesopelagic fishes. Marine Ecology Progress Series, 395: 109–118. http://www.jstor.org/stable/24874245

Kalish, J. M., Greenlaw, C. F., Pearcy, W. G., and Holliday, D. V. 1986. The biological and acoustical structure of sound scattering layers off Oregon. Deep-Sea Research Part A. Oceanographic Research Papers, 33: 631–653. https://doi.org/10.1016/0198-0149(86)90058-0

Kloser, R. J., Ryan, T. E., Keith, G., and Gershwin, L. 2016. Deep-scattering layer, gas-bladder density, and size estimates using a two-frequency acoustic and optical probe. ICES Journal of Marine Science, 73: 2037–2048. https://doi.org/10.1093/icesjms/fsv257

Kloser, R. J., Ryan, T., Sakov, P., Williams, A., and Koslow, J. A. 2002. Species identification in deep water using multiple acoustic frequencies. Canadian Journal of Fisheries and Aquatic Sciences, 59: 1065–1077. https://doi.org/10.1139/f02-076

Køgeler, J. W., Falk-Petersen, S., Kristensen, Å., Pettersen, F., and Dalen, J. 1987. Density- and sound speed contrasts in sub-Arctic zooplankton. Polar Biology, 7: 231–235. https://doi.org/10.1007/BF00287419

Kohonen, T. 1982. Self-organized formation of topologically correct feature maps. Biological Cybernetics, 43: 59–69. https://doi.org/10.1007/BF00337288

Kondo, Y., Salibian-Barrera, M., and Zamar, R. 2012. A robust and sparse K-means clustering algorithm. http://arxiv.org/abs/1201.6082

Korneliussen, R. 2000. Measurement and removal of echo integration noise. ICES Journal of Marine Science, 57: 1204–1217. https://doi.org/10.1006/jmsc.2000.0806

Korneliussen, R. J. 2002. Analysis and presentation of multifrequency echograms. PhD thesis, University of Bergen, Department of Physics, Bergen, Norway. 182 pp.

Korneliussen, R. J. 2010. The acoustic identification of Atlantic mackerel. ICES Journal of Marine Science, 67: 1749–1758. https://doi.org/10.1093/icesjms/fsq052

Korneliussen, R. J., Diner, N., Ona, E., Berger, L., and Fernandes, P. G. 2008. Proposals for the collection of multifrequency acoustic data. ICES Journal of Marine Science, 65: 982–994. https://doi.org/10.1093/icesjms/fsn052

Korneliussen, R. J., Heggelund, Y., Eliassen, I. K., and Johansen, G. O. 2009. Acoustic species identification of schooling fish. ICES Journal of Marine Science, 66: 1111–1118, https://doi.org/10.1093/icesjms/fsp119

Korneliussen, R. J., Heggelund, Y., Eliassen, I. K., Øye, O. K., Knutsen, T., and Dalen, J. 2009. Combining multibeam-sonar and multifrequency echosounder data: examples of the analysis and imaging of large euphausiid schools. ICES Journal of Marine Science, 66: 991–997. https://doi.org/10.1093/icesjms/fsp092

Korneliussen, R. J., Heggelund, Y., Macaulay, G. J., Patel, D., Johnsen, E., and Eliassen, I. K. 2016. Acoustic identification of marine species using a feature library. Methods in Oceanography, 17: 187–205. https://doi.org/10.1016/j.mio.2016.09.002

Korneliussen, R. J., and Ona E. 2002. An operational system for processing and visualizing multifrequency acoustic data. ICES Journal of Marine Science, 59: 293–313. https://doi.org/10.1006/jmsc.2001.1168

Korneliussen, R. J., and Ona, E. 2003. Synthetic echograms generated from the relative frequency response. ICES Journal of Marine Science, 60: 636–640. https://doi.org/10.1016/S1054-3139(03)00035-3

Koslow, J. A., Kloser, R., and Stanley, C. A. 1995. Avoidance of a camera system by a deepwater fish, the orange roughy (*Hoplostethus atlanticus*). Deep-Sea Research Part 1: Oceanographic Research Papers, 42: 233–244. https://doi.org/10.1016/0967-0637(95)93714-P

Kraeutner, P. H., and Bird, J. S. 1999. Beyond interferometry, resolving multiple angles-of-arrival in swath bathymetric imaging. *In* Riding the Crest into the 21st Century, Oceans '99 MTS/IEEE Conference Proceedings, Seattle, WA., pp. 37–45. Holland Publications, Escondido, CA. 1602 pp. https://doi.org/10.1109/OCEANS.1999.799704

Kubilius, R., and Ona, E. 2012. Target strength and tilt-angle distribution of the lesser sandeel (*Ammodytes marinus*). ICES Journal of Marine Science, 69: 1099–1107. https://doi.org/10.1093/icesjms/fss093

Lavery, A. C., Schmitt, R. W., and Stanton, T. K. 2003. High-frequency acoustic scattering from turbulent oceanic microstructure: The importance of density fluctuations. The Journal of the Acoustical Society of America, 114: 2685–2697. https://doi.org/10.1121/1.1614258

Lavery, A. C., Wiebe, P. H., Stanton, T. K., Lawson, G. L., Benfield, M. C., and Copley, N. 2007. Determining dominant scatterers of sound in mixed zooplankton populations. The Journal of the Acoustical Society of America, 122: 3304–3326. https://doi.org/10.1121/1.2793613

Lawson, C. L., and Hanson, R. J. 1974. Solving Least Squares Problems. Prentice-Hall, New Jersey. 337 pp.

Lee, W., Lavery, A. C., and Stanton, T. K. 2012. Orientation dependence of broadband acoustic backscattering from live squid. The Journal of the Acoustical Society of America, 131: 4461–4475. https://doi.org/10.1121/1.3701876

Lefort, R., Fablet, R., Berger, L., and Boucher, J-M. 2012. Spatial Statistics of Objects in 3-D Sonar Images: Application to Fisheries Acoustics. IEEE Geoscience and Remote Sensing Letters, 9: 56–59. https://doi.org/10.1109/LGRS.2011.2160328

Legendre, P., and Legendre, L. 2012. Numerical Ecology, Developments in Environmental Modelling, Volume 24. Elsevier, Amsterdam. 1006 pp.

Lemon, D., Johnston, P., Buermans, J., Loos, E., Borstad, G., and Brown, L. 2012. Multiple-frequency moored sonar for continuous observations of zooplankton and fish. IEEE Ocean 2012 Conference, Hampton Roads, VA, USA, 14–19 October 2012. pp. 1-6. https://doi.org/10.1109/OCEANS.2012.6404918

Lek, S., Delacoste, M., Baran, P., Dimopoulos, I., Lauga, J., and Aulagnier, S. 1996. Application of neural networks to modelling nonlinear relationships in ecology. Ecological Modelling, 90: 39–52. https://doi.org/10.1016/0304-3800(95)00142-5

Lilja, J., Marjomäki, T. J., Jurvelius, J., Rossi, T., and Heikkola, E. 2004. Simulation and experimental measurement of side-aspect target strength of Atlantic salmon (*Salmo salar*) at high frequency. Canadian Journal of Fisheries and Aquatic Sciences, 61: 2227–2236. https://doi.org/10.1139/f04-166

Love, R. H. 1978. Resonant acoustic scattering by swimbladder-bearing fish. The Journal of the Acoustical Society of America, 64: 571–580. https://doi.org/10.1121/1.382009

Lowndes, A. G. 1942. The displacement method of weighting living aquatic organisms. Journal of Marine Biological Association of the United Kingdom, 25: 555–574. https://doi.org/10.1017/S0025315400055144

MacLennan, D. N., and Holliday, D. V. 1996. Fisheries and plankton acoustics: past, present, and future. ICES Journal of Marine Science, 53: 513–516. https://doi.org/10.1006/jmsc.1996.0074

MacQueen, J. 1967. Some methods for classification and analysis of multivariate observations. *In* Proceedings of the Fifth Berkeley Symposium on Mathematical Statistics and Probability, Volume 1: Statistics, pp. 281–297. Ed. by L. M. Le Cam, and J. Neyman. University of California Press, Berkeley. 666 pp. https://projecteuclid.org/euclid.bsmsp/1200512992

Mair, A. M., Fernandes, P. G., Lebourges-Dhaussy, A., and Brierley, A. S. 2005. An investigation into the zooplankton composition of a prominent 38 kHz scattering layer in the North Sea. Journal of Plankton Research, 27: 623–633. https://doi.org/10.1093/plankt/fbi035

McQuinn, I. H., Dion, M., and St. Pierre, J-F. 2013. The acoustic multifrequency classification of two sympatric euphausiid species (*Meganyctiphanes norvegica* and *Thysanoessa raschii*), with empirical and SDWBA model validation. ICES Journal of Marine Science, 70: 636–649. https://doi.org/10.1093/icesjms/fst004

McClatchie, S., and Coombs, R. F. 2005. Low target strength fish in mixed species assemblages: the case of orange roughy. Fisheries Research, 72: 185–192. https://doi.org/10.1016/j.fishres.2004.11.008

Medwin, H., and Clay, C. S. 1998. Fundamentals of Acoustical Oceanography, Academic Press, Boston. 712 pp.

Menke, W. 2012. Geophysical Data Analysis: Discrete Inverse Theory, Volume 45. MATLAB Edition, Academic Press, San Diego. 330 pp.

Moum, J. N., Farmer, D. M., Smyth, W. D., Armi, L., and Vagle, S. 2003. Structure and Generation of Turbulence at Interfaces Strained by Internal Solitary Waves Propagation Shoreward over the Continental Shelf. Journal of Physical Oceanography, 33: 2093–2122. https://doi.org/10.1175/1520-0485(2003)033<2093:SAGOTA>2.0.CO;2

Nakashima, B. S. 1990. Escapement from a Diamond IX midwater trawl during acoustic surveys for capelin (*Mallotus villosus*) in the Northwest Atlantic. Journal du Conseil International pour l'Exploration de la Mer, 47: 76–82. https://doi.org/10.1093/icesjms/47.1.76

Nero, R. W., and Magnuson, J. J. 1989. Characterisation of Patches Along Transects Using High-Resolution 70-Khz Integrated Acoustic Data. Canadian Journal of Fisheries and Aquatic Sciences, 46: 2056–2064. https://doi.org/10.1139/f89-254

Novarini, J. C., and Bruno, D. R. 1982. Effects of the sub-surface bubble layer on sound propagation. The Journal of the Acoustical Society of America, 72: 510–514. https://doi.org/10.1121/1.388107

O'Driscoll, R. L., Oeffner, J., and Dunford, A. J. 2013. *In situ* target strength estimates of optically verified southern blue whiting (*Micromesistius australis*). ICES Journal of Marine Science, 70: 431–439. https://doi.org/10.1093/icesjms/fss177

Okumura, T., Masuya, R., Takao, Y., and Sawada, K. 2003. An application of the boundary element method to acoustic scattering of marine organism. The Journal of the Marine Acoustical Society of Japan, 30: 206–213. https://doi.org/10.3135/jmasj.30.206

Olden, J. D., and Jackson, D. A. 2002. Illuminating the "black box": a randomization approach for understanding variable contributions in artificial neural networks. Ecological Modelling, 154(1): 135–150. https://doi.org/10.1016/S0304-3800(02)00064-9

Ona, E. 1987. The equivalent beam angle and its effective value when applying an integrator threshold. ICES Document CM 1987/B: 35.

Ona, E. 1990. Physiological factors causing natural variations in acoustic target strength of fish. Journal of the Marine Biological Association of the United Kingdom, 70: 107–127. https://doi.org/10.1017/S002531540003424X

Ona, E. 2003. An expanded target-strength relationship for herring. ICES Journal of Marine Science, 60: 493–499. https://doi.org/10.1016/S1054-3139(03)00031-6

Ona, E., and Mitson, R. B. 1996. Acoustic sampling and signal processing near the seabed: the dead zone revisited. ICES Journal of Marine Science, 53: 677–690. https://doi.org/10.1006/jmsc.1996.0087

Pedersen, A. 2006. Effects of nonlinear sound propagation in fisheries research. PhD thesis, University of Bergen, Norway. 308 pp.

Pedersen, G., and Korneliussen, R. J. 2009. The relative frequency response derived from individually separated targets of northeast Arctic cod (*Gadus morhua*), saithe (*Pollachius virens*), and Norway pout (*Trisopterus esmarkii*). ICES Journal of Marine Science, 66: 1149–1154. https://doi.org/10.1093/icesjms/fsp070

Peña, M. 2007. Latent variable spaces for the construction of topology preserving mappings. Computing and Information Systems Technical Reports, 41: 14299. ISSN 1461-6122

Peña, M. 2018. Robust clustering methodology for multi-frequency acoustic data: A review of standardization, initialization and cluster geometry. Fisheries Research, 200: 49–60. https://doi.org/10.1016/j.fishres.2017.12.013

Peña, M., and Calise, L. 2016. Use of SDWBA predictions for acoustic volume backscattering and the Self-Organizing Map to discern frequencies identifying *Meganyctiphanes norvegica* from mesopelagic fish species. Deep-Sea Research Part I: Oceanographic Research Papers, 110: 50–64. https://doi.org/10.1016/j.dsr.2016.01.006

Peña, M., Carbonell, A., Tor, A., Alvarez-Berastegui, D., Balbín, R., dos Santos, A., and Alemany, F. 2015. Nonlinear ecological processes driving the distribution of marine decapod larvae. Deep-Sea Research Part I: Oceanographic Research Papers, 97: 92–106. https://doi.org/10.1016/j.dsr.2014.11.017

Peña, M., Georgakarakos, S., and Boyra, G. 2008. Visualisation of the clustering of acoustic echotraces using Topology Preserving Mapping. Application to juvenile anchovy in the Bay of Biscay, ICES Document CM 2008/R: 15.

Petitgas, P. 2001. Geostatistics in fisheries survey design and stock assessment: models, variances and applications. Fish and Fisheries, 2: 231–249. https://doi.org/10.1046/j.1467-2960.2001.00047.x

R Core Team. 2016. R: A language and environment for statistical computing. R Foundation for Statistical Computing, Vienna, Austria. http://www.R-project.org/.

Rand, W. M. 1971. Objective criteria for the evaluation of clustering methods. Journal of the American Statistical Association, 66(336): 846–850, https://doi.org/10.1080/01621459.1971.10482356.

Ramani, N., and Patrick, P. H. 1992. Fish detection and identification using neural networks-some laboratory results. IEEE Journal of Oceanic Engineering, 17(4): 364–368. https://doi.org/10.1109/48.180305

Reeder, D. B., and Stanton, T. K. 2004. Acoustic scattering by axisymmetric finite-length bodies: An extension of a two-dimensional conformal mapping method. The Journal of the Acoustical Society of America, 116: 729–746. https://doi.org/10.1121/1.1648681

Reid, D. G. (Ed.). 2000. Report on echo trace classification. ICES Cooperative Research Report No. 238. 107 pp.

Renfree, J. S., and Demer, D. A. 2016. Optimizing transmit interval and logging range while avoiding aliased seabed echoes. ICES Journal of Marine Science, 73: 1955–1964. https://doi.org/10.1093/icesjms/fsw055

Rice, S. O. 1954. Mathematical analysis of random noise. *In* Selected Papers on Noise and Stochastic Process, pp. 133–294. Ed. by N. Wax. Dover Publications, New York. 352 pp.

Rose, G. A., and Leggett, W. C. 1988. Hydroacoustic signal classification of fish schools by species. Canadian Journal of Fisheries and Aquatic Sciences, 45: 597–604. https://doi.org/10.1139/f88-073

Ross, T., Keister, J. E., and Lara-Lopez, A. 2013. On the use of high-frequency broadband sonar to classify biological scattering layers from a cabled observatory in Saanich Inlet, British Columbia. Methods in Oceanography, 5: 19–38. https://doi.org/10.1016/j.mio.2013.05.001

Rouesseeuw, P. J. 1987. Silhouettes: A graphical aid to the interpretation and validation of cluster analysis. Journal of Computational and Applied Mathematics, 20: 53–65. https://doi.org/10.1016/0377-0427(87)90125-7.

Rumelhart, D., Hinton, G., and Williams, R. 1986. Learning internal representations by error propagation. *In* Parallel Distributed Processing: Explorations in the Microstructure of Cognition, pp. 318–362. Ed. by D. E. Rumelhart, and J. L. McClelland. The MIT Press, Cambridge, MA. 567 pp.

Ryan, T. E., and Kloser, R. J. 2016. Improved estimates of orange roughy biomass using an acoustic–optical system in commercial trawlnets. ICES Journal of Marine Science, 73: 2112–2124. https://doi.org/10.1093/icesjms/fsw009

Ryan, T. E., Kloser, R. J., and Macaulay, G. J. 2009. Measurement and visual verification of fish target strength using an acoustic-optical system attached to a trawlnet. ICES Journal of Marine Science, 66: 1238–1244. https://doi.org/10.1093/icesjms/fsp122

Sato, M., Horne, J. K., Parker-Stetter, S. L., and Keister, J. E. 2015. Acoustic classification of coexisting taxa in a coastal ecosystem. Fisheries Research, 172: 130–136. https://doi.org/10.1016/j.fishres.2015.06.019

Sawada, K., Takahashi, H., Abe, K., Ichii, T., Watanabe, K., and Takao, Y. 2009. Target-strength, length, and tilt-angle measurements of Pacific saury (*Cololabis saira*) and Japanese anchovy (*Engraulis japonicus*) using an acoustic-optical system. ICES Journal of Marine Science, 66: 1212–1218. https://doi.org/10.1093/icesjms/fsp079

Scalabrin, C., Diner, N., and Weill, A. 1994. Automatic shoal recognition and classification based on MOVIES-B software. Oceans Engineering for Today's Technology and Tomorrow's Preservation. Proceedings of Oceans 94, Brest, 13–16 September 1994. IEEE, Brest: II 319–II 324. doi.org/10.1109/OCEANS.1994.364062

Scalabrin, C., and Massé, J. 1993. Acoustic detection of the spatial and temporal distribution of fish shoals in the Bay of Biscay. Aquatic Living Resources, 6: 269–283. https://doi.org/10.1051/alr:1993027

Schwarz, G. 1978. Estimating the Dimension of a Model. The Annals of Statistics, 6: 461–464. https://projecteuclid.org/euclid.aos/1176344136

Scoulding, B., Chu, D., Ona, E., and Fernandes, P. G. 2015. Target strengths of two abundant mesopelagic fish species. The Journal of the Acoustical Society of America, 137: 989–1000. https://doi.org/10.1121/1.4906177

Shotton, R., and Bazigos, G. P. 1984. Techniques and considerations in the design of acoustic surveys. Rapports et Procès-Verbaux des Réunions du Conseil International pour l'Exploration de la Mer, 184. 34–57.

Simmonds, J. E., Armstrong, F., and Copland, P. J. 1996. Species identification using wideband backscatter with neural network and discriminant analysis. ICES Journal of Marine Science, 53: 189–195. https://doi.org/10.1006/jmsc.1996.0021

Simmonds, E. J., and Fryer, R. J. 1996. Which are better, random or systematic surveys? A simulation using North Sea herring as example. ICES Journal of Marine Science, 53: 39–50. https://doi.org/10.1006/jmsc.1996.0004

Simmonds, E. J., and MacLennan, D. N. 2005. Fisheries Acoustics: Theory and Practice, 2nd edition, Blackwell Publishing, Oxford. 437 pp.

Simmonds, E. J., Williamson, N. J., Gerlotto, F., and Aglen, A. 1992. Acoustic survey design and analysis procedures: a comprehensive review of current practice. ICES Cooperative Research Report No. 187. 131 pp.

Smith, J. N., Ressler, P. H., and Warren, J. D. 2010. Material properties of euphausiids and other zooplankton from the Bering Sea. The Journal of the Acoustical Society of America, 128: 2664–2680. https://doi.org/10.1121/1.3488673

Soule, M. A., Barange, M., and Hampton, I. 1995. Evidence of bias in estimates of target strength obtained with a split-beam echo-sounder. ICES Journal of Marine Science, 52: 139–144. https://doi.org/10.1016/1054-3139(95)80022-0

Stanton, T. K. 1985. Density estimates of biological sound scatterers using sonar echo peak PDFs. The Journal of the Acoustical Society of America, 78: 1868–1873. https://doi.org/10.1121/1.392773

Stanton, T. K. 1988. Sound scattering by cylinders of finite length. I. Fluid cylinders. The Journal of the Acoustical Society of America, 83: 55–63. https://doi.org/10.1121/1.396184

Stanton, T. K. 1989. Sound scattering by cylinders of finite length. III. Deformed cylinders. The Journal of the Acoustical Society of America, 86: 691–705. https://doi.org/10.1121/1.398193

Stanton, T. K., Chu, D., and Reeder, D. B. 2004. Non-Rayleigh acoustic scattering characteristics of individual fish and zooplankton. IEEE Journal of Ocean Engineering, 29: 260–268. 10.1109/JOE.2004.828208

Stanton, T. K., Chu, D., and Wiebe, P. H. 1996. Acoustic scattering characteristics of several zooplankton groups. ICES Journal of Marine Science, 53: 289–295. https://doi.org/10.1006/jmsc.1996.0037

Stanton, T. K, Chu, D., and Wiebe P. H. 1998a. Sound scattering by several zooplankton groups. II. Scattering models. The Journal of the Acoustical Society of America, 103: 236–253. https://doi.org/10.1121/1.421110

Stanton, T. K, Chu, D., Wiebe, P. H., Martin, L. V., and Eastwood, R. L. 1998b. Sound scattering by several zooplankton groups. I. Experimental determination of dominant scattering mechanism. The Journal of the Acoustical Society of America, 103: 225–235. https://doi.org/10.1121/1.421469

Stanton, T. K., Chu, D., Wiebe, P. H., and Clay, C. S. 1993. Average echoes from randomly oriented random-length finite cylinders: Zooplankton models. The Journal of the Acoustical Society of America, 94: 3463–3472. https://doi.org/10.1121/1.407200

Stanton T. K., and Clay, C. S. 1986. Sonar echo statistics as a remote-sensing tool: Volume and seabed. IEEE Journal of Oceanic Engineering, 11: 79–95. https://doi.org/10.1109/JOE.1986.1145139

Stanton, T. K, Clay, C. S., and Chu, D. 1993. Ray representation of sound scattering by weakly scattering deformed fluid cylinders: Simple physics and application to zooplankton. The Journal of the Acoustical Society of America, 94: 3454–3462. https://doi.org/10.1121/1.407199

Stanton, T. K., Sellers, C., and Jech, J. M. 2012. Resonance classification of mixed assemblages of fish with swimbladders using a modified commercial broadband acoustic echosounder at 1–6 kHz. Canadian Journal of Fisheries and Aquatic Sciences, 69: 854–868. https://doi.org/10.1139/f2012-013

Stanton, T. K., Wiebe, P. H., Chu, D., Benfield, M. C., Scanlon, L., Martin, L., and Eastwood, R. L. 1994a. On acoustic estimates of zooplankton biomass. ICES Journal of Marine Science, 51: 505–512. https://doi.org/10.1006/jmsc.1994.1051

Stanton, T. K., Wiebe, P. H., Chu, D., and Goodman, L. 1994b. Acoustic characterisation and discrimination of marine zooplankton and microstructure. ICES Journal of Marine Science, 51: 469–479. https://doi.org/10.1006/jmsc.1994.1048

Stoner, A. W., Ryer, C. H., Parker, S. J., Auster, P. J., and Wakefield, W. W. 2008. Evaluating the role of fish behavior in surveys conducted with underwater vehicles. Canadian Journal of Fisheries and Aquatic Sciences, 65: 1230–1243. https://doi.org/10.1139/F08-032

Strutt, J. W. (Lord Rayleigh). 1919. XXXI. On the problem of random vibrations in one, two, or three dimensions. The London, Edinburgh, and Dublin Philosophical Magazine and Journal of Science, 37(220): 321–347. https://doi.org/10.1080/14786440408635894

Sund, O. 1935. Echo Sounding in Fishery Research. Nature, 135: 953. https://doi.org/10.1038/135953a0

Sæther M. 2009. Transducer with stable opening angle over a wide frequency-range. Design, construction and measurements. *(In Norwegian)*. Department of Physics and Technology, University of Bergen, Norway. 88 pp.

Tarantola, A. 2005. Inverse Problem Theory and Methods for Model Parameter Estimation. Society for Industrial and Applied Mathematics, Philadelphia. 339 pp. https://doi.org/10.1137/1.9780898717921

Theodoridis, S., and Koutroubas, K. 2008. Pattern Recognition, 4th edition. Academic Press, Cambridge, MA. 984 pp.

Tibshirani, R., Walther, G., and Hastie, T. 2001. Estimating the number of data clusters via the gap statistic. Journal of the Royal Statistical Society: Series B (Statistical Methodology), 63: 411–423. https://doi.org/10.1111/1467-9868.00293

Tichy, F. E., Solli, H., and Klaveness, H. 2003. Nonlinear effects in a 200-kHz sound beam and consequences for target-strength measurement. ICES Journal of Marine Science, 60: 571–574. https://doi.org/10.1016/S1054-3139(03)00033-X

Tomczak, M., Haffner, G. D., and Fronaes, E. 2002. False-bottom acoustic echo in mid water? A note on how to evaluate and prevent the interference. IEEE Journal of Oceanic Engineering, 27: 870–872. https://doi.org/10.1109/JOE.2002.804059

Torgersen, T., and Kaartvedt, S. 2001. *In situ* swimming behaviour of individual mesopelagic fish studied by split-beam echo target tracking. ICES Journal of Marine Science, 58: 346–354. https://doi.org/10.1006/jmsc.2000.1016

Traykovski, L. V. M., Stanton, T. K., Wiebe, P. H., and Lynch, J. F. 1998. Model-based covariance mean variance classification techniques: Algorithm development and application to the acoustic classification of zooplankton. IEEE Journal of Oceanic Engineering, 23: 344–364. https://doi.org/10.1109/48.725230

Trenkel, V. M., Berger, L., Bourguignon, S., Doray, M., Fablet, R., Massé, J., Mazauric, V., *et al*. 2009. Overview of recent progress in fisheries acoustics made by Ifremer with examples from the Bay of Biscay. Aquatic Living Resources, 22: 433–445. https://doi.org/10.1051/alr/2009027

Trenkel, V. M., Mazauric, V., and Berger, L. 2008. The new fisheries multibeam echosounder ME70: description and expected contribution to fisheries research. ICES Journal of Marine Science, 65: 645–655. https://doi.org/10.1093/icesjms/fsn051

Trevorrow, M. V., Mackas, D. L., and Benfield, M. C. 2005. Comparison of multifrequency acoustic and *in situ* measurements of zooplankton abundance in Knight Inlet, British Columbia. The Journal of the Acoustical Society of America, 117(6): 3574–3588. https://doi.org/10.1121/1.1920087

Urick, R. J. 1983. Principles of Underwater Sound, 3rd Edition, McGraw-Hill, New York. 444 pp.

Urmy, S. S., and Horne, J. K. 2016. Multi-scale responses of scattering layers to environmental variability in Monterey Bay, California. Deep-Sea Research Part I: Oceanographic Research Papers, 113: 22–32. https://doi.org/10.1016/j.dsr.2016.04.004

Urmy, S. S., Horne, J. K., and Barbee, D. H. 2012. Measuring the vertical distributional variability of pelagic fauna in Monterey Bay. ICES Journal of Marine Science, 69: 184–196. https://doi.org/10.1093/icesjms/fsr205

Warren, J. D., and Smith, J. N. 2007. Density and sound speed of two gelatinous zooplankton: ctenophore (*Mnemiopsis leidyi*) and lion's mane jellyfish (*Cyanea capillata*). The Journal of the Acoustical Society of America, 122: 574–580. https://doi.org/10.1121/1.2739433

Watkins, J. L., and Brierley, A. S. 1996. A post-processing technique to remove background noise from echo integration data. ICES Journal of Marine Science, 53: 339–344. https://doi.org/10.1006/jmsc.1996.0046

Weston, D. E. 1967. Sound propagation in the presence of bladder fish. *In* Underwater Acoustics, Volume 2, pp. 55–88. Ed. by V. M. Albers. Plenum Press, New York. 416 pp.

Weill, A., Scalabrin, C., and Diner, N. 1993. MOVIES–B: an acoustic detection description software. Application to shoal species' classification. Aquatic Living Resources, 6: 255–267. https://doi.org/10.1051/alr:1993026

Wiebe, P. H., Chu, D., Kaartvedt, S., Hundt, A., Melle, W., Ona, E., and Batta-Lona, P. 2010. The acoustic properties of *Salpa thompsoni*. ICES Journal of Marine Science, 67: 583–593. https://doi.org/10.1093/icesjms/fsp263

Wileman, D. A., Ferro, R. S. T., Fonteyne, R., and Millar, R. B. 1996.Manual of methods of measuring the selectivity of towed fishing gears. ICES Cooperative Research Report No. 215. 126 pp.

Williams, K., Punt, A. E., Wilson, C. D., and Horne, J. K. 2011. Length-selective retention of walleye pollock, *Theragra chalcogramma*, by midwater trawls. ICES Journal of Marine Science, 68: 119–129. https://doi.org/10.1093/icesjms/fsq155

Woillez, M., Ressler, P. H., Wilson, C. D., and Horne, J. K. 2012. Multifrequency species classification of acoustic-trawl survey data using semi-supervised learning with class discovery. The Journal of the Acoustical Society of America, 131: EL184–EL190. https://doi.org/10.1121/1.3678685

Ye, Z. 1997a. Resonant scattering of acoustic waves by ellipsoid air bubbles in liquids. The Journal of the Acoustical Society of America, 101: 681–685. https://doi.org/10.1121/1.418279

Ye, Z. 1997b. Low-frequency acoustic scattering by gas-filled prolate spheroids in liquids. The Journal of the Acoustical Society of America, 101: 1945–1952. https://doi.org/10.1121/1.418225

Ye, Z., Hoskinson, E., Dewey, R. K., Ding, L., and Farmer, D. M. 1997. A method for acoustic scattering by slender bodies. I. Theory and verification. The Journal of the Acoustical Society of America, 102: 1964–1976. https://doi.org/10.1121/1.419650

Yeh, C. 1967. Scattering of acoustic waves by a penetrable prolate spheroid. I. Liquid prolate spheroid. The Journal of the Acoustical Society of America, 42: 518–521. https://doi.org/10.1121/1.1910614

Zampolli, M., Jensen, F. B., and Tesei, A. 2009. Benchmark problems for acoustic scattering from elastic objects in the free field and near the seafloor. The Journal of the Acoustical Society of America, 125(1): 89–98. https://doi.org/10.1121/1.3027446

Zwolinski, J. P., Emmett, R. L., and Demer, D. A. 2011. Predicting habitat to optimize sampling of Pacific sardine (*Sardinops sagax*). ICES Journal of Marine Science, 68: 867–879. https://doi.org/10.1093/icesjms/fsr038

Annex 1: Case studies by methods described in Section 6

Table A1.1 Case studies referring to methods described in Section 6

Case study	Order	Species	Methods used	Link to CRR	Source
Benoit-Bird	1	Mesopelagics	Adaptive sampling based on *r(f)*	Guiding sampling	Moline and Benoit-Bird (2016)
Lawson and Fielding	2	*Euphausia superba*	SDWBA models used to determine *r(f)* limits for species ID	Applications of models, determining parameters for *r(f)* during surveys	
De Robertis	3	Various	Z-score	*r(f)*, feature library, data preprocessing	De Robertis *et al*. (2010)
Korneliussen	4	Various	Bayesian classification	*r(f)*, feature library, data preprocessing	Korneliussen *et al*. (2016)
Campanella	5	Reef fish	Robust Sparse K-Means (RSKC)	Unsupervised clustering	Campanella and Taylor (2016)
Sakinan	6		Artificial neural networks		

A1.1 Case Study 1: Adaptive sampling based on real-time target classification by means of ΔMVBS (and more)

Acoustic attenuation reduces the effective range of ship-mounted echosounders, particularly in the case of higher frequencies commonly used to detect and classify micronekton and nekton aggregations. Work undertaken by researchers from the University of Delaware and Oregon State University applied autonomous technology and classification techniques to carry out a detailed study of nektonic organisms in the mesopelagic zone. Kongsberg's Remote Environmental Monitoring Unit (REMUS) autonomous underwater vehicle (AUV) fitted with Simrad EK60 echosounders (38 and 120 kHz), logging and processing computers, and navigational equipment was used for the study, providing a stable platform with increased effective range and resolution at operational depths beyond that of ship-mounted systems (Moline *et al*., 2015).

The AUV's computer dedicated to processing data and communication of synthesized results for navigational purposes ran Echoview processing software to analyse data in real time, as well as a custom application for communicating the processed data-output product. Data processing comprised standard preliminary steps, such as seabed removal, depth correction, and noise removal, followed by an advanced workflow for automated and objective target classification:

1. detection of individual targets in each frequency,
2. elimination of targets present in only one of the two frequencies,
3. filtering of targets based on the expected difference in volume scattering across frequencies for the target species,
4. conversion of target strength to (a) length estimates and (b) density within a depth interval,
5. combining length and density to estimate biomass,

6. integration over a specified time- and depth-interval, and
7. application of binary-based approach to ascertain whether a biomass threshold has been met.

Once the threshold criteria have been met, this is communicated by the custom application to the navigation system, resulting in a change of survey plan, i.e. greater survey effort in the immediate area containing the targets of interest.

If required, the software data-processing workflow can easily be updated to adjust the classification routine for different species/targets of interest and other applications. Workflow steps to identify squid and an example of the threshold determination process are shown in Figures A1.1 and A1.2, respectively, and expected difference in volume scattering across frequencies (refer to step 3) is detailed in Benoit-Bird *et al.* (2008).

Such on-board analysis and classification process for guided sampling allows fine-scale measurements of spatial variability of targets of interest and contributes to enhancing our understanding of ecological processes such as predator/prey interactions, biogeochemical cycling, energy transfer, and the interactions between these processes throughout the entire water column (Benoit-Bird *et al.*, 2016).

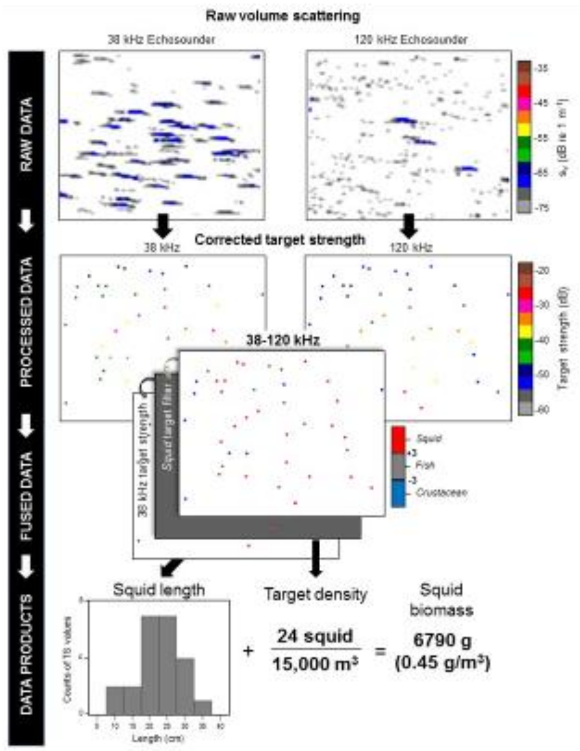

Figure A1.1. Raw data collected off the Californian coast in 2013 was analysed following this diagrammatic representation of data processing, synthesis, and data-product generation. Squid were the target organisms, and targets were classified to identify presence/absence of squid as a data product for use in AUV decision-making and autonomy. From Moline and Benoit-Bird (2016).

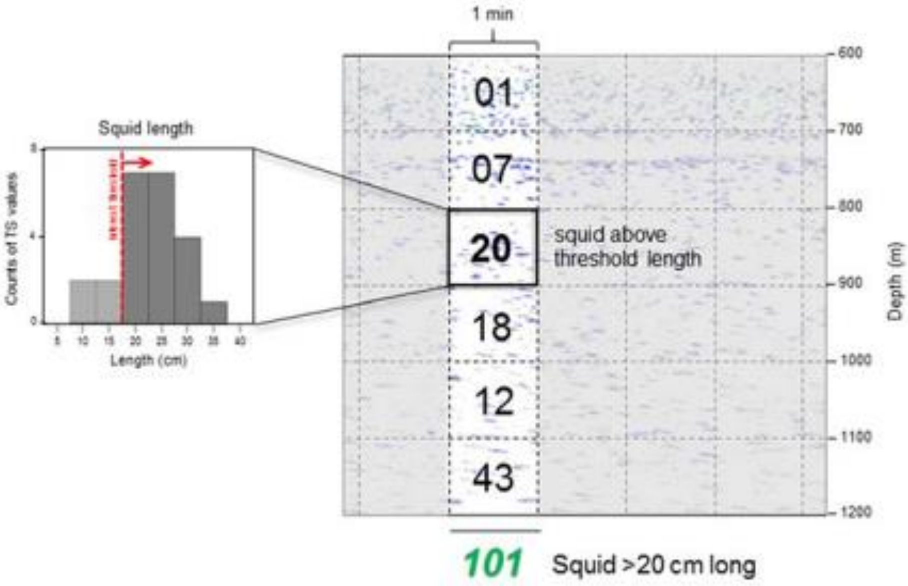

Figure A1.2. Threshold determination for guided sampling, using example data from off California in 2013. Squid number and length criteria feed into vehicular navigation. From Moline and Benoit-Bird (2016).

References

Benoit-Bird, K., Gilly, W., Au, W., and Mate, B. 2008. Controlled and *in situ* target strengths of the jumbo squid *Dosidicus gigas* and identification of potential acoustic scattering sources. The Journal of the Acoustical Society of America, 123: 1318–1328. https://doi.org/10.1121/1.2832327

Benoit-Bird, K., Southall, B., and Moline, M. 2016. Predator-guided sampling reveals biotic structure in the bathypelagic. Proceedings of the Royal Society B: Biological Sciences, 283(1825): 20152457. https://doi.org/10.1098/rspb.2015.2457

Campanella, F., and Taylor, J. C. 2016. Investigating acoustic diversity of fish aggregations in coral reef ecosystems from multifrequency fishery sonar surveys. Fisheries Research, 181: 63–76. https://doi.org/10.1016/j.fishres.2016.03.027

De Robertis, A., McKelvey, D. R., and Ressler, P. H. 2010. Development and application of an empirical multifrequency method for backscatter classification. Canadian Journal of Fisheries and Aquatic Sciences, 67: 1459–1474. https://doi.org/10.1139/F10-075

Korneliussen, R. J., Heggelund, Y., Macaulay, G. J., Patel, D., Johnsen, E., and Eliassen, I. K. 2016. Acoustic identification of marine species using a feature library. Methods in Oceanography, 17: 187–205. https://doi.org/10.1016/j.mio.2016.09.002

Moline, M. A., and Benoit-Bird, K. 2016. Sensor Fusion and Autonomy as a Powerful Combination for Biological Assessment in the Marine Environment. Robotics, 5(1): 4. https://doi.org/10.3390/robotics5010004

Moline, M. A., Benoit-Bird, K., O'Gorman, D., and Robbins, I. C. 2015. Integration of scientific echo sounders with an adaptable autonomous vehicle to extend our understanding of animals from the surface to the bathypelagic. Journal of Atmospheric and Oceanic Technologies, 32: 2173–2186. https://doi.org/10.1175/JTECH-D-15-0035.1

A 1.2 Case study 2: dB difference based on theoretical models of Antarctic krill

Antarctic krill (*Euphausia superba*) are one of the key species in the Antarctic marine foodweb, both as prey to a wide variety of dependent species as well as being commercially harvested (Atkinson *et al*., 2009; Nicol *et al*., 2011). They are considered to influence ocean biogeochemistry and, therefore, the carbon pump (Tovar-Sanchez *et al*., 2007). Antarctic krill are also notable for their formation of dense and typically monospecific aggregations (Watkins, 1986) that lend themselves to acoustic quantification and classification.

The commercial exploitation of krill is managed under the direction of the Convention for the Conservation of Antarctic Marine Living Resources (CCAMLR). This management is informed by acoustic surveys of krill density and distribution using an historical international synoptic survey (hereafter CCAMLR 2000 survey; Hewitt *et al*., 2004; Watkins *et al*., 2004; Fielding *et al*., 2011), national interannual surveys (Reiss *et al*., 2008; Fielding *et al*., 2014; Kinsey *et al*., 2015; Skaret *et al*., 2015), national research programmes (Cox *et al*., 2015) and future plans for fishing vessels (Watkins *et al*., 2015). In addition to CCAMLR-related efforts, acoustic techniques are also commonly used in studies of krill ecology and predator–prey interactions (Nowacek *et al*., 2011; Schmidt *et al*., 2011).

The current classification method employed by these studies to attribute acoustic data to krill utilizes a dB-differences technique (or relative frequency response) applied to the S_v data typically averaged over 50 pings (reflecting a horizontal resolution of 100 s or 500 m at a survey speed of 10 knots) and 5 m vertical resolution. An objective method for identification was initially followed using the two-frequency dB fixed windows of Maduriera *et al*. (1993) and Watkins and Brierley (2002) of $S_{V120\text{kHz}-38\text{kHz}}$ 2–12 or 2–16 dB re m^{-1}, respectively, derived empirically from aggregations of known composition based on concurrent net sampling. Often such dual-, and later multifrequency, approaches have been used in conjunction with thresholding as an additional step to exclude more weakly scattering targets than krill. Thresholds are typically based on likely minimum numerical densities, sometimes in combination with estimates of visual acuity, sensing distances, and minimum packing densities (Lawson *et al*., 2008).

In 2005, the use of fixed dB windows changed to survey-specific windows derived using an empirically validated scattering model, the stochastic distorted-wave Born approximation (SDWBA; McGehee *et al*., 1998; Demer and Conti, 2003), which allowed the inclusion of more frequencies into the identification technique (in principle, any frequency combination, but in practical application, $S_{v120\text{kHz}-38\text{kHz}}$ and $S_{v200\text{kHz}-120\text{kHz}}$) and provided a means to constrain the dB windows to the size range of krill measured in the survey area, thereby minimizing the chance of misclassifying backscattering from other types of scatterer as krill associated with the use of a broad fixed window. Parameterization of the SDWBA for Antarctic krill with material properties, target shape, target anatomy, and orientation will all influence the dB windows generated to identify krill. Of these parameters, orientation has a particularly strong influence on the modelled target strength of krill, although the morphology has also been shown to contribute significantly to TS (Calise and Skaret, 2011).

The parameterization of the SDWBA currently used by the Antarctic studies above includes the density contrast (g) and sound–speed contrast (h) taken from Foote (1990), the generic krill shape described by McGehee *et al*. (1998), and updated by Demer and Conti (2003) to be 40% fatter, and a normal distribution of orientations of N[–20°, 28°]. This orientation N[mean°, standard deviation°] was estimated by a least-squares inversion of the full SDWBA model using the krill length distributions measured during the CCAMLR 2000 survey and compared with the observed differences in volume-backscattering strengths (S_v) at 120 and 38 kHz (Conti and Demer, 2006; CCAMLR, 2010).

As an example of its use, the technique is applied to acoustic data collected as part of the British Antarctic Surveys Western Core Box (WCB; Fielding *et al*., 2014) during RRS "James Clark Ross" cruise 304 (JR304). To parameterize the SDWBA for target identification, the length frequency distribution of Antarctic krill (Figure A1.3) were collected from trawls made using an RMT8 (rectangular midwater trawl) with a 4.5-mm mesh size and mouth opening of 8 m^2. Trawls were targeted on krill swarms using the acoustic data, and up to 100 krill were measured from each trawl for total length (TL) from the anterior edge of the eye to the tip of the telson and rounded down (Morris *et al*., 1988). Volume backscattering strength data (S_v; dB re 1 m^{-1}) were collected solely during daylight using a calibrated Simrad EK60 operating at 38, 70, 120, and 200 kHz; in this specific case, a 30 km transect (along WCB leg 4_1) is used as the example. The raw acoustic data were cleaned for attenuated signal (following Ryan *et al*., 2015), background noise (following Watkins and Brierley, 1996) and impulsive "spike" noise (following Fielding *et al*., 2014) using the software Echoview™. Finally, the cleaned data were averaged into 500 m horizontal and 5 m vertical cells on which the identification procedure was carried out.

The target strength of krill modelled using the SDWBA, parameterized as detailed above, was calculated for 38, 120, and 200 kHz (Figure A1.4 left panel). The variable dB windows for $S_{v120kHz-38kHz}$ (0.4 to 14.3 dB re 1 m^{-1}) and $S_{v200kHz-120kHz}$ (−5.3 to 3.9 dB re 1 m^{-1}) were calculated as the minimum and maximum ΔS_v values based on the distribution of 95% of the krill length frequencies estimated from a cumulative distribution function (with tails of 2.5% at each end) and rounded to smaller/larger 10 mm (this results in a window for 20–60 mm sized krill during JR304, Figure A1.4 right panel). Using these windows, 53.5% of the total nautical area scattering coefficient (s_A, m^2 nautical miles^{-2}) was attributed to krill using the $S_{v120kHz-38kHz}$, and this is was further reduced to 44.9% using the $S_{v200kHz-120kHz}$ window (Table A1.2)

Compared with the traditional fixed $S_{v120kHz-38kHz}$ window of 2–16 dB re 1 m^{-1}, this survey-specific window allows, via the lower limit of 0.4, for the possibility of large krill (60 mm) that are found in the catches, via the upper limit of 14.3 dB re 1 m^{-1}, avoids possible contamination by smaller non-krill scatterers; the addition of the $S_{v200kHz-120kHz}$ criteria further increases the likelihood of accurate classification. The model-based approach to defining context-specific dB windows hence offers substantial flexibility and utility, although its accuracy, of course, hinges on accurate knowledge of the krill length distribution and proper model parameterization. Ongoing efforts are, therefore, seeking to characterize possible seasonal, spatial, and vertical variability of these parameters (e.g. Chu and Wiebe, 2005).

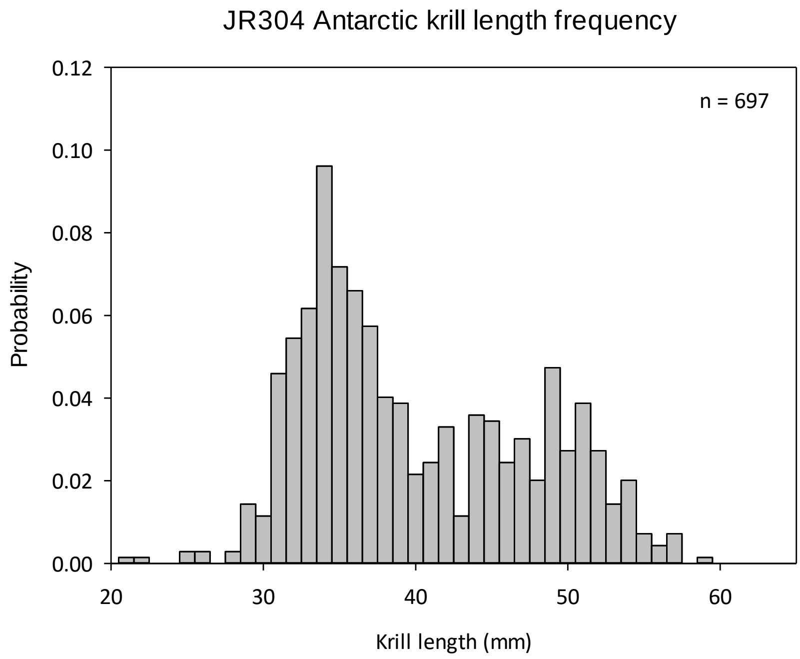

Figure A1.3 Antarctic krill length frequency probability density function. Antarctic krill total length (TL) in mm. In all, 697 krill were measured from 7 net hauls.

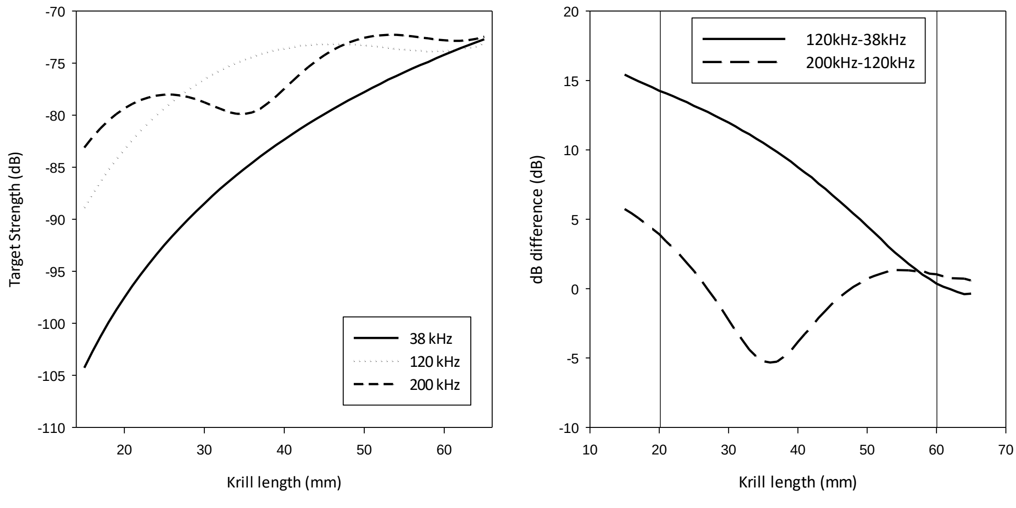

Figure A1.4. Left panel: Antarctic krill target strength at 38, 120 and 200 kHz calculated using the SDWBA, parameterized using values of g and h given in Foote (1990), a fatness coefficient of 40% (Demer and Conti, 2004) applied to the 2-D shape representation described by McGehee *et al.* (1998), and an orientation of N[-20°, 28°] after CCAMLR, 2010. Right panel: dB differences calculated for $S_{v120kHz-38kHz}$ and $S_{v200kHz-120kHz}$. The red shaded box identifies the $S_{v120kHz-38kHz}$ window for cruise JR304 and the blue shaded box identifies the $S_{v200kHz-120kHz}$ window.

Table A1.2. 120 kHz nautical area scattering coefficient (s_A) integrated to 250 m across transect for cleaned resampled data, data identified as krill using $S_{v120kHz\text{–}38kHz}$, and data identified as krill using $S_{v120kHz\text{–}38kHz}$ and $S_{v200kHz\text{–}120kHz}$.

	Cleaned resampled 120 kHz (Figure A2.3c)	$S_{v120kHz\text{–}38kHz}$ identified krill targets (Figure A2.3d)	$S_{v120kHz\text{–}38kHz}$ and $S_{v200kHz\text{–}120kHz}$ identified krill targets (Figure A2.3e)
Nautical area scattering coefficient (s_A, m^2 nautical mile^{-2})	169.58	90.80	76.07

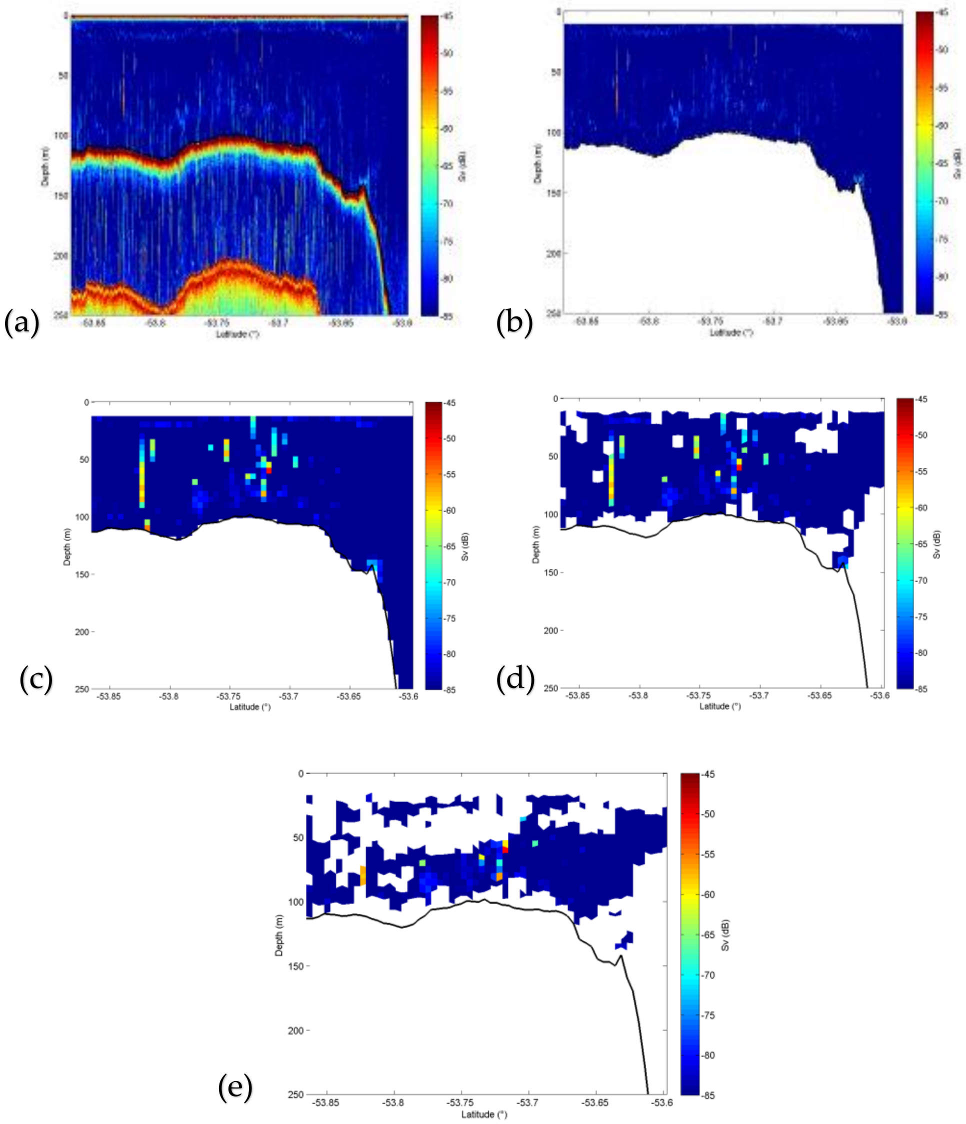

Figure A1.5. (a) Raw 120 kHz acoustic backscatter data (S_v, dB re 1 m^{-1}); (b) cleaned 120-kHz acoustic backscatter data; (c) averaged (500 m horizontal by 5 m vertical) 120 kHz acoustic backscatter data; (d) 120 kHz acoustic backscatter data identified as krill using $S_{v120kHz\text{–}38kHz}$; and (e) 120 kHz acoustic backscatter data identified as krill using $S_{v120kHz\text{–}38kHz}$ and $S_{v200kHz\text{–}120kHz}$. The seabed is delineated by the black line.

References

Atkinson, A., Siegel, V., Pakhomov, E. A., Jessopp, M. J., and Loeb, V. 2009. A re-appraisal of the total biomass and annual production of Antarctic krill. Deep-Sea Research Part I: Oceanographic Research Papers, 56: 727–740. https://doi.org/10.1016/j.dsr.2008.12.007

Calise, L., and Skaret, G. 2011. Sensitivity investigation of the SDWBA Antarctic krill target strength model to fatness, material contrast and orientation. CCAMLR Science, 18: 97–122.

CCAMLR. 2010. Report of the Fifth Meeting of the Subgroup on Acoustic Survey and Analysis Methods (Cambridge, UK, 1 to 4 June 2010). Scientific Committee for the Conservation of Antarctic Marine Living Resources SC-CCAMLR. Document No. SC-CAMLR-XXIX/06.

Chu, D., and Wiebe, P. H. 2005. Measurements of sound-speed and density contrasts of zooplankton in Antarctic waters. ICES Journal of Marine Science, 62: 818–831. https://doi.org/10.1016/j.icesjms.2004.12.020

Conti, S. G., and Demer, D. A. 2006. Improved parameterization of the SDWBA for estimating krill target strength. ICES Journal of Marine Science, 63: 928–935. https://doi.org/10.1016/j.icesjms.2006.02.007

Cox, M. J., Ladroit, Y., Escobar-Flores, P., and O'Driscoll, R. L. 2015. A biomass estimate of Antarctic krill *Euphausia superba*) at the Balleny Islands. CCAMLR working group paper WG-EMM-15/17. 14 pp.

Demer, D. A., and S. G. Conti. 2003. Validation of the stochastic distorted-wave, Born-approximation model with broad-bandwidth, total target-strength measurements of Antarctic krill. ICES Journal of Marine Science, 60: 625–635, Erratum, 61: 155–156. https://doi.org/10.1016/j.icesjms.2003.12.002

Fielding, S., Watkins, J., Cossio, A., Reiss, C., Watters, G., Calise, L., Skaret, G., *et al*. 2011. The ASAM 2010 assessment of krill biomass for Area 48 from the Scotia Sea CCAMLR 2000 synoptic survey. Working Group on Ecosystem Monitoring and Management (Busan, Republic of Korea, 11 to 22 July 2011). Commission for the Conservation of Antarctic Marine Living Resources (CCAMLR). Document No. SC-CAMLR-XXX/03. 9 pp.

Fielding, S., Watkins, J. L., Trathan, P. N., Enderlein, P., Waluda, C. M., Stowasser, G., Tarling, G. A., *et al*. 2014. Interannual variability in Antarctic krill (*Euphausia superba*) density at South Georgia, Southern Ocean: 1997–2013. ICES Journal of Marine Science, 71(9): 2578–2588. https://doi.org/10.1093/icesjms/fsu104

Foote, K. G. 1990. Speed of sound in *Euphausia superba*. The Journal of the Acoustical Society of America, 87: 1405–1408. https://doi.org/10.1121/1.399436

Hewitt, R. P., Watkins, J., Naganobu, M., Sushin, V., Brierley, A. S., Demer, D., Kasatkina, S., *et al*. 2004. Biomass of Antarctic krill in the Scotia Sea in January/February 2000 and its use in revising an estimate of precautionary yield. Deep-Sea Research Part II: Topical Studies in Oceanography, 51(12–13): 1215–1236. https://doi.org/10.1016/j.dsr2.2004.06.011

Kinzey, D., Watters, G. M., and Reiss, C. S 2015. Selectivity and biomass measures in an age-based assessment of Antarctic krill (*Euphausia superba*). Fisheries Research, 168: 72–84. https://doi.org/10.1016/j.fishres.2015.03.023

Lawson, G. L., Wiebe, P. H., Stanton, T. K., and Ashjian, C. J. 2008. Euphausiid distribution along the Western Antarctic Peninsula - Part A: Development of robust multi-frequency acoustic techniques to identify euphausiid aggregations and quantify euphausiid size, abundance, and biomass. Deep-Sea Research Part II: Topical Studies in Oceanography, 55: 412–431. https://doi.org/10.1016/j.dsr2.2007.11.010

Madureira, L. S. P., Ward, P., and Atkinson, A. 1993. Differences in backscattering strength determined at 120 and 38 kHz for three species of Antarctic macroplankton. Marine Ecology Progress Series, 93: 17–24.

McGehee, D. E., O'Driscoll, R. L., and Martin Traykovski, L. V. 1998. Effects of orientation on acoustic scattering from krill at 120 kHz. Deep-Sea Research Part II: Part II: Topical Studies in Oceanography, 45(7): 1273–1294. https://doi.org/10.1016/S0967-0645(98)00036-8

Morris, D. J., Watkins, J. L., Ricketts, C., Buchholz, F., and Priddle, J. 1988. An assessment of the merits of length and weight measurements of Antarctic krill *Euphausia superba*. British Antarctic Survey Bulletin, 79: 27–50.

Nicol, S., Foster, J., and Kawaguchi, S. 2011. The fishery for Antarctic krill - recent developments. Fish and Fisheries, 13: 30–40. https://doi.org/10.1111/j.1467-2979.2011.00406.x

Nowacek, D. P., Friedlaender, A. S., Halpin, P. N., Hazen, E. L., Johnston, D. W., Read, A. J., Espinasse, B., *et al*. 2011. Super-aggregations of krill and humpback whales in Wilhelmina Bay, Antarctic Peninsula. Plos One 6(4): e19173. https://doi.org/10.1371/journal.pone.0019173

Reiss, C. S., Cossio, A. M., Loeb, V., and Demer, D. A. 2008. Variations in the biomass of Antarctic krill (*Euphausia superba*) around the South Shetland Islands, 1996–2006. ICES Journal of Marine Science, 65: 497–508. https://doi.org/10.1093/icesjms/fsn033

Ryan, T. E., Downie, R. A., Kloser, R. J., and Keith, G. 2015. Reducing bias due to noise and attenuation in open-ocean echo integration data. ICES Journal of Marine Science, 72: 2482–2493. https://doi.org/10.1093/icesjms/fsv121

Schmidt, K., Atkinson, A., Steigenberger, S., Fielding, S., Lindsay, M. C. M., Pond, D. W., Tarling, G. A., *et al*. 2011. Seabed foraging by Antarctic krill: Implications for stock assessment, bentho-pelagic coupling, and the vertical transfer of iron. Limnology and Oceanography, 56: 1411–1428. 10.4319/lo.2011.56.4.1411

Skaret, G., Krafft, B. A., Calise, L., Watkins, J., Pedersen, R., and Godø, O. R. 2015. Evaluation of Antarctic krill biomass and distribution off the South Orkney Islands 2011-2015. Document WG-EMM-15/54. CCAMLR, Hobart, Australia.

Tovar-Sanchez, A., Duarte, C. M., Hernández-León, S., and Sañudo-Wilhelmy, S. A. 2007. Krill as a central node for iron cycling in the Southern Ocean. Geophysical Research Letters, 34: L11601. https://doi.org/10.1029/2006GL029096

Watkins, J. L. 1986. Variations in the size of Antarctic krill, *Euphausia superba* Dana, in small swarms. Marine Ecology Progress Series, 31: 67–73.

Watkins, J. L., and Brierley, A. S. 1996. A post-processing technique to remove background noise from echo-integration data. ICES Journal of Marine Science, 53: 339–344. https://doi.org/10.1006/jmsc.1996.0046

Watkins, J. L., and Brierley, A. S. 2002. Verification of the acoustic techniques used to identify Antarctic krill. ICES Journal of Marine Science, 59: 1326–1336. https://doi.org/10.1006/jmsc.2002.1309

Watkins, J. L., Hewitt, R., Naganobu, M., and Sushin, V. 2004. The CCAMLR 2000 Survey: a multinational, multi-ship biological oceanography survey of the Atlantic sector of the Southern Ocean. Deep-Sea Research Part II: Topical Studies in Oceanography, 51: 1205–1213. https://doi.org/10.1016/j.dsr2.2004.06.010

A1.3 Case study 3: Application of frequency response for species classification during acoustic surveys in Alaska

Motivation

Acoustic–trawl surveys of walleye pollock (*Gadus chalcogrammus*) are regularly conducted in Alaska to support fisheries management (Karp and Walters, 1994). During these surveys, acoustic backscatter measurements are allocated to species based on the examination of echograms by experienced analysts and targeted trawling of aggregations with pelagic and bottom trawls (Honkalehto *et al*., 2009). By the mid-2000s, echosounder technology had progressed to the point that acoustic data were routinely being collected at 4–5 frequencies (i.e. 18, 38, 120, 200 kHz and sometimes 70 kHz) but the multifrequency information was not being used for species classification.

At the time, instrumentation, methods, and software for routine multifrequency acoustic measurement via multiple narrowband echosounders (Higginbottom *et al*., 2000; Korneliussen and Ona, 2002; Korneliussen *et al*., 2008) were becoming available, and promising results that had used multifrequency information to inform acoustic species classifications (Fernandes *et al*., 2006, and references therein) were being reported. In the areas of Alaska where pollock are surveyed, the pelagic communities are generally dominated by a few species, as is often the case in high-latitude areas. These areas are likely to be environments where the use of frequency response as the basis for acoustic classification could be informative.

At the outset, the study chose to quantify the frequency response of dominant scatterers in the survey areas and evaluate how a relatively simple classification approach would perform in distinguishing among major scattering groups observed in pollock surveys in Alaska. The aim was to develop a method that could be implemented during routine surveys. In addition, only frequency response (i.e. rather than backscatter strength or other information such as previous distributions of each species or echotrace characteristics of aggregations; Reid, 2000), would be considered as this was thought to be less dependent on fish density and behaviour and thus potentially a more robust classifier. Thus, the goals were to 1) document the frequency response of the organisms encountered during these surveys and 2) develop an objective technique to classify backscatter to taxonomic categories that could be easily integrated with survey operations and the software tools available at the time.

Methods

An empirical approach was undertaken; a library of the relative frequency response was compiled in instances where species composition had been shown, by trawl sampling, to be dominated by a single species or taxon (see De Robertis *et al*., 2010 for details). Survey trawls where ≥ 4 frequencies were available ($n = 375$) were screened by catch composition, and those trawls where the catch composition was dominated by a single species or group were included in further analysis.

Initial analysis of frequency response revealed that spatially averaging acoustic data was essential to reduce variability (see Section 5.6.5 and Figure 1 in De Robertis *et al*., 2010) and low signal-to-noise data needed to be identified and removed from further consideration (see Section 5.6.4 and De Robertis and Higginbottom, 2007) to avoid artefacts from noise. Backscatter occurring in the trawl path was isolated to maximize the probability that the trawl catch reflected the species causing the backscatter, and the frequency response for cells with above a minimum threshold ($S_v > -70$ dB re 1 m^{-1}), and a signal-to-noise ratio of > 10 dB was computed in 5 m × 5 ping analysis cells. This cell size was empirically determined based on a decrease in the variance of the frequency response with increasing cell size (cf. Figure 1 in De Robertis *et al*., 2010). Histograms of the pairwise frequency response revealed that the spatially averaged observations (expressed in logarithmic units, i.e. $\Delta S_{vf1-f2} = S_{v,f1} - S_{v,f2}$) generally could be approximated by a normal distribution (i.e. the mean and standard deviation were used to summarize pairwise frequency measurements).

A Z-score (normal deviate, $\overline{Z}$) approach was used to summarize the relative frequency response and to evaluate the degree to which an unclassified measurement corresponds to the relative frequency response of a known class of scatterers in the database of ground-truthed frequency differences (De Robertis *et al*., 2010). One practical advantage of this approximation is that this provided a metric that could be summarized using the post-processing tools employed during the surveys (i.e. no additional software or processing steps were required). The average Z-score across all frequency pairs provides a convenient measure of confidence in the cell classification, expressed in units of standard deviations relative to the measured relative frequency response for taxon *m*. For example, a backscatter observation with a $\overline{Z}_{pollock}$ of 0.5 compared is much more consistent with backscatter from pollock than one with a $\overline{Z}_{pollock}$ of 2.5, as 2.5 standard deviations is much farther from the mean than 0.5 standard deviations.

A workflow[1], which did not require user input, was developed that allowed the Z-score relative to those for taxa in the trawl ground-truthed library for a given set of acoustic measurements (Figure A1.6**)** classifying backscatter to taxonomic classes (e.g. pollock vs. euphausiids) as a binary decision based on Z-score alone (see De Robertis *et al*., 2010 for details). The Z-scores were used to generate a classification in which the label corresponding to a library component (e.g. Z-score relative to pollock is computed using the pollock mean and s.d. at each frequency pair tabulated in the library) is assigned to each backscatter observation. In addition, the aggregate frequency response of multiple adjacent cells is considered in the classification as one and is unlikely to observe high average Z-scores if the species identification is correct (i.e. cases in which many observations are in the tails of the expected distribution are removed as multiple observations from the tails of the distribution are unlikely). The spatially averaged $\overline{Z}$ was also used as an index of classification certainty as the units of $\overline{Z}$ describe how well the sample conforms to the measured frequency response of a given class. For example, one would expect a spatially averaged $\overline{Z}$ of 1 for a given species and deviations from this (either spatially or temporally) should cause one to consider the effectiveness of the classification.

[1]An example implementation and tutorial is available at: http://support.echoview.com/WebHelp/Data_Processing/Classification/dB_difference_z_score.htm

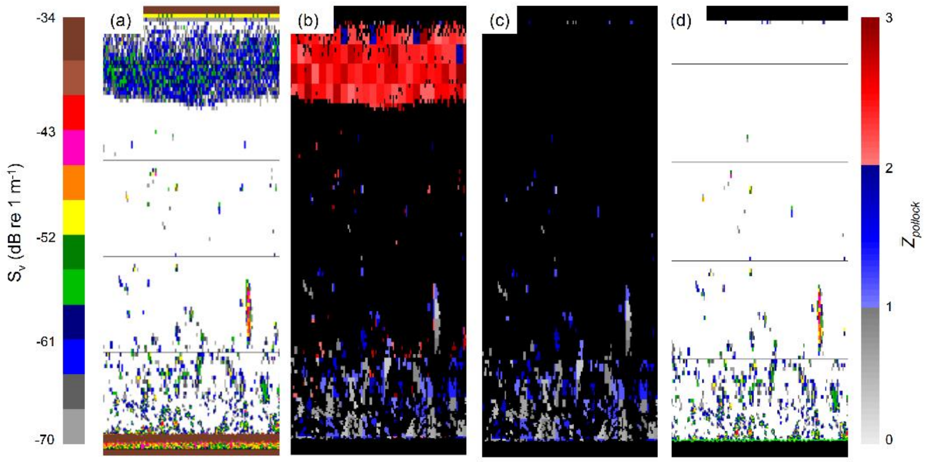

Figure A1.6. Example of implementation of the Z-score method in the eastern Bering Sea: (a) original 38 kHz echogram showing backscatter from demersal and pelagic walleye pollock (*Gadus chalcogrammus*) and a near-surface layer of unknown composition; (b) synthetic echogram of $\overline{Z}_{pollock}$ summarizing the frequency responses at 18, 38, 120, and 200 kHz; results are shown for all samples above the integration threshold of −70 dB re 1 m^{-1} at 38 kHz; (c) as in (b), but implementing criteria excluding neighbouring cells where cells are, on average, only marginally consistent with pollock (De Robertis *et al.*, 2010). (d) 38 kHz echogram showing all samples with a frequency response consistent with that of pollock. Colour scales for 38 kHz S_v (left) and pollock (right) are shown, and black horizontal lines demarcate 25 m depth intervals. Reprinted with permission from De Robertis *et al.* (2010).

Results

A library of frequency responses was established by extracting acoustic data from a sizeable number of trawl sites with almost pure catches of pollock (n = 56 hauls) and euphausiids (n = 27) and small sample sizes of other species [n = 2–4 for capelin (*Mallotus villosus*), myctophids (Myctophidae), eulachon (*Thaleichthys pacificus*), and Pacific ocean perch (*Sebastes alutus*)]. These measurements (Figure A1.6) characterized the expected frequency response for pollock and euphausiids (Figure A1.7) and produced preliminary results for other less well-sampled species. Overall (see De Robertis *et al.*, 2010 for details), the data showed that (i) walleye pollock frequency responses were similar along a wide range of body size, (ii) fish with large gas-filled swimbladders (pollock, Pacific ocean perch, capelin) had similar frequency response, (iii) myctophids showed evidence of resonance close to 38 kHz, (iv) areas where jellyfish were captured show higher backscatter at 18 kHz, and (v) eulachon, which lack a swimbladder, showed evidence of higher backscatter at 120 kHz, consistent with the predictions of Gauthier and Horne (2004).

Pollock backscatter automatically classified using the Z-score method (i.e. based on frequency response alone with no user input) and the standard survey technique (i.e. based on trawls and expert examination of echograms) compared favourably in the eastern Bering Sea (Figure A1.8). The consistency between the estimates of pollock abundance based on the two methods indicates that, in the case of pollock in the eastern Bering Sea, the assumptions of the Z-score method are largely met. Similarly, the $\overline{Z}_{pollock}$ for backscatter identified as pollock was consistently in the range expected for pollock (1–1.2), which provides some confidence that the backscatter classified as pollock had a consistent frequency response over space and among cruises.

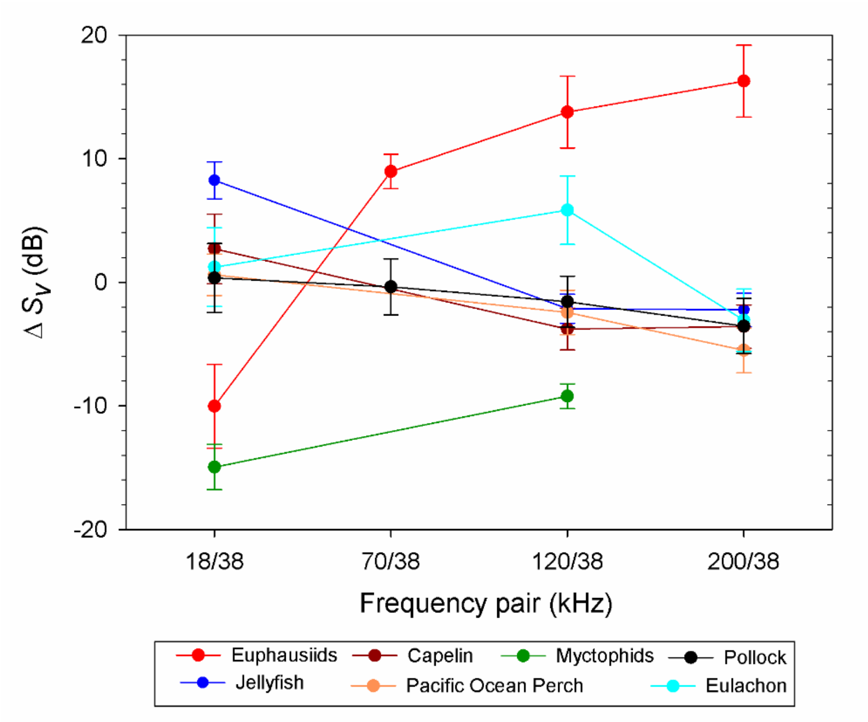

Figure A1.7. Means and standard deviations of frequency response (ΔS_v) estimated for groups of fish and invertebrates commonly encountered during acoustic–trawl surveys in the Gulf of Alaska and eastern Bering Sea. Reprinted with permission from De Robertis *et al.* (2010).

Discussion

The similarity between Z-score and survey pollock classifications indicates that an abundance index of pollock approximating that from a traditional survey can successfully be made with species identification based solely on relative frequency response in this environment. However, one must keep in mind that the eastern Bering Sea midwater fish community is dominated by a few abundant species (e.g. Honkalehto *et al.*, 2009; De Robertis and Cokelet, 2012) and acoustic species classification based on relative frequency response and other methods will be more challenging in more diverse environments.

The Z-score method is now routinely implemented during surveys of Alaska pollock. It is primarily used to generate real-time synthetic echograms to establish whether observed backscatter has a frequency response consistent with pollock. This is used as an additional source of information to inform the decision to deploy a trawl during surveys and as a source of information when backscatter is being allocated to species by an analyst. In addition, the method has been used for species classification in cases where trawl samples are not available (De Robertis and Cokelet, 2012) or as an initial filter to exclude backscatter that is unlikely to be from the target species (De Robertis *et al.*, 2017).

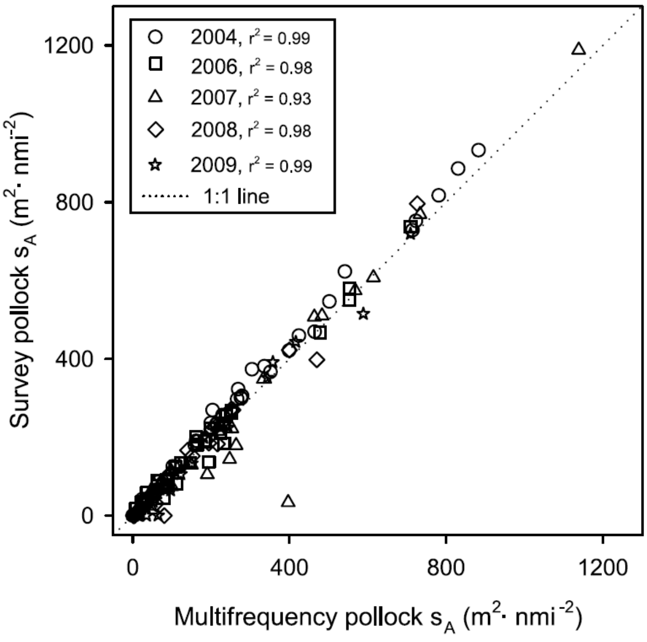

Figure A1.8. Comparison of pollock backscatter based on multifrequency identification of pollock, with pollock backscatter identified in the acoustic survey for five surveys between 2004 and 2009. Each point represents a transect mean. The figure legend lists the *r*² resulting from linear regression of the multifrequency **and survey pollock abundance in each year. The outlier from 2007 shows a transect in which aggregations of rockfish were misidentified by the** Z-score **method as pollock due to their similar frequency response. Reprinted with permission from De Robertis *et al.* (2010).**

In addition, the Z-score method has been used as the basis for acoustic identification of euphausiids during the pollock surveys (Ressler *et al.*, 2012), and the measured euphausiid frequency response has been used in dual-frequency classifications (e.g. Benoit-Bird *et al.*, 2011; De Robertis and Cokelet, 2012). The euphausiid classifications appear to be robust. Follow-up trawl sampling principally captured euphausiids in areas with a frequency response expected for euphausiids (e.g. Ressler *et al.*, 2012; Simonsen *et al.*, 2016), which lends support to the acoustic classifications. In addition, a limited number of measurements of euphausiid frequency response using the same method produced very similar frequency responses for euphausiids in both the Barents Sea (Ressler *et al.*, 2015) and the Gulf of Alaska (Simonsen *et al.*, 2016). Although the ability to distinguish zooplankton from other scatterers based on frequency response is by no means novel (e.g. Watkins and Brierley, 2002), the method appears to be relatively robust to the assumptions made in the environments tested. There is substantial interest in euphausiid abundance, and the Z-score classification method has facilitated several studies of euphausiid population dynamics and predator–prey relationships (e.g. Sigler *et al.*, 2012; Ressler *et al.*, 2014, 2015; Hunt *et al.*, 2016; Simonsen *et al.*, 2016). An acoustic-based euphausiid abundance index based on this method is routinely considered as an "ecosystem indicator" as part of fisheries management deliberations in Alaska (Bolt and Zador, 2009).

The method described in this case study is quite simple. It was, by design, restricted to the arithmetic operations available in the software package used during these surveys at the time. For example, all frequency pairs are weighted equally, although some species may differ at some frequencies (e.g. compare eulachon and other species in Figure A1.7). Treating all frequency pairs equally will dilute the differences in frequency response. However, despite these inherent simplifications, the method has proved relatively robust and useful in separating species with large frequency differences (e.g. fish and zooplankton) in studies of relatively simple high-latitude ecosystems. However, it is unlikely that the method is sensitive enough to robustly distinguish between acoustically similar groups such as fish with non-resonant swimbladders fish [e.g. walleye pollock and rockfish (*Sebastes* spp.)]. This, if achievable, will require more sophisticated methods for characterizing frequency-dependent scattering measurements and their variance and will require other sources of information such as measurements over a broader frequency range.

It is important to recognize that success for methods of acoustic species classification will be situation-dependent. These methods typically rely on assumptions (e.g. that the primary scatterers largely do not coincide in space and that they differ in frequency response) and it should be expected that acoustic classifications are likely to fail under some circumstances. The utility and effectiveness of any approach is situation-dependent; classification success depends on the species composition, relative abundance, relative frequency response, and spatial overlap of the species assemblage present in the environment. To avoid making incorrect interpretations, it is important to be able to identify the situations under which a particular method will provide useful results (i.e. it may be unavoidable to make mistakes, but it may be possible to identify incorrect classifications so that incorrect inferences can be avoided). In this context, a goodness-of-fit criterion is a useful metric; a poor fit with the expected acoustic properties may indicate a violation of the underlying assumptions, and the goodness-of-fit should be monitored and suspect results critically investigated. The method described here provides a goodness-of-fit criterion (the Z-score) which can be used as a measure of confidence in the classification, and it has proved robust in several applications. It is straightforward to implement and can be adapted to other situations if the necessary parameters can be generated from empirical observations or theoretical predictions (Sakinan and Gücü, 2017). It could certainly be improved upon, e.g. using more sophisticated statistics (Anderson *et al*., 2007; Korneliussen, 2010), incorporating sources of information other than frequency response (Woodd-Walker *et al*., 2003), or averaging observations within aggregations to reduce variability (Korneliussen *et al*., 2009), format treatment of species mixtures (Woillez *et al*., 2012), and in some applications such additional considerations will be necessary. However, the method has proven useful in some applications in low-diversity ecosystems, and it may prove useful in other applications.

References

Anderson, C. I. H., Horne, J. K., and Boyle, J. 2007. Classifying multi-frequency fisheries acoustic data using a robust probabilistic classification technique. The Journal of the Acoustical Society of America, 121(6): El230–El237. https://doi.org/10.1121/1.2731016

Benoit-Bird, K. J., Kuletz, K., Heppell, S., Jones, N., and Hoover, B. 2011. Active acoustic examination of the diving behavior of murres foraging on patchy prey. Marine Ecology Progress Series, 443: 217–235, doi:10.3354/meps09408. http://www.jstor.org/stable/24875288

Boldt, J., and Zador, S. (Eds). 2009. Ecosystem Considerations for 2010. North Pacific Management Council, Anchorage, AK 99501. 191 pp. Available at http://www.afsc.noaa.gov/refm/docs/2009/ecosystem.pdf

De Robertis, A., and Cokelet, E. D. 2012. Distribution of fish and macrozooplankton in ice-covered and open-water areas of the Eastern Bering Sea. Deep-Sea Research Part II: Topical Studies in Oceanography, 65–70: 217–229. https://doi.org/10.1016/j.dsr2.2012.02.005

De Robertis, A., and Higginbottom, I. 2007. A post-processing technique to estimate the signal-to-noise ratio and remove echosounder background noise ICES Journal of Marine Science, 64: 1282–1291. https://doi.org/10.1093/icesjms/fsm112

De Robertis, A., McKelvey, D., and Ressler, P. H. 2010. Development and application of empirical multi-frequency methods for backscatter classification. Canadian Journal of Fisheries and Aquatic Sciences, 67: 1459–1474. https://doi.org/10.1139/F10-075

De Robertis, A., Taylor, K., Wilson, C. D., and Farley, E. V. 2017. Abundance and distribution of Arctic cod (*Boreogadus saida*) and other pelagic fishes over the U.S. Continental Shelf of the Northern Bering and Chukchi Seas. Deep-Sea Research Part II: Topical Studies in Oceanography, 135: 51–65. https://doi.org/10.1016/j.dsr2.2016.03.002

Fernandes, P. G., Korneliussen, R. J., Lebourges-Dhaussy, A., Masse, J., Iglesias, M., Diner, N., Ona, E., *et al*. 2006. The SIMFAMI project: species identification methods from acoustic multi-frequency information. Final Report to the EC Number Q5RS-2001-02054 (Report accessible from any of the authors).

Gauthier, S., and Horne, J. K. 2004. Acoustic characteristics of forage fish species in the Gulf of Alaska and Bering Sea based on Kirchhoff-approximation models. Canadian Journal of Fisheries and Aquatic Sciences, 61(10): 1839–1850. https://doi.org/10.1139/f04-117

Higginbottom, I. R., Pauly, T. J., and Heatley, D. C. 2000. Virtual echograms for visualization and post-processing of multiple-frequency echosounder data. *In* Proceedings of the Fifth European Conference on Underwater Acoustics, ECUA 2000, pp. 1497–1502. Ed. by M. E. Zakharia, P. Chevret, and P. Dubail. Office for Official Publications of the European Communities, Luxembourg.

Honkalehto, T., Jones, D., McCarthy, A., McKelvey, D., Guttormsen, M. A., Willams, K., and Williamson, N. J. 2009. Results of the echo integration-trawl survey of walleye pollock (*Theragra chalcogramma*) on the U.S. and Russian Bering Sea shelf in June and July 2008. NOAA Technical Memorandum NMFS-AFSC-194. 67 pp.

Hunt, G. L., Ressler, P. H., Gibson, G. A., De Robertis, A., Aydin, K., Sigler, M. F., Ortiz, I., *et al*. 2016. Euphausiids in the Eastern Bering Sea: A synthesis of recent studies of euphausiid production, consumption and population control. Deep-Sea Research Part II: Topical Studies in Oceanography, 134: 204–222. https://doi.org/10.1016/j.dsr2.2015.10.007

Karp, W. A., and Walters, G. E. 1994. Survey assessment of semi-pelagic gadoids: the example of walleye pollock, *Theragra chalcogramma* in the Eastern Bering Sea. Marine Fisheries Review, 56: 8–22.

Korneliussen, R. J. 2010. The acoustic identification of Atlantic mackerel. ICES Journal of Marine Science, 67: 1749–1758. https://doi.org/10.1093/icesjms/fsq052

Korneliussen, R. J., Diner, N., Ona, E., Berger, L., and Fernandes, P. 2008. Proposals for the collection of multifrequency acoustic data. ICES Journal of Marine Science, 65: 982–994. https://doi.org/10.1093/icesjms/fsn052

Korneliussen, R. J., Heggelund, Y., Eliassen, I. K., and Johansen, G. O. 2009. Acoustic species identification of schooling fish. ICES Journal of Marine Science, 66: 1111–1118. https://doi.org/10.1093/icesjms/fsp119

Korneliussen, R. J., and Ona, E. 2002. An operational system for processing and visualizing multi-frequency acoustic data. ICES Journal of Marine Science, 59: 293–313. https://doi.org/10.1006/jmsc.2001.1168

Reid, D. G. 2000. Report on echo trace classification. ICES Cooperative Research Report No. 238. 107 pp.

Ressler, P. H., Dalpadado, P., Macaulay, G. J., Handegard, N., and Skern-Mauritzen, M. 2015. Acoustic surveys of euphausiids and models of baleen whale distribution in the Barents Sea. Marine Ecology Progress Series, 527: 13–29. https://doi.org/10.3354/meps11257

Ressler, P. H., De Robertis, A., and Kotwicki, S. 2014. The spatial distribution of euphausiids and pollock in the eastern Bering Sea does not imply top-down control by predation. Marine Ecology Progress Series, 503: 111–122. https://doi.org/10.3354/meps10736

Ressler, P. H., De Robertis, A., Warren, J. D., Smith, J. D., and Kotwicki, S. 2012. Developing an acoustic index of euphausiid abundance to understand trophic interactions in the Bering Sea ecosystem. Deep-Sea Research Part II: Topical Studies in Oceanography, 65–70: 184–195. https://doi.org/10.1016/j.dsr2.2012.02.015

Sakınan, S., and Gücü, A. C. 2017. Spatial distribution of the Black Sea copepod, *Calanus euxinus*, estimated using multi-frequency acoustic backscatter. ICES Journal of Marine Science, 74: 832–849. https://doi.org/10.1093/icesjms/fsw183

Sigler, M. F., Kuletz, K. J., Ressler, P. H., Friday, N. A., Wilson, C. D., and Zerbini, A. N. 2012. Marine predators and persistent prey in the southeast Bering Sea. Deep-Sea Research Part II: Topical Studies in Oceanography, 65–70: 292–303. https://doi.org/10.1016/j.dsr2.2012.02.017

Simonsen, K. A., Ressler, P. H., Rooper, C., and Zandor, S. G. 2016. Spatio-temporal distribution of euphausiids: an important component to understanding ecosystem processes in the Gulf of Alaska and eastern Bering Sea. ICES Journal of Marine Science, 73: 2020–2036. https://doi.org/10.1093/icesjms/fsv272

Watkins, J. L., and Brierley, A. S. 2002. Verification of the acoustic techniques used to identify Antarctic krill. ICES Journal of Marine Science, 59: 1326–1336. https://doi.org/10.1006/jmsc.2002.1309

Woillez, M., Ressler, P. H., Wilson, C. D, and Horne, J. K. 2012. Multifrequency species classification of acoustic-trawl survey data using semi-supervised learning with class discovery. The Journal of the Acoustical Society of America, 131: EL184–EL190. https://doi.org/10.1121/1.3678685

Woodd-Walker, R. S., Watkins, J. L., and Brierley, A. S. 2003. Identification of Southern Ocean acoustic targets using aggregation backscatter and shape characteristics. ICES Journal of Marine Science, 60: 641–649. https://doi.org/10.1016/S1054-3139(03)00062-6

A1.4 Case study 4: Identification of mackerel, sandeel, and capelin by means of LSSS in three different ecosystems

The LSSS software

The Large Scale Survey System (LSSS) software analyses acoustic backscatter from marine organisms such as zooplankton and pelagic and demersal fish. It is designed for efficient post-processing of large amounts of echosounder and sonar data and contains tools to isolate echotraces by creating regions and assigning categories to these regions. The LSSS preprocessing facility (KORONA) carries out time-intensive automated processing of acoustic data. With automatic categorization the primary intention is to provide information that allows more objective scrutiny of the echograms and, second, to accelerate manual scrutiny.

Populating the feature library

Data were processed in a standardized manner to remove noise, bad data, and to average data. Acoustic multifrequency data that originated from registrations that were monospecific according to biological sampling were used to populate a library of statistical properties of measured acoustical variables. In its current implementation, the logarithmic relative frequency responses, R(f), and the scattering strength, S_v, are main acoustic variables used by the LSSS (Korneliussen *et al*., 2016). The procedure and theory for extracting the statistical properties, as implemented in LSSS, are described in Korneliussen *et al*. (2016). The content of the feature library is used to group the scatterers into scattering-classes. The acoustic feature library contains statistical properties, such as mean, variance, and covariance of the acoustic variables for each of the acoustic library categories (ALC).

Species identification – acoustic categorization

Data processing started, as described above, and continued by detecting schools and categorizing acoustic targets. Two types of automatic categorization were used simultaneously: one based on scattering models through inversio**n** (Section 6.1.2) **a**nd one based on an acoustic feature library described here. The acoustic variables in the library are expected to be lognormal distributed, and the number of acoustic variables equals the number of available frequencies ($R(f)$ at all frequencies, f, except 38 kHz, where $S_v(38)$ is used), e.g. 6 for RV "G. O. Sars" until 2016. The method also works for broadband data as it can be split into several narrower bands, so after 2016, the number of variables could be e.g. 25 on board RV "G. O. Sars".

A multidimensional, lognormal probability density function (PDF) is fitted to the data and compared to the content of the feature library. As such, multidimensional comparison is difficult to visualize. The comparison is shown for one dimension only. Figure A1.9 shows the fitted PDF for two hypothetical acoustic library categories (ALC). Since $R(x)_{\omega 2} > R(x)_{\omega 1}$, which indicates category ω_2 as the most likely if the separation is based on one feature only. Note that $R(f) = 10\log_{10}[r(f)]$.

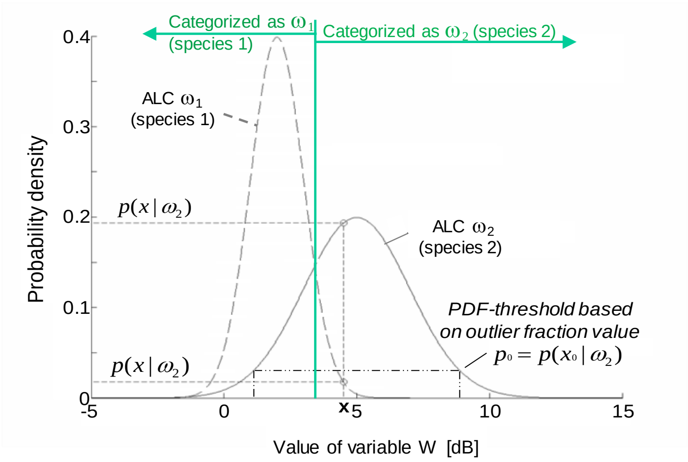

Figure A1.9. Probability density function of one acoustic variable W (i.e. one dimension) for two acoustic library categories (ALC) is used to determine if measurement x (of acoustic variable W) is most likely to originate in species 1 or 2. Here p(x|ω2) > p(x|ω1) indicates species 2 as the most likely. In practice, many such comparisons between different features and categories contribute to the chosen category.

Figure A1.10 shows two dimensions, *R(70)* and *R(200)*, of the hyper ellipses of the same acoustic library categories (ALC). The covariances among the individual acoustic variables are considered as well as the variance. This means that the contours of the distributions will be ellipses, whose axes are not necessarily parallel with those of the property–space axes. The use of covariance in addition to variance gives more accurate distribution functions and better separation between the different acoustic library categories. The centre of the ellipses represents the mean, and the size and tilt of the ellipses represents the variances and covariance of these acoustic variables, *R(70)* and *R(200)*. The separation of the ellipses visualizes the ability to distinguish the categories. In this case, there are three spatial resolutions – pixels, cells, and entire schools. Each point in the cell resolution is averaged over many samples, which in turn gives smaller variances that appear as smaller ellipses with better separation. Additional good separations between the categories may be found by similar visualizations of other pairs of variables.

Multifrequency data from each pixel are tested against the properties of the acoustic library categories (ALC; further details below). The most probable ALC are associated with that pixel. This is determined by the probability that the tested data belongs to a specific acoustic library category. The categorization method is based on Bayes decision theory (Theodoridis and Koutroumbas, 2008). Measurements on new backscatter are compared to the content of the feature library to decide which, if any, of the existing ALC the new measurements are close to. The details of the categorization algorithm are described in Korneliussen *et al.* (2016).

Application of the procedures described above results in a library containing statistical features of acoustical measurements. Figures A1.11 and A1.12 show two different ways of visualizing the statistical properties of the variables in a feature library.

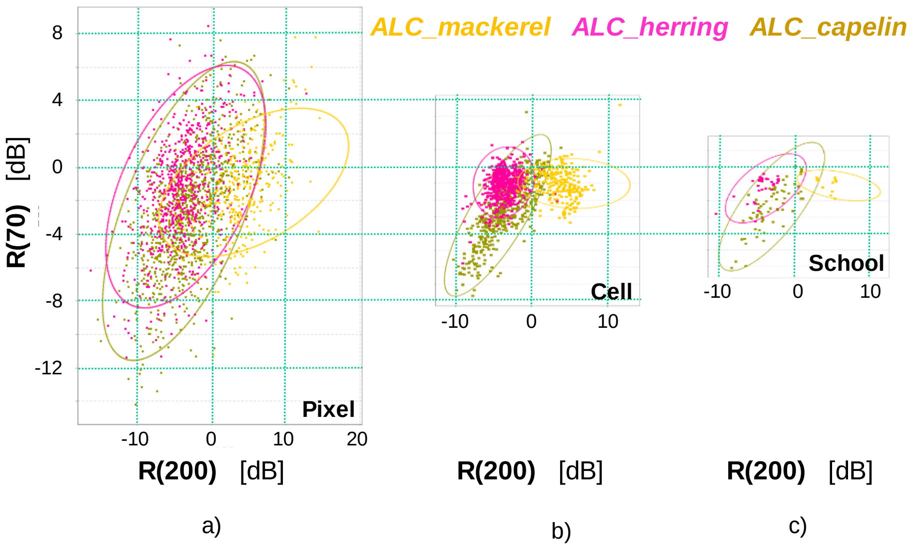

Figure A1.10. Acoustic variables *R(70)* and *R(200)* at different spatial resolutions for three acoustic library categories (ALC): (a) pixel resolution; (b) cell resolution (800 pixels averaged spatially); (c) school resolution (one value per identified school).

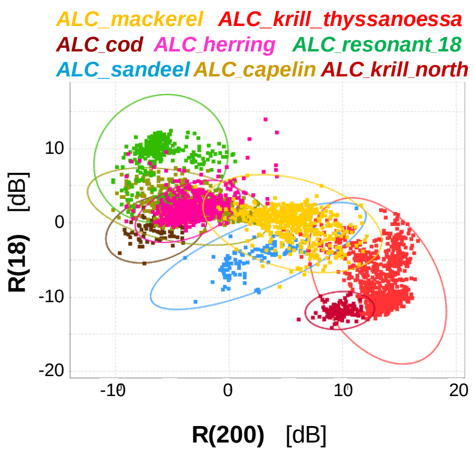

Figure A1.11. Logarithmic relative frequency responses *R(18)* vs. *R(200)* at cell resolution (800 samples averaged) for the *ALC* of importance for the case studies. The ellipses are statistical boundaries on each category that contain 90% of the observations. The plot shows that for the features *R(18)* vs. *R(200)*, *ALC_mackerel* is almost completely separated from *ALC_resonant_18*, while *ALC_herring* has partial overlap with both *ALC_mackerel* and *ALC_resonant_18*. In addition to *R(18)* and *R(200)*, using more features improves the separation of categories.

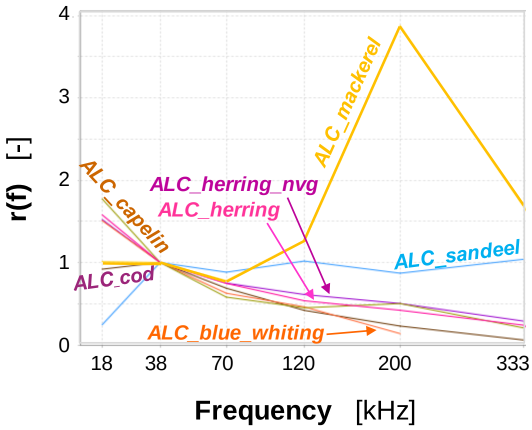

Figure A1.12. Relative frequency responses, *r(f)*, of the acoustic library categories (*ALC*). The categories are generated from ground-truthed backscatter of *Scomber scombrus* L. (*ALC_mackerel*), *Ammodytes marinus* L. (*ALC_sandeel*), *Mallotus villosus* L. (*ALC_capelin*), *Gadus morhua* L. (*ALC_cod*), *Micromesistius poutassou* L. (*ALC_blue_whiting*) and *Clupea harengus* L. (*ALC_herring* and *ALC_herring_nvg*). The *ALC_herring_nvg* category is trained on Norwegian spring-spawning herring, while the *ALC_herring* category also includes North Sea herring.

Multifrequency acoustic data were collected according to existing protocols (Korneliussen *et al.*, 2008) with the intention of combining and analysing coincident observations from several echosounders operating at different frequencies. This requires the use of calibrated systems (Foote *et al.*, 1987; Demer *et al.*, 2015) operated at the same pulse-duration (in these data, 1 ms) and ensonifying nearly the same volume of water at all frequencies. Data were collected during three surveys using Simrad EK60 echosounders mounted in a tightly packed configuration on a protruding keel (Korneliussen, 2010). All surveys were used for stock abundance estimation. The surveys were:

1. Survey number 2004113
   RV "G. O. Sars" in October–November 2004 in the northern part of the North Sea and southern part of the Norwegian Sea targeting Atlantic mackerel (*Scomber scombrus*). The survey was selected to compare the categorization method with an earlier method (Korneliussen, 2010).
2. Survey number 2014807
   RV "Eros" in 2014 in the North Sea targeting sandeel (*Ammodytes marinus*). The survey was selected because it observed small schools on and just above the seabed, which provides a challenge to the categorization process.
3. Survey number 2014116
   RV "G. O. Sars" in the Barents Sea in 2014 for investigation of the complete ecosystem (which is the survey selected for identification of capelin, which is acoustically similar to herring and cod in the same waters).

Data from the three surveys were processed stepwise through independent processing modules, i.e. the output from one processing module was the input of the next module. The processing was as follows:

1. Discrimination – removal of unwanted signal
   a. Remove spike-noise (originating in unsynchronized instruments or sonars on nearby ships). Median value of surrounding pixels replaces removed values.
   b. Replace negative spikes, i.e. drop in values with a vertical extent (originating in pings blocked by a bubble cloud). Median value of surrounding pixels replaces removed values.

   c. Quantify and remove ambient noise from the remaining data.
2. Align data spatially
   a. Correct data for horizontal and vertical placement of transducers and for the frequency-dependent system delay.
3. Group data in schools and seabed (grouping in tracks not used in these case studies)
   a. Detect seabed.
   b. Detect extent of the schools.
4. Categorize data
   a. Categorize all pixels. (Categorization of some pixels may not be conclusive). To speed up processing, only pixels below the surface blind zone and above the detected seabed are attempted to be categorized.
   b. Categorize all pixels inside the detected schools as a unit. The results are usually more conclusive than pixels categorized individually. Results of school categorization takes precedence over pixel categorization.
   c. Use inversion to investigate if the measured backscatter of a pixel originates from zooplankton. To speed up the processing, pixels categorized as fish are not investigated further.

The processing modules of points 4.a and 4.b do not use all frequencies at all ranges. For example, at ranges beyond 300 m, 200 kHz data are not used even if they are available; at ranges beyond 350 m, 120 kHz data are not used. *ALC_mackerel* requires 200 kHz to be identified, so there is no attempt to identify *ALC_mackerel* at ranges 300 m beyond the transducer. The processing module of point 4.c needs to use all specified frequencies. If the frequencies 18, 38, 70, 120, 200, and 333 kHz are specified, there will be no attempt to fit a zooplankton scattering model to the measured data beyond the maximum specified range of 333 kHz, which may be 110 m.

The settings for pixel categorization and school categorization were the same for all surveys, except that the selection of acoustic library categories to be identified was different due to geographical considerations. For example, as Atlantic mackerel is unlikely to be found far north in the Barents Sea in late September, the acoustic library category *ALC_mackerel* was not used in that case study. *ALC_mackerel* is based on acoustic data verified to be Atlantic mackerel and is used to identify mackerel.

Acoustic aggregations appearing as schools may not necessarily contain only one species. Assuming that a school may contain more than one species requires that different parts of the school are automatically tested for acoustic properties. If the test is inconclusive or does not conclude that the school is monospecific, the school is processed as if it contains multiple species. Processing individual pixels of a school usually leaves many pixels uncategorized, which gives values of s_A too low for the automatic categorization of the school. Most schools in the investigation areas were expected to be monospecific. The disadvantage of getting values for s_A too low for many schools was evaluated to be larger than sometimes being wrong about schools being monospecific.

For this study, schools were assumed to be monospecific. In cases where all the echoes from a school have similar relative frequency responses, it may be assumed that the aggregation contains only scatterer type and potentially only one species. Note, that the result of the categorization is an acoustic category, not a species. The s_A was stored at a horizontal resolution of 0.1 nautical miles both for the original manual scrutiny and for the automatic categorization. Table A1.3 shows the acoustic library categories used by the categorization modules in the different case studies.

Table A1.3. Categories and species compared in the surveys. The second column is the target species. The third and fourth columns are the similar scrutinize category and acoustic library category (ALC) believed to originate in the target species. The final column contains ALC that were identified simultaneously with the target library category. If the backscatter of a pixel is not most likely to originate in the target ALC, or if the probability is below the probability threshold, $s_v = 0$ for that pixel.

Survey	Biological target species	Scrutinize category	ALC[G]	Number of training schools	Training schools collection year	ALC used to remove backscatter
2004113	*Scomber scombrus* L.	Mackerel	*ALC_mackerel*	35	1999 2005	*ALC_resonant_18*[A] *ALC_krill_north*[B] *ALC_krill_thyssanoessa*[C] *ALC_herring*[D]
2014807	*Ammodytes marinus* L.	Sandeel	*ALC_sandeel*	44	2008 2009	*ALC_resonant_18*[A] *ALC_krill_north*[B] *ALC_krill_thyssanoessa*[C] *ALC_herring*[D]
2014116	*Mallotus villosus* L.	Capelin	*ALC_capelin*	67	2008 2014	*ALC_resonant_18*[A] *ALC_krill_north*[B] *ALC_krill_thyssanoessa*[C] *ALC_herring_nvg*[E] *ALC_cod*[F]

[A] *ALC_resonant_18* were trained from 4 shoals of zooplankton that were resonant at 18 kHz.
[B] *ALC_krill_north* was trained from 24 schools of *Meganictiphanes norwegica* L.
[C] *ALC_krill_thyssanoessa* trained from 8 shoals of *Thyssanoessa inermis* L.
[D] *ALC_herring* were trained from 40 schools of *Clupea harengus* L.
[E] *ALC_herring_nvg* were trained from 9 schools of Norwegian spring-spawning herring.
[F] *ALC_cod* were trained from 10 schools of *Gadus morhua* L. These were actually schools of cod.
[G] Acoustic library categories are always in *italic* and preceded by *ALC_*

The acoustic library categories resulting (*ALC*) from processing points 4.a and 4.b are mapped to scrutiny categories. The results of the scrutiny categories are stored to a database and, for each survey, that result is compared to the data scrutiny carried out during the surveys.

Results

The s_A values from the automatic categorization and the manual scrutiny for the three surveys show that the automatic categorization and the manual scrutiny are strongly correlated, especially for large s_A (Figure A1.13 a and c). A notable characteristic, especially for capelin, is that the values from the automatic categorization are equal to or slightly smaller than the manual scrutiny, except for small values of s_A. Furthermore, there are many small-to-moderate values from the automatic categorization that give zero s_A for the manual scrutiny, especially for sandeel. Subsequent inspection of the manually scrutinised sandeel survey echograms showed that some sandeel schools were clearly scrutinized incorrectly. This objective check of the manual scrutiny is one advantage of the automatic process. There was high spatial conformity between the manual scrutiny and the automatic categorization (Figures A1.11 and A1.13b) and the correlation between the two methods was high except for low values of s_v where the correlation varied considerably (Figure A1.13c).

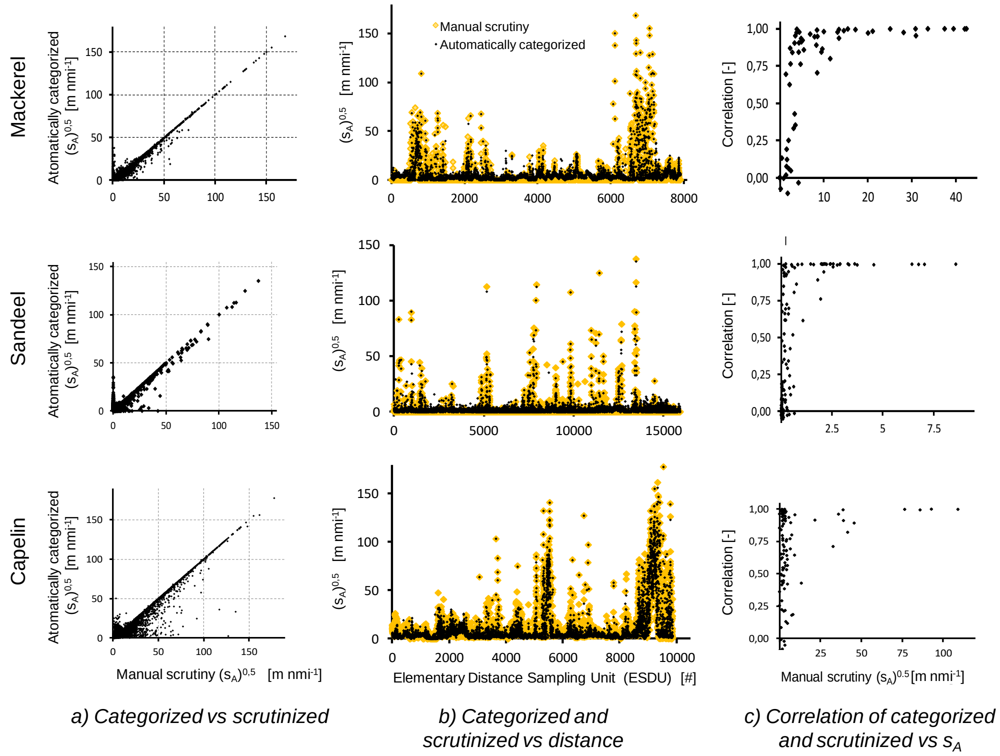

Figure A1.13. Comparison of automatic categorization (acoustic library categories) and manual scrutiny (scrutiny categories) for Atlantic mackerel, sandeel, and capelin. s_A are stored in the database at a horizontal resolution of 0.1 nautical miles and shown here as $s_A^{0.5}$ to better show the dynamics. a) Automatically categorized acoustic library category compared to manually scrutinized. b) Automatically categorized (black) and manually scrutinized (orange) as a function of distance travelled. c) Correlation between s_A from acoustic library category (resulting from automatic categorization) and s_A for similar scrutiny category (resulting from manual scrutiny) for the same 100 x 0.1 nautical miles distance.

The overall correlations between manual scrutiny and automatic categorization are very high for all surveys (Table A1.4). For mackerel and sandeel, the total acoustic abundance of the automatic categorization and the manual scrutiny were within 2% of each other. The slight difference is explained by the observation that manually drawn school integration regions are always slightly larger than the automatically drawn school regions. The capelin data correlation is close to 1 (Table A1.4), but the automatic categorization resulted in a 15% lower s_A than the manual scrutiny. This may be due to school categorization failing so that some schools are not being categorized as a unit, but as individual pixels. This, in turn, leaves many pixels uncategorized and some of the pixels being wrongly identified as cod or herring instead of capelin. In that case, masking the measurements with pixels identified as capelin will give values that are too low.

Table A1.4. Comparison of manual scrutiny and automatic categorization. The s_A(200) **samples are averaged over 0.1 nautical miles. Column 6 gives number of samples, column 7 the total** s_A **of automatic detection relative to** s_A **of manual scrutiny.**

Survey	Biological target species	Scrutinize category	ALC	Correlation	$s_{A,200}$ samples	$\Sigma s_A(200)_{auto}/\Sigma s_A(200)_{man}$
2004113	*Scomber scombrus* L.	Mackerel	*ALC_mackrel*	0.996	7 913	0.985
2014807	*Ammodytes marinus* L.	Sandeel	*ALC_sandeel*	0.998	17 925	0.994
2014116	*Mallotus villosus* L.	Capelin	*ALC_capelin*	0.976	9 869	0.855

Discussion

Averge values of *R(f)* at the school resolution level for the main acoustic library categories (*ALC_mackerel*, *ALC_sandeel*, and *ALC_capelin*) were used in the three surveys and some other categories with features similar to *ALC_capelin* (*herring*, *cod*, *blue whiting*). The mean *r(f)* values of *ALC_mackerel* and *ALC_sandeel* are quite different from the other acoustic library categories (Figure A1.10 – *r(f)* not logarithmic), which makes reliable automatic categorization likely. However, the variation (uncertainty) of *r(200)*, (not shown) is typically three–fivefold the mean value of *r(200)* at school resolution and around 10–20-fold the mean value at pixel level. This makes occasional misclassifications likely, especially at pixel level. In other words, misclassification is more likely if the scattering regions cannot be grouped into single fish tracks or schools of somewhat stronger scattering regions.

The good results from *ALC_mackerel* were expected because the *r(f)* of *ALC_mackerel* is markedly different from other categories. The *r(f)* of *ALC_sandeel* is also quite different from the other categories, so a high similarity between manual scrutiny and automatic categorization was also expected. The sample correlation coefficient is high for large s_A, thus the total correlation also becomes large. The less common alternative, the rank correlation coefficient (Walpole *et al*., 2002), gives equal weight to all values and results in a somewhat lower correlation. However, it is the large values that have most influence on the abundance estimates, and it is, therefore, felt that the use of sample correlation is more appropriate.

The high correlation between manual scrutiny and automatic categorization of *ALC_capelin* was unexpected, especially since the *r(f)* of *ALC_capelin* in the feature library is like that of *ALC_cod* and *ALC_herring_nvg*. The manual scrutiny of *ALC_capelin* is reliable in this case due to the low water temperature in which *ALC_capelin* is often found, the location in the water column, the schooling behaviour, and the results of the biological sampling. It was expected that additional, non-acoustic characteristics would be needed for a high correlation between manual scrutiny and automatic categorization. Difference in school shapes has previously been used to improve automatic categorization (Scalabrin *et al.*, 1996; Korneliussen *et al.*, 2009a), but that was not used in this case as the scattering regions mostly formed large layers and not schools of limited size, so morphology was not considered to be reliable. A reduction in the *a priori* probability of *ALC_herring* and *ALC_cod*, e.g. from 1 to 0.8, may be defended due to the low water temperature. Such a reduction in the *a priori* probability did, in fact, improve both correlations, and improved, to some degree, the ratio between automatic categorization and manual scrutiny.

Each acoustic library category should contain a sufficient quantity of data for each category for extraction of statistical properties, preferably from more than one survey. Poor training of one category in the acoustic feature library can lead to unreliable results, as would the use of data from uncalibrated echosounders. Uncalibrated instruments give biased s_A values and, therefore, an incorrect relative frequency response. The uncritical use of fully automated species identification during operational surveys is inadvisable. Although these surveys showed good agreement between automatic categorization and manual scrutiny, the relative frequency responses may potentially change with water temperature, fat content, specimen size, and species behaviour, so that similarly good results may not be found in other cases. A solution to this problem is to build an acoustic library that allows for seasonal variations in the scattering properties. Alternatively, one species may be used to build up several acoustic library categories, like *ALC_mackerel_spring*, *ALC_mackerel_summer*, etc.

Automatic categorization may be used to reanalyse data from old surveys to obtain a new and objective view of those data and to analyse data that have no temporally relevant ground-truth information available such as data collected with autonomous underwater vehicles or with ocean observatories. Automatic categorization is reliable for the large s_A values present in the case studies. Furthermore, automatic categorization can provide a more objective view to assist manual scrutiny and, from experience, speeds up the scrutinizing process (as allocation of scrutiny categories to echotraces can be taken with confidence faster than otherwise and requires less consideration by the scrutiny team). The speed and objectivity of the scrutiny naturally also improves with the use of reliable echotrace detection, as the acoustic library categorization becomes more reliable and because less time is needed to draw school regions.

Efficient and effective scrutinizing of acoustic data in a resource-limited environment requires attention to the time required to produce abundance estimates. The use of automatic categorization contributes to this aim and is particularly important for surveys which require abundance estimates at their completion, such as the joint Russian and Norwegian surveys of Barents Sea capelin (Eriksen, 2012) and the Norwegian surveys of North Sea sandeel (Johnsen *et al.*, 2009).

A future enhancement is to incorporate more of the information that the scrutinizing operator has at hand, such as the local geography, and use it to automatically adjust the *a priori* probability, such as reducing the probability of finding Atlantic mackerel in the Barents Sea during winter. The methods for acoustic categorization presented here can be applied to wideband acoustic data, although this has not been shown here. Wideband data improve range resolution and hence improve single fish detection and tracking. Wideband backscatter can be split into several frequency bands to give an increased number of points in the $r(f)$ curve, which should lead to improved species identification.

References

Demer, D. A., Berger, L., Bernasconi, M., Bethke, E., Boswell, K., Chu, D., Domokos, R., *et al*. 2015. Calibration of acoustic instruments. ICES Cooperative Research Report No. 326. 130 pp.

Eriksen, E. (Ed). 2012. Survey report from the joint Norwegian/Russian ecosystem survey in the Barents Sea August-October 2012. IMR/PINRO Joint Report Series No. 2/2012. 139 pp.

Foote, K. G., Knudsen, H. P., Vestnes, G., MacLennan, D. N., and Simmonds, E. J., 1987. Calibration of acoustic instruments for fish density estimation: a practical guide. ICES Cooperative Research Report No. 144. 69 pp.

Johnsen, E., Pedersen, R., and Ona, E. 2009. Size-dependent frequency response of sandeel schools. ICES Journal of Marine Science, 66: 1100–1105. https://doi.org/10.1093/icesjms/fsp091

Korneliussen, R. J. 2010. The acoustic identification of Atlantic mackerel. ICES Journal of Marine Science, 67: 1749–1758. https://doi.org/10.1093/icesjms/fsq052

Korneliussen, R. J., Heggelund, Y., Eliassen, I. K., and Johansen, G. O. 2009a. Acoustic species identification of schooling fish. ICES Journal of Marine Science, 66: 1111–1118. https://doi.org/10.1093/icesjms/fsp119

Korneliussen, R., Heggelund, Y., Macaulay, G. J., Patel, D., Johnsen, E., and Eliassen, I. 2016. Acoustic identification of marine species using a feature library. Methods in Oceanography, 17: 187–205. https://doi.org/10.1016/j.mio.2016.09.002

Scalabrin, C., Diner, N., Weill, A., Hillion, A., and Mouchot, M-C. 1996. Narrowband acoustic identification of monospecific fish shoals. ICES Journal of Marine Science, 53: 181–188. https://doi.org/10.1006/jmsc.1996.0020

Theodoridis, S., and Koutroumbas, K. 2008. Pattern Recognition, 4th edition. Academic Press, Cambridge, MA. 984 pp.

Walpole, R. E., Myers, R. H. Myers, S., and Ye, K. 2002. Probability & Statistics for Engineers & Scientists, seventh edition. Prentice-Hall, New Jersey. 730 pp.

A1.5: Case study 5 Acoustic diversity and classification of fish aggregations in coral reefs eco-systems

Introduction

Acoustic surveys have been used successfully for several decades as an assessment tool for small pelagic or demersal fish populations in high-latitude areas where species diversity and the general complexity of the systems are relatively low. So far, very few fisheries acoustic assessments have been carried out for fish species in coral and rocky reef systems (Costa *et al*., 2014). The high diversity of these areas and the inability to identify species using only sonar (echosounders) have limited the use of this technology. Groundtruthing can be very challenging due to the nature of the seabed, inhibiting the use of extractive methods like trawlnets. To respond to the increasing need for reliable large-scale data for the management of these important ecosystems, there is a need to improve fisheries acoustics and develop alternative approaches for target classification in these areas.

In this case study, we evaluate previously defined metrics that describe the shape (geometric) and acoustic backscatter (energetic) properties (Nero and Magnuson, 1989; Reid, 2000; Scalabrin and Massè, 1993; Haralabous and Georgarakos, 1996; Korneliussen *et al*., 2009) of Caribbean reef fish aggregations and schools in order to investigate the acoustic diversity and identify meaningful patterns that could help classify the acoustic signatures to species groups or guilds rather than individual species. We use an unsupervised statistical clustering method in order to describe the acoustic variability of the coral reef areas. Underwater video surveys of fish aggregations and schools from remotely operated vehicle (ROV) were used to guide our interpretation of the unsupervised classification. The research was conducted in the US Virgin Islands and Puerto Rico in spring 2011, 2013, and 2014.

Methods

Acoustics

The acoustic surveys were carried out on board the NOAA ship "Nancy Foster" using Simrad EK 60 split-beam echosounders operating at three frequencies (38, 120, 200 kHz). The survey design was generally based on parallel transects. The intertransect distance, transect length, and direction varied among sampling sites and were chosen according to the characteristics of the reef.

The acoustic backscatter was processed using the software Echoview (Version 7.0, Echoview, Pty Ltd., Hobart, Tasmania). Background noise and other unwanted backscatter (e.g. bubbles, plankton) were removed to get a "clean" echogram. The S_v echograms were averaged at each frequency and an image filtering procedure was used to stabilize the data by removing the small samples and better identifying the schools, as described in Korneliussen *et al*. (2009). The synthetic echogram obtained was used to detect schools by applying the SHAPES (SHoal Analysis and Patch Estimation System) algorithm in Echoview (Barange, 1994).

A series of parameters describing the energetic, morphological structure and position of the school in the water column were exported. These metrics provide detailed information of the acoustic characteristics and behaviour of fish aggregations. The full list of metrics used is shown in Table A1.5. The remaining backscatter was not identified as the school was excluded from further analysis for this case study. This low-density backscatter most likely belongs to a large number of species that have individual swimming behaviour and are analysed with other approaches (e.g. echo counting).

An unsupervised robust sparse K-means (RSKM) clustering approach was used for the classification of the aggregations (Kondo *et al*., 2012). This method is a derived form of k-means that is able to reduce the negative effect of using a large number of variables, and it is able to deal with the presence of outliers in the dataset.

Species composition and schooling behaviour of the fish communities in the area were detected using videos and still images taken by an ROV (Super Phantom S2 and Sub-Atlantic Mohawk18). Fish schools and aggregations observed by the ROV were paired with the closest aggregations and clusters from the analysis of the echosounder surveys. Fish behaviour (e.g. packing density, number of fish in the schools, school shape, distance from the seabed) was also evaluated as were coupling patterns in clusters with species observed. Figure A1.14 summarizes the general workflow of the approach used.

Table A1.5. List of school features used for school classification.

Class	School descriptor	Unit	Description	Reference
Energetic	MVBS 38, 120, 200 kHz (MVBS38, MVBS120, MVBS200)	db re 1 m^{-1}	Mean volume backscattering coefficient	Simmonds and MacLennan (2005)
	S_v max 38, 120, 200 kHz (sv_max38, sv_max120, sv_max200)	db re 1 m^{-1}	Maximum volume backscattering coefficient	Simmonds and MacLennan (2005)
	Horizontal roughness 38 kHz (hor_rough)	db re 1 m^{-1}	Measure of the dispersion of acoustic energy in the horizontal direction	Nero and Magnuson (1989)
	Vertical roughness 38 kHz (ver_rough)	Db re 1 m^{-1}	Measure of the dispersion of acoustic energy in the vertical direction	Nero and Magnuson (1989)
	Skewness 38 kHz (skew)	-	Skewness of the sample values in a school	Lawson *et al*. (2001)
	Standard deviation (s.d.)	-	Standard deviation of the S_v values in the school	
	Coefficient of variation (*CV*)	-	Coefficient of variation of the S_v values in the school	
	r(200) 200/38 (freq_resp200)	db re 1 m^{-1}	Relative frequency response: volume-backscattering coefficient at 200 kHz relative to 38 kHz considered as reference frequency	Korneliussen and Ona (2003)
	r(120) 120/38 (freq_resp120)	db re 1 m^{-1}	Relative frequency response: volume-backscattering coefficient at 120 kHz relative to 38 kHz	Korneliussen and Ona (2003)

			considered as reference frequency	
Geometric	Corrected length (length)	m	Horizontal dimension in the plane of the echogram corrected for known beam geometry	Reid (2000)
	Corrected thickness (thick)	m	Vertical dimension in the plane of the echogram corrected for known beam geometry	Reid (2000)
	Corrected perimeter (perim)	m	Length of the perimeter (in the plane of the echogram) corrected for known beam geometry	Reid (2000)
	Corrected area (area)	m^2	Cross-sectional area (in the plane of the echogram) of a school represented by a region on an echogram corrected for known beam geometry	Reid (2000)
	Image compactness (compact)	-	Measure of the shape of a school calculated as the ratio between the perimeter and the area	Reid (2000)
	3D school volume (vol_3d)	m^3	Estimated volume of a school assuming it is cylindrical	
	Rectangularity (rectangul)	-	(Length * thickness)/area	Scalabrin and Massè (1993); Haralabous and Georgarakos (1996)
	Circularity (circul)	-	$(4\pi$*area)/perimeter^2	Korneliussen *et al*. (2009)
	Uneveness (unev)	-	Relation between the school perimeter and the rectangle perimeter computed from the school height and length	Weill *et al*. (1993)
	Fractal dimension (fractal)	-	Index of shape complexity (Ln (perimeter/4) × 2)/Ln(number of samples)	Nero and Magnuson (1989); Barange (1994)
	Elongation (elong)	-	Length/thickness	Coetzee (2000)

Bathymetric	Depth mean (school depth)	m	The distance from the sea surface to the geometric centre of the fish school
	Mean distance seabed (dist)	m	The distance from the seabed to the geometric centre of the fish school
	Depth (depth)	m	

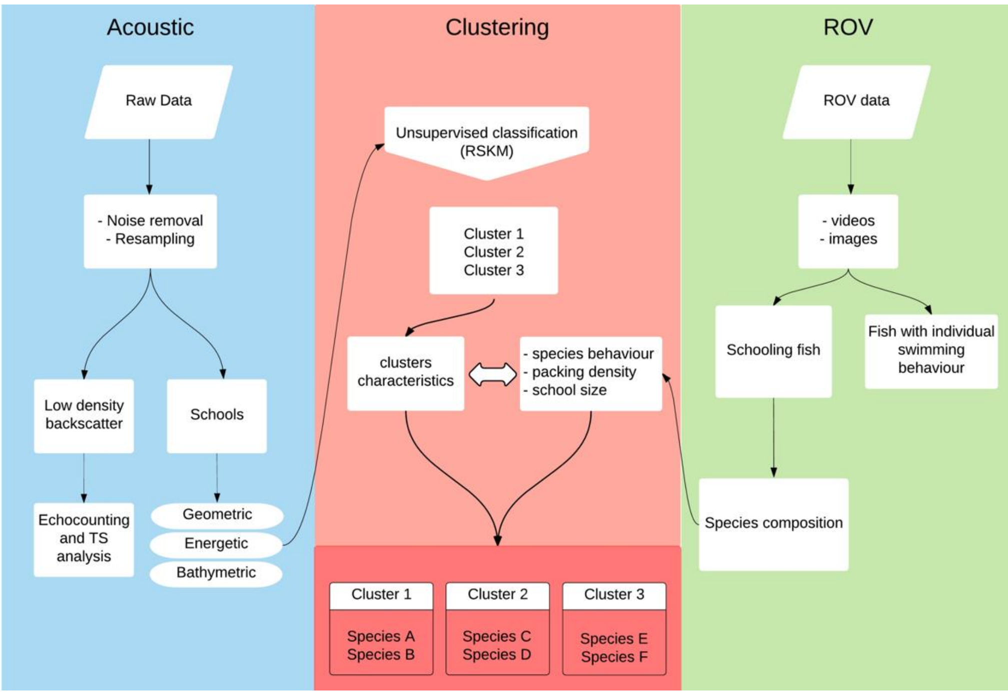

Figure A1.14. Workflow for analysis and classification of multifrequency echosounder data of the fish schools. Low density backscatter detected from individual fish are logged and analysed using echo counting (not discussed further here).

Results and discussion

The clustering identified five distinct aggregation groups. Different names were associated with the clusters based on the characteristics observed. The clusters were named: "high energy" (Cluster 1), "moderate energy" (Cluster 2), "low energy" (Cluster 3), "very low energy" (Cluster 4), and "serpentine" (Cluster 5). The first four clusters were well separated based on the energetic parameters. The "serpentine" cluster showed a stronger separation from the others for geometric parameters. The results of clustering are shown in Figure A1.15 on a principal component analysis (PCA) biplot.

The variables that were most influential in the clustering were the energetic parameters (maximum S_v and MVBS) followed by several geometric parameters (rectangularity, length, elongation, perimeter, and thickness; Figure A1.16). Bathymetric variables and frequency response were relatively unimportant.

In all, seven ROV dives were carried out and the videos were visually inspected to identify the species that formed schools, aggregations, or loose groups that could be associated with the clusters we analysed acoustically (Figure A1.17 and Table A1.6). The deployment of the ROV occurred within ca. 2 h from the acoustic surveys. Packing density, size of the schools, and number of schools detected were the features observed in the ROV videos to help the coupling with the acoustic clusters.

Based on these results, we can say that the "high energy" and the "moderate energy" clusters include mainly large-bodied predator species and commercially important species. In contrast, the remaining clusters may include small-bodied species that are not typically harvested but still have important ecological roles in the system.

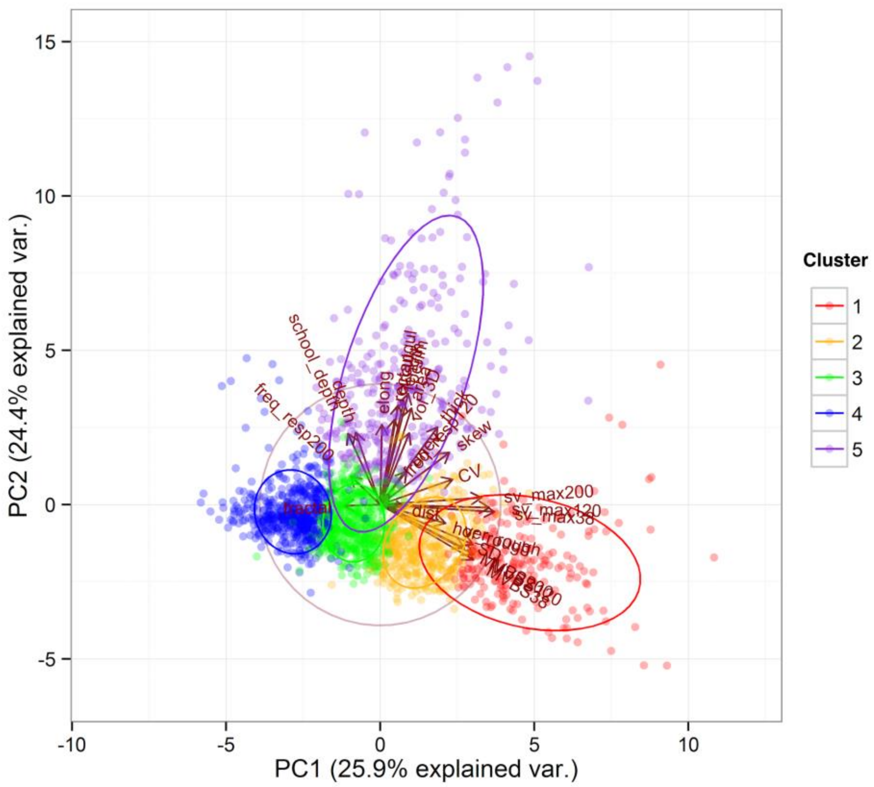

Figure A1.15. Clustering results plotted in a PCA biplot.

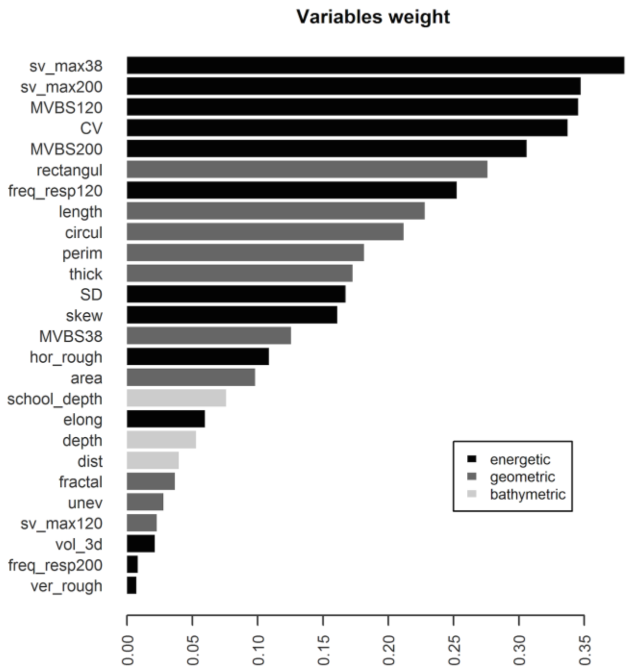

Figure A1.16. Weights of the clustering features estimated by the RSKM algorithm.

This study is the first work that describes the acoustic patterns and diversity of fish aggregations in a coral reef system, building the basis for a more extensive use of acoustic techniques in diverse and complex ecosystems. The approach used could identify consistent patterns in the acoustic backscatter and shape of schools ascribable to the different morphologies of individuals and behaviours of groups and schools of coral reef fish.

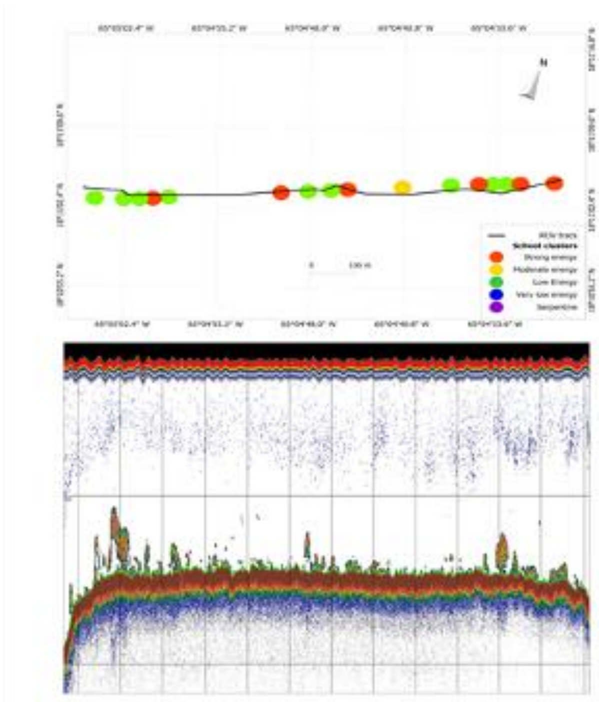

Figure A1.17. Example of the association between acoustic transect and ROV. The top panel shows the distribution of school clusters around the ROV transect. The echogram of the entire acoustic transect is shown in the bottom panel.

Table A1.6. Association of the acoustic clusters with the species and their behaviours observed in the ROV videos.

Cluster	Acoustic features	Candidate species	Behaviour
High energy	High backscattering High thickness Large size schools	Large carangids: Caranx ruber, Caranx latus Spadefish: Chaetodipterus faber	Moderate to highly packed schools Organized and coordinated schools
Moderate energy	High/moderate backscattering Moderate size schools	Small size carangids: *Selar crumenophtalmus* Dog and gray snapper: *Lutjianus jocu, L. griseus* Bermuda chub: *Kyphosus sectatrix* Triggerfish: *Canthidermis sufflamis*	Moderate to highly packed schools with smaller body size Organized and coordinated schools
Low energy	Moderate/low backscattering Moderate size schools	Black durgon: *Melichtys niger* Creole wrasse: *Clepticus parrae* Damselfish:	Moderate/low packing density Shoaling behaviour
Very low energy	Low backscattering Small schools	Small mixed species	Low packing density Shoaling behaviour
Serpentine	Moderate/low backscattering Highly elongated Large size schools	Creole wrasse: *Clepticus parrae* Damselfish Small planktivorous	Large and elongated schools Organized and coordinated movements

References

Barange, M. 1994. Acoustic identification, classification and structure of biological patchiness of the Agulhas Bank and its relation to frontal features. South African Journal of Marine Science, 14: 333–347. https://doi.org/10.2989/025776194784286969

Coetzee, J. 2000. Use of a shoal analysis and patch estimation system (SHAPES) to characterise sardine schools. Aquatic Living Resources, 13: 1–10. https://doi.org/10.1016/S0990-7440(00)00139-X

Costa, B., Taylor, J. C., Kracker, L., Battista, T., and Pittman, S. 2014. Mapping reef fish and the seascape: using acoustics and spatial modeling to guide coastal management. PLoS One 9(1): e85555. https://doi.org/10.1371/journal.pone.0085555

Haralabous, J., and Georgakarakos, S. 1996. Artificial neural networks as a tool for species identification of fish schools. ICES Journal of Marine Science, Volume 53: 173–180. https://doi.org/10.1006/jmsc.1996.0019

Kondo, Y., Salibian-Barrera, M., and Zamar, R. 2012. A robust and sparse K-means clustering algorithm. http://arxiv.org/abs/1201.6082

Korneliussen, R. J., Heggelund, Y., Eliassen, I. K., and Johansen, G. O. 2009. Acoustic species identification of schooling fish. ICES Journal of Marine Science, 66: 1111–1118. https://doi.org/10.1093/icesjms/fsp119

Korneliussen, R. J., and Ona, E. 2003. Synthetic echograms generated from the relative frequency response. ICES Journal of Marine Science, 60: 636–640. https://doi.org/10.1016/S1054-3139(03)00035-3

Lawson, G. L., Barange, M., and Fréon, P. 2001. Species identification of pelagic fish schools on the South African continental shelf using acoustic descriptors and ancillary information. ICES Journal of Marine Science, 58: 275–287. https://doi.org/10.1006/jmsc.2000.1009

Nero, R. W., and Magnuson, J. J. 1989. Characterization of patches along transects using high-resolution 70-kHz integrated acoustic data. Canadian Journal of Fisheries and Aquatic Sciences, 46: 2056–2064. https://doi.org/10.1139/f89-254

Reid, D. G. 2000. Report on echo trace classification. ICES Cooperative Research Report No. 238. 115 pp.

Scalabrin, C., and Massé, J. 1993. Acoustic detection of the spatial and temporal distribution of fish shoals in the Bay of Biscay. Aquatic Living Resources, 6: 269–283. https://doi.org/10.1051/alr:1993027

Simmonds, E. J., and MacLennan, D. N. 2005. Fisheries Acoustics: Theory and Practice. Blackwell Publishing, Oxford. 437 pp.

Weill, A., Scalabrin, C., and Diner, N. 1993. MOVIES-B: an acoustic detection description software. Application to shoal species' classification. Aquatic Living Resources, 6: 255–267. https://doi.org/10.1051/alr:1993026

A1.6 Case study 6 Identification of the small pelagic fish in the northeastern Mediterranean Sea by means of an artificial neural network

Motivation

The northeast corner of the Mediterranean Sea is one of the warmest and most saline parts of the entire basin (Marullo *et al.*, 1999). The area has been highly affected by the invasion of alien species introduced to the Mediterranean through the man-made Suez Canal. The intensity and distributional range of this invasion is likely to expand further towards the western extent of the basin with increasing temperatures (Raitsos *et al.*, 2010). For management purposes, prediction of the potential future changes is important, and a detailed characterization of the current ecological conditions is necessary. In the study area, the role of the pelagic migrant Lessepsian fish has become more noticeable, and their commercial catch has been increasing (Gücü *et al.*, 2010). However, knowledge of their habitat characteristics and their interactions with local species has been limited. This work was conducted to characterize the spatial distribution of small pelagic fish in this area using hydroacoustics, trawl, and CTD between 2009 and 2011 (Figure A1.18). Species identification was challenging due to the lack of previous expert knowledge of their acoustic characteristics. Therefore, unsupervised and supervised classification techniques were utilized to assist species identification. Supervised classification techniques, such as artificial neural network (ANN), are powerful classification tools in cases where introduced patterns are distinct with regard to several descriptors (Lek and Guégan, 2000). In this work, the school identification process began with an exploration of the patterns within the school dataset, grouping the similar components, and finally labelling each distinct group using the trawl dataset. The supervised method, ANN, was useful for fine-tuning the relatively subjective initial classification rather than automatic recognition and classification of fish schools. Furthermore, different size groups of the same species showed different characteristics, and ANN was used to discriminate between juvenile and adult aggregations.

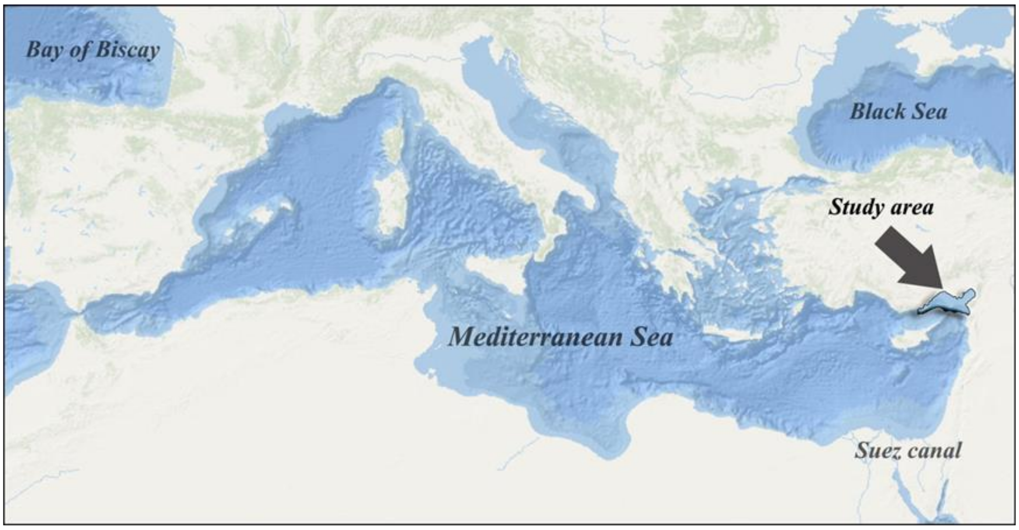

Figure A1.18. The study area in the northeast corner of the Mediterranean Sea.

Methods

The acoustic data were collected with a pole-mounted split-beam Simrad EY60 120 kHz echosounder and processed with the Echoview software and its virtual ecogram operators. Fish aggregations were detected and characterized using the ''Schools detection'' module. The trawl catch data were the primary basis for interpretation of the size and species composition and relative contribution to the total abundance. The positions of the trawl stations were selected based on the fish school types observed on the echograms throughout the survey. In all, 131 trawls were conducted in 5 surveys. The towing speed varied between 2.8 and 4.5 knots, and the duration was determined based on the fish distribution on echograms; nevertheless, maximum duration was 30 minutes. The study area was divided into eight subsections in east-to-west and inshore-to-offshore coverage. Most dominant species (biomass and spatial coverage) were selected and ranked according to their biomass proportions. As relative abundance in the catch undergoes high uncertainty, the individual trawl catches were regarded as representative only of presence/absence of the species, and allocation was done in accordance with the ranking. An initial K-means clustering was used to group similar schools based on school descriptors. Subsequently, the trawl catch compositions were associated with these clusters based on spatial information. For this interpretation, all fish schools located within 4 nautical miles of the centre of a trawl haul were used. Schools within the trawl area were manually assigned to the species, taking in account trawl catch composition and k-means cluster labels. Factors associated with schooling behaviour of the fish, such as school density, depth preference, geographical location, total depth, and position in the water column, were also considered during allocation. This approach rather than directly using the catch composition was taken due to uncertainties, including vessel avoidance, variation in catchability of species, and net performance. The descriptor metrics of this set of identified schools were exported to be used as a learning set.

Supervised scrutinization was conducted in three stages:

1. The classification success of the identified schools located near trawl sites were tested.
2. The test was applied to the entire dataset. Initial labelling extended to the entire dataset manually, taking into account k-means labelling and the subjectively identified patterns. ANN was used to test the consistency of this subjective identification and apply fine-tuning. Inconsistencies within the learning set with respect to spatial continuity (e.g. depth, position, and distance to shore) were eliminated.
3. The test was repeated by discriminating the juvenile schools of *Sardinella aurita* within the learning set.

Training and testing was performed by cross validation with ten folds, meaning that the dataset was randomly partitioned into ten subsets and by an iterative process, one set was used for training and the rest were used for testing. The neural network model was composed of ten descriptors, six outputs representing major species groups, and eight nodes at the hidden layer, which were determined by testing the performance of the model using a range of different node numbers.

Results and discussion

In total, 110 different species were observed in all trawl hauls, including untargeted species such as bottom-dwelling flatfish. Only 34 species were observed more than 13 times (10% of the total number of hauls). Most (84%) of the pelagic and semi-pelagic fish were captured in nearshore areas at depths < 50 m. In total, 3231 fish schools were acoustically detected; however, only 2841 of them were used in the analysis. K-means analysis using tenfold cross-validation resulted in 5–8 different clusters. The larger number of clusters provided better resolution, but increased the uncertainties by potentially creating artificial subclusters. The final decision on the number of clusters

($n = 6$) was a trade-off between resolution and convenience for use. In clustering S_v, mean and depth were the most influencing parameters. The schools with higher S_v-mean located at shallower depths ca. < 50 m were the most discrete group (Figure A1.19a).

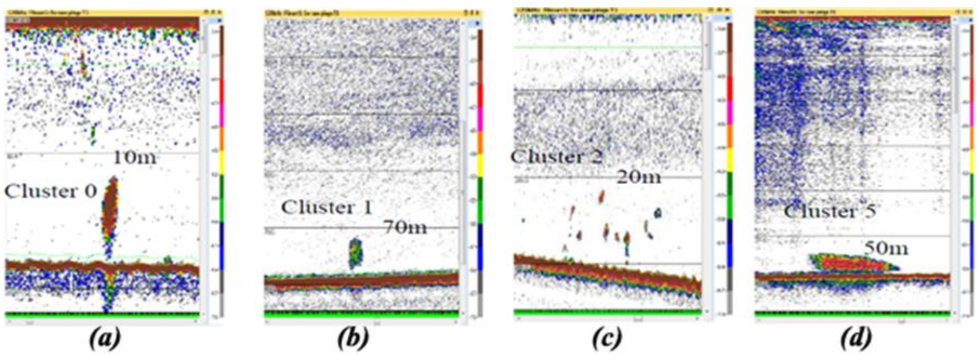

Figure A1.19. Example schools for the different groups characterized by clustering. Depth **and energetic density were the main discriminators where association with the seabed was also important.**

Results obtained from clustering were then checked for their consistency with the trawling results regarding depth, energetic features of the school (S_v mean), and morphometric descriptors. Figure A1.20 shows an example of the location of the selected fish schools near trawl stations. At these points, schools with known clusters labels were assigned species based on corresponding image pattern and trawl information. The labelling obtained for the schools located near trawl stations was then used as input for ANN for identification of the remaining schools in the entire dataset. The performance of the learning set was assessed by tenfold cross-validation test: the accuracy was 87.5% for *Sardinella aurita*. School distribution per species in selected datasets was rather homogeneous, changing between 11% and 1.7%. Two exceptions were *S. aurita*, with a strong dominancy of 37%, and *Etrumeus teres*, which accounted for only 8%. Although the accuracy of the classification seems promising, the significance of the *S. aurita* dominance in the learning set could have led to misclassification. This was due to the model's tendency to prioritize this discretely abundant group with bias (false positives). As a result, the *Sardinella* group appeared to dominate the dataset, accounting for an average of 59% of the backscatter. In a further step, ANN was used to test the *S. aurita* classification with respect to developmental stage (juveniles and adults). Because the adult and the juvenile fish form dissimilar schools, changing in size, density, and school morphometry, a subset of data attributed only to this species was subjected to the test.

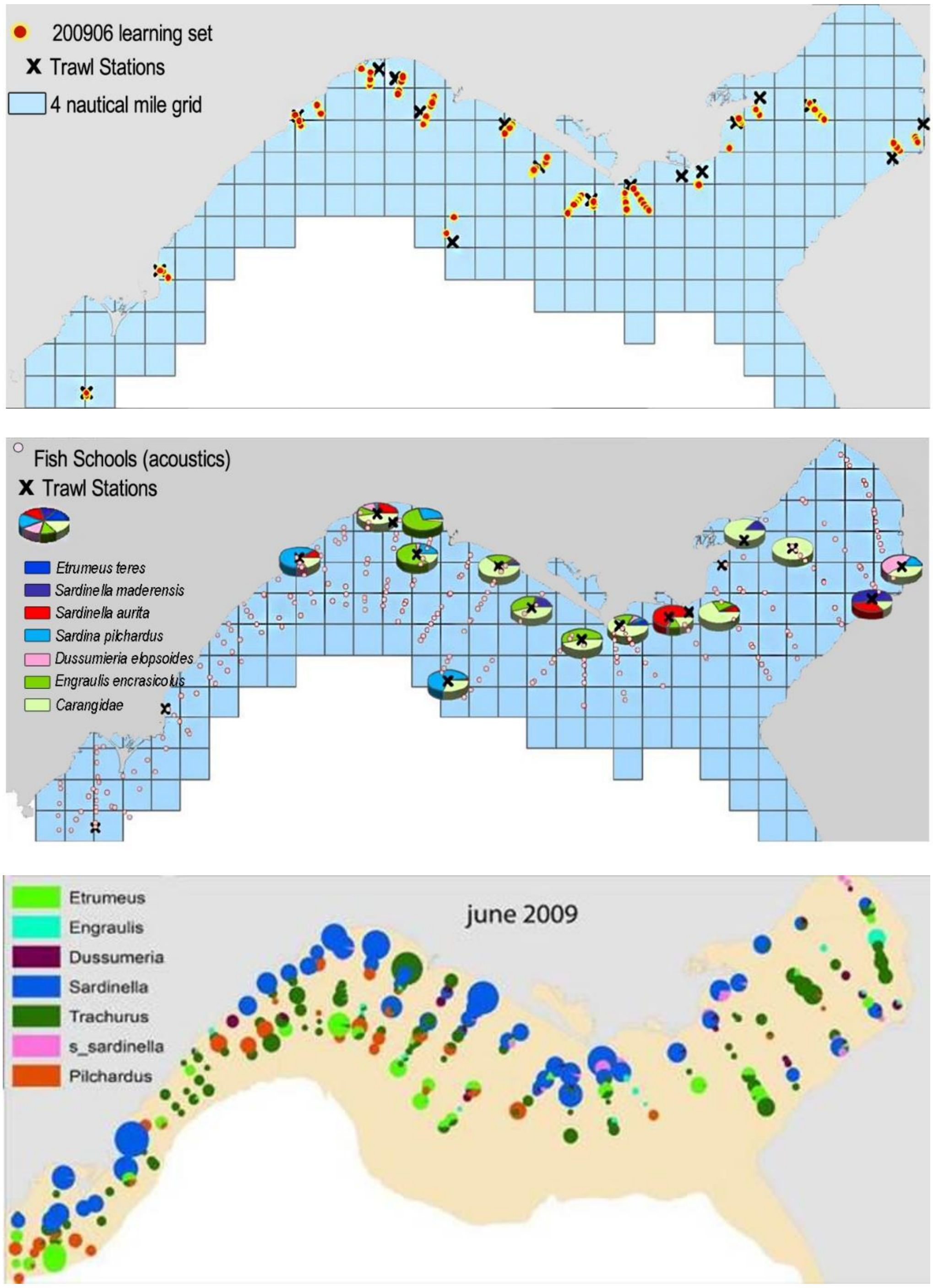

Figure A1.20. Examples from June 2009. Upper panel: position of the identified fish schools and the nearest trawl haul within a 4-nautical-mile grid. Middle panel: the species composition from trawls and position of the entire fish schools. Lower panel: map of identified fish schools.

As June corresponds to spawning and October corresponds to the appearance of juveniles, typological differences in fish schools were assessed. In the two October surveys, juvenile distribution was almost identical, tending to accumulate at the outer edge of river plumes. Adult *S. aurita* schools were widely distributed all along the coast in the study area within the 0–50 m bathymetric range. Specifically, the largest acoustic densities and trawl catches for *S. aurita* were observed in the Bay of Mersin where the chlorophyll concentration was the highest and species classification results were consistent. This difference was captured with ANN and helped distinguish nursery areas of this species. This study lacked multifrequency acoustics observations. Frequency responses have been used as a powerful discriminator in several studies (Fässler *et al*., 2007; De Robertis *et al*., 2010). In this case, when overall descriptors were considered, the school depth was the most important parameter. One reason for this could be the effect of temperature. Since there was a constant thermal stratification during both survey seasons, the species partitioned the habitat based on their temperature preferences.

Conclusion

ANN was used for fine-tuning the species identification procedure of initially subjectively classified fish schools. Fine-tuning involved cross-validation tests where all samples in the training dataset were used for both training and validation; hence, the validation of every possible sample in the dataset. ANN, furthermore, helped characterize the distribution areas of different life stages of the most dominant species in the area (*S. aurita*). Although automatic recognition and classification of schools with ANN may not be possible in case of similarity in school patterns of different species, it may assist overall in decision-making.

References

De Robertis, A., McKelvey, D. R., and Ressler, P. H. 2010. Development and application of an empirical multifrequency method for backscatter classification. Canadian Journal of Fisheries and Aquatic Sciences, 67(9): 1459–1474. https://doi.org/10.1139/F10-075

Fässler, S. M., Santos, R., García-Núñez, N., and Fernandes, P. G. 2007. Multifrequency backscattering properties of Atlantic herring (*Clupea harengus*) and Norway pout (*Trisopterus esmarkii*). Canadian Journal of Fisheries and Aquatic Sciences, 64(2): 362–374. https://doi.org/10.1139/f07-013

Gücü, A. C., Ok, M., and Sakınan, S. 2010. Past and present of fish fauna in the NE Levant Sea and factor facilitating the colonization by Lessepsian fishes. *In* EastMed (2010) Report of the SubRegional Technical meeting on the Lessepsian migration and its impact on Eastern Mediterranean fishery. GCP/INT/041/ECGRE-ITA/TD-04, pp. 88–110.

Lek, S., and Guégan, J. F. (Eds). 2000. Artificial Neuronal Networks: Application to Ecology and Evolution. SpringerVerlag, New York. 262 pp.

Marullo, S., Santoleri, R., Malanotte-Rizzoli, P., and Bergamasco, A. 1999. The sea surface temperature field in the Eastern Mediterranean from advanced very high resolution radiometer (AVHRR) data: Part II. Interannual variability. Journal of Marine Systems, 20(1): 83–112. https://doi.org/10.1016/S0924-7963(98)00072-4

Raitsos, D. E., Beaugrand, G., Georgopoulos, D., Zenetos, A., Pancucci-Papadopoulou, A. M., Theocharis, A., and Papathanassiou, E. 2010. Global climate change amplifies the entry of tropical species into the Eastern Mediterranean Sea. Limnology and Oceanography, 55: 1478–1484. https://doi.org/10.4319/lo.2010.55.4.1478

Annex 2: Case studies illustrating the need for target classification

The following case study is not referred to in Section 6 but it illustrates the need for a target classification method.

A2.1 Case study 7 Acoustic buoys in tuna purse-seine fisheries

Since 2010, tuna fishing companies use acoustic buoys more often. In 2015, it is estimated that almost 100% (Delgado de la Molina *et al*., 2014; Lopez *et al*., 2014) of fish aggregating devices (FADs) are equipped with an acoustic buoy to (i) locate the FADs and (ii) evaluate how much fish is located under that FAD.

Acoustic buoys are using transducers with 50, 130, 190, and 200 kHz. The companies that build these buoys are making ca. 100 000 buoys per year for use by tuna fishing companies worldwide (Figure A2.1).

For example, Gaertner *et al*. (2015) estimate that in 2013, ca. 17 300 acoustic buoys were used in the Atlantic Ocean.

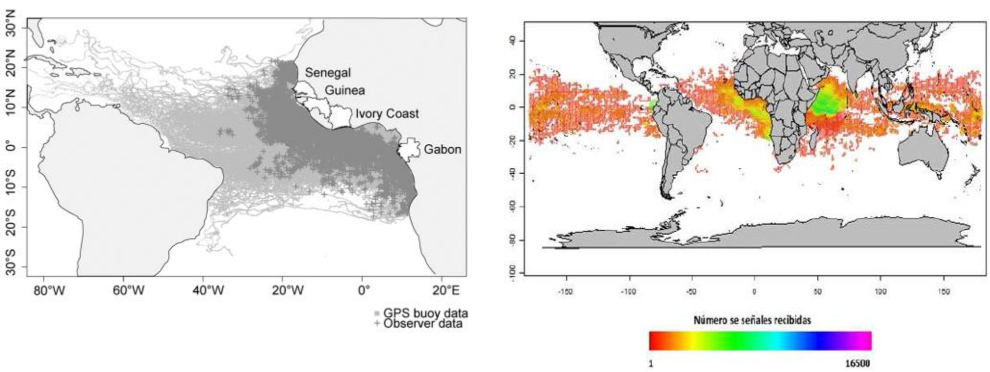

Figure A2.1. Worldwide distribution of tuna buoys.

New generation echosounder buoys are being used with two frequencies. Furthermore, the buoy manufacturers are using new filters and ways to integrate the acoustic data, but there is a lack of standardization so that they cannot be compared equally.

The fishing market and consumers are also requesting size and species differentiation, thus some of the buoy manufacturers are developing acoustic buoys with two transducers with difference frequencies.

As can be seen in Figures A2.2–A2.3, buoys and FADs used by tuna vessels in the Atlantic are well distributed from 20°N to 20°S and from Africa to the South American coast.

This information, according to Santiago *et al*. (2016), can be used to estimate a relative acoustic index or abundance. TTV Ltd. made an initial relative abundance evaluation in 2013; what can be seen when all companies share their acoustic and biologic information? Moreover, the future trend gives us the possibility to differentiate size and species.

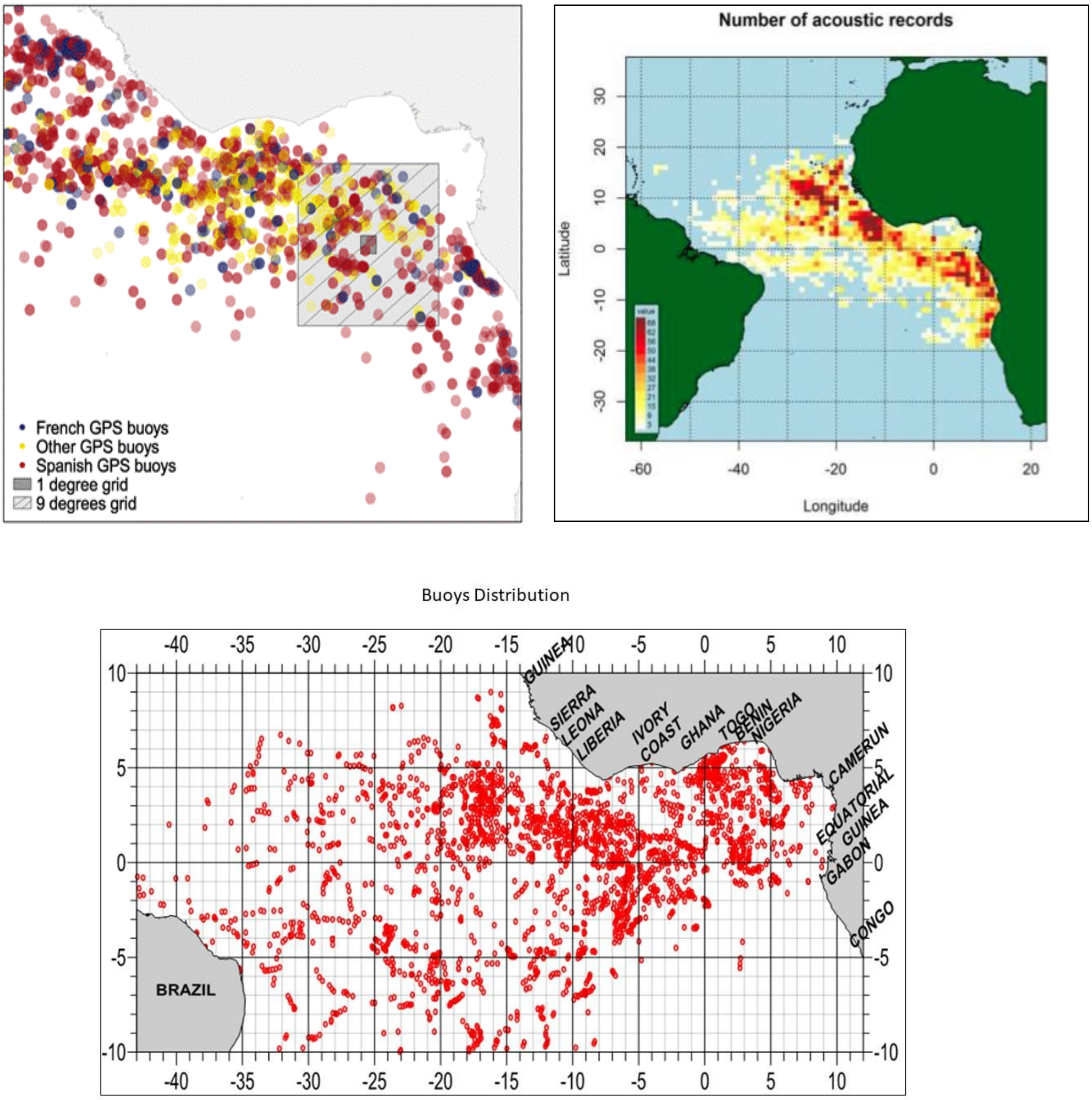

Figure A2.2. Acoustic buoy distribution in the Atlantic Ocean. Sources: Maufroy *et al*. (2015), ANABAC and OPAGAC fleet data (2011), and TTV fleet (2013).

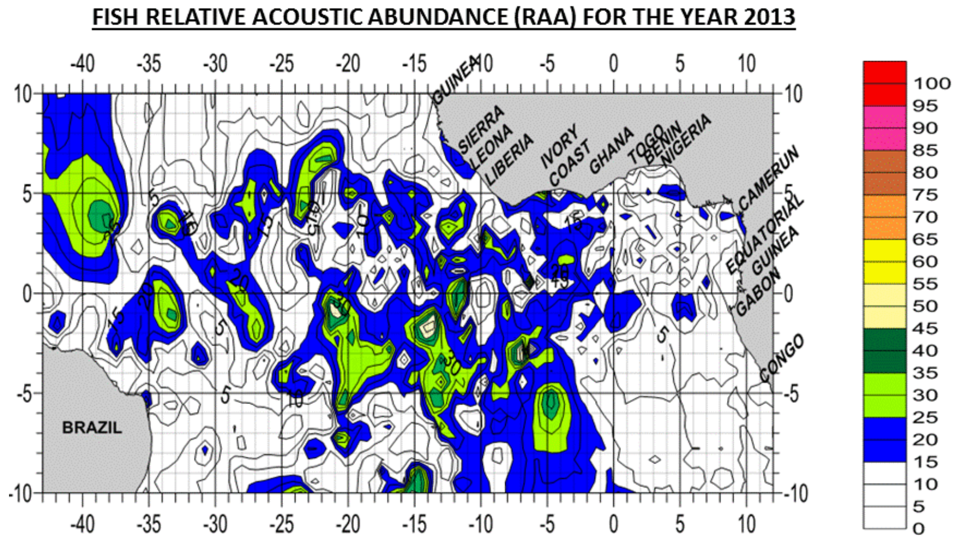

Figure A2.3. Fish relative abundance (tonnes) map using acoustic bouy data.

Conclusion

Buoy acoustic information could speed up the process for a more selective fishery. Moreover, this information could help to estimate biomass or relative acoustic abundance of the highly migratory species.

Buoy technology is currently at the level of discrimination but the market has stronger needs, i.e. identification of specific sizes and species.

References

Delgado de la Molina, A., Ariz, J., Murua, H., and Santana, J. C. 2015. Spanish fish aggregating device management plan. Preliminary data. Collective Volume of Scientific Papers, ICCAT, 71(1): 515–524.

Gaertner, D., Ariz, J., Bez, N., Clermidy, S., Moreno, G., Murua, H., and Soto, M. 2016. Objectives and first results of the CECOFAD project. Collective Volume of Scientific Papers, ICCAT, 72(2): 391–405.

Lopez, J., Moreno, G., Sancristobal, I., and Murua, J. 2014. Evolution and current state of the technology of echo-sounder buoys used by Spanish Tropical tuna purse seiners in the Atlantic, Indian and Pacific Oceans. Fisheries Research, 155: 127–137. https://doi.org/10.1016/j.fishres.2014.02.033

Maufroy, A., Kaplan, D. M., Bez, N., Delgado de la Molina, A., Murua, H., Floch, L., and Chassot, E. 2015. Drifting Fish Aggregation device (dFADs) of the Atlantic Ocean: how many? ICCAT Document No. SCRS/2015/086.

Santiago, J., Lopez, J., Moreno, G., Murua, H., Quincoces, I., and Soto, M. 2016. Towards a tropical tuna buoy-derived abundance index (TT-BAI). Collective Volume of Scientific Papers, ICCAT, 72(3): 714–724.

10 Author contact information

Editor

Rolf J. Korneliussen
Institute of Marine Research
Nordnesgaten 50, 5005 Bergen, Norway
rolf.korneliussen@hi.no
+47 48 89 73 88

Authors

Laurent Berger
Ifremer Bretagne Centre
ZI de la Pointe du Diable, CS 10070,
29280 Plouzané
France
Laurent.Berger@ifremer.fr
+33 29822 47000

Fabio Campanella
NOAA Southeast Fisheries
Science Center
101 Pivers Island Road, Beaufort, NC
28516-9722
USA
fabio.campanella@noaa.gov
+1 252 728 8754

Dezhang Chu
NOAA Northwest Fisheries
Science Center
2725 Montlake Blvd. East, Seattle,
WA 98112
USA
dezhang.chu@noaa.gov
+1 508 289 3318

David Demer
NOAA Southeast Fisheries
Science Center
8901 La Jolla Shores Drive, La Jolla, CA
92037-1508
USA

Alex De Robertis
NOAA Alaska Fisheries
Science Center
7600 Sand Point Way N.E., Seattle
WA 98115
USA
Alex.DeRobertis@noaa.gov
+1 206 526 4789

Réka Domokos
NOAA Pacific Islands Fisheries
Science Center
2570 Dole Street, Honolulu
HI 96822-2396
USA
reka.domokos@noaa.gov
+1 808 983 5368

Mathieu Doray
Ifremer Nantes Centre
Rue de l'île d'Yeu
44311 Nantes Cédex 03
France
Mathieu.Doray@ifremer.fr
+33 24037 4169

Sophie Fielding
British Antarctic Survey
High Cross Madingley Road, Cambridge,
CB3 OET
UK
s.fielding@bas.ac.uk

Sascha M. M. Fässler
Cantonal office for Environment
and Energy
Basel-Stadt, Hochbergerstrasse 158
4019 Basel
Switzerland
sascha.faessler@bs.ch;
sascha.fassler@gmail.com
+41 6163 92322

Stéphane Gauthier
DFO Institute of Ocean Sciences
9860 West Saanich Road, Sidney BC V8L
4B2
Canada
stephane.gauthier@dfo-mpo.gc.ca

Sven Gastauer
Antarctic Climate and Ecosystems
CRC/Australian Antarctic Division
Private Bag 80
7001 Hobart, Tasmania
Australia
Sven.gastauer@utas.edu.au
+61 4 3130 0139

John Horne
University of Washington
Seattle, Washington 98195-5020
USA
jhorne@u.washington.edu
+1 206 526 4618

Briony Hutton
Myriax–Echoview
Hobart, Tasmania
Australia
briony.hutton@echoview.com

Federico Iriarte Ahón
Albor Tecnologico S.A.C.
Jr. Santa Rosa 191, int. 510
Cercado de Lima
Perú
federico.iriarte@albortecnologico.com;
faya2005s@yahoo.com
+51 96 71 60 23 8

J. Michael Jech
University of Washington
166 Water Street,
Woods Hole MA 02543
USA
michael.jech@noaa.gov
+1 508 495 2353

Rudy Kloser
CSIRO
Marine and Atmospheric Research
Castray Esplande,
Hobart Tasmania 7001
Australia
enquiries@csiro.au

Gareth Lawson
Woods Hole Oceanographic Institution
266 Woods Hole Road, MS#34
Woods Hole, MA 02543-1050
USA
glawson@whoi.edu
+1 508 289 3713

Anne Lebourges-Dhaussy
L'Institut de Recherche pour le Développement (IRD)
Centre de Bretagne, F-29280 Plouzané
France
Anne.Lebourges.Dhaussy@ird.fr
+33 (2) 9822 4505

Ian McQuinn
Maurice Lamontagne Institute 850
Route de la Mer Mont-Joli
Québec G5H 3Z4
Canada
Ian.McQuinn@dfo-mpo.gc.ca
+1 418 775 0627

Marian Peña
IEO Centro Oceanográfico de Baleares
Muelle de Poniente s/n, E-07015 Palma de Mallorca
Spain
marian.pena@ieo.es

Ben Scoulding
CSIRO
Marine and Atmospheric Research
Castray Esplande, Hobart Tasmania 7001
Australia
ben.scoulding@csiro.au
+61 3 6231 5588

Serdar Sakinan
Wageningen University and Research
1970 AB IJmuiden
Netherlands
serdar.sakinan@wur.nl

Matthias Schaber
Thünen Institute of Sea Fisheries
Palmaille 9, 22767 Hamburg
Germany
matthias.schaber@thuenen.de

J. Christopher Taylor
NOAA Southeast Fisheries
Science Center
101 Pivers Island Road
Beaufort
NC 28516-9722
USA
Chris.Taylor@noaa.gov
+1 252 838 0833

Charles H. Thompson
NOAA Southeast Fisheries
Science Center
Room 2010, 1021 Balch Blvd.
Stennis Space Center
MS 39529
USA
charles.thompson@noaa.gov